ANKARA YILDIRIM BEYAZIT UNIVERSITY

GRADUATE SCHOOL OF NATURAL AND APPLIED SCIENCES



THERMAL AND MECHANICAL CHARACTERIZATION OF GRAPHENE NANOPLATELETS/SHAPE MEMORY POLYMER NANOCOMPOSITES

M.Sc. Thesis by

Hasan TOPAÇLI

Department of Materials Engineering

July, 2021

ANKARA

THERMAL AND MECHANICAL CHARACTERIZATION OF GRAPHENE NANOPLATELETS/SHAPE MEMORY POLYMER NANOCOMPOSITES

A Thesis Submitted to

The Graduate School of Natural and Applied Sciences of

Ankara Yıldırım Beyazıt University

In Partial Fulfillment of the Requirements for the Degree of Master of Science

in Materials Engineering, Department of Material Engineering

by

Hasan TOPAÇLI

July, 2021

ANKARA

M.Sc. THESIS EXAMINATION RESULT FORM

We have read the thesis entitled **"THERMAL and MECHANICAL CHARACTERIZATION of GRAPHENE NANOPLATELETS/SHAPE MEMORY POLYMER NANOCOMPOSITES"** completed by **HASAN TOPAÇLI** under the supervision of **ASST. PROF. DR. MEHMET FATİH ÖKTEM** and we certify that in our opinion it is fully adequate, in scope and in quality, as a thesis for the degree of Master of Science.

Asst. Prof. Dr. Mehmet Fatih ÖKTEM

Supervisor

Prof. Dr. Güven ÇANKAYA

Jury Member

Prof. Dr. Mustafa ACARER

Jury Member

Prof. Dr. Sadettin ORHAN

Director

Graduate School of Natural and Applied Sciences

ETHICAL DECLARATION

I hereby declare that, in this thesis which has been prepared in accordance with the Thesis Writing Manual of Graduate School of Natural and Applied Sciences,

- All data, information and documents are obtained in the framework of academic and ethical rules,
- All information, documents and assessments are presented in accordance with scientific ethics and morals,
- All the materials that have been utilized are fully cited and referenced,
- No change has been made on the utilized materials,
- All the works presented are original,

and in any contrary case of above statements, I accept to renounce all my legal rights.

Date: **Signature:**

Name & Surname: Hasan TOPAÇLI

ACKNOWLEDGMENTS

First of all, I would like to express my sincere thanks to my advisor, Asst. Prof. Dr. Mehmet Fatih ÖKTEM, for his support, kindly approach and scientific guidance during my studies.

I must also express my profound appreciations to my mother, my father, and my sister for providing me endless support throughout my life. The completion of this study would not have been possible without their prays.

2021, July **Hasan TOPAÇLI**

THERMAL AND MECHANICAL CHARACTERIZATION OF GRAPHENE NANOPLATELETS/SHAPE MEMORY POLYMER NANOCOMPOSITES

ABSTRACT

Shape memory polymers in recent years can be named as one of the most important materials developed. It is of great technological and scientific importance with its ability to react to external stimuli and to restore the deformation of the material to its original state. Thanks to the potential of shape memory polymers, it has a wide range of uses in advanced aerospace, commercial applications, and biomedical fields. The biocompatibility of polyurethane-based shape memory polymers has made these materials suitable for medical products. In recent years, with the positive results obtained in studies on the biocompatibility of graphene-based materials, the number of studies in the biomedical field has increased. In this study, it was aimed to improve the thermal and mechanical properties of SMP MP3510 polyurethane-based polymer produced by Mitsubishi Heavy Industries without losing its biocompatibility feature. Differential scanning calorimeter and thermogravimetric analyzes to examine the thermal properties of nanocomposites obtained by adding 0.1%, 0.3% and 0.5% by weight graphene nanoplatelets using a hybrid method including ultrasonic mixing-high-speed mechanical mixing and high-speed mechanical mixing method, 3-point bending test and Shore D hardness test to examine their mechanical properties, fourier transform infrared spectroscopy analysis to examine the chemical structure, scanning electron microscopy to examine the distribution of graphene nanoplatelets from the cross-sectional area of nanocomposites, and atomic force microscopy and scanning electron microscopy analyzes to examine the effect of graphene nanoplatelets on the surface morphology of nanocomposites were carried out.

Keywords: Shape memory polymer nanocomposite, graphene nanoplatelets, biocompatibility, thermal and mechanical properties

GRAFEN NANOLEVHA/ŞEKİL HAFIZALI POLİMER NANOKOMPOZİTLERİN TERMAL VE MEKANİK KARAKTERİZASYONU

ÖZ

Şekil hafızalı polimerleri son yıllarda geliştirilen en önemli malzemelerden biri olarak adlandırabiliriz. Dış uyaranlara tepki vermesi ve malzemede oluşturulan deformasyonu malzemenin ilk haline getirebilmesi özelliğiyle teknolojik ve bilimsel açıdan büyük öneme sahiptir. Şekil hafızalı polimerlerin sahip olduğu potansiyel sayesinde gelişmiş havacılık, ticari uygulamalar ve biyomedikal alanda geniş bir kullanım alanına sahiptir. Poliüretan bazlı şekil hafızalı polimerlerin biyo uyumluluk özelliği göstermesi bu malzemeleri tıbbi ürünler için uygun hale getirmiştir. Son yıllarda grafen bazlı malzemelerin biyo uyumluluk özelliği üzerinde yapılan çalışmalarda elde edilen olumlu sonuçlar ile biyomedikal alanda yapılan çalışmaların sayısı artmıştır. Bu çalışmada, Mitsubishi Heavy Industries firmasının üretmiş olduğu SMP MP3510 poliüretan bazlı polimerinin biyo uyumluluk özelliğini kaybetmeden termal ve mekanik özelliklerini iyileştirmek hedeflendi. Yüksek hızda mekanik karıştırma yöntemi ve ultrasonik karıştırma ile yüksek hızda mekanik karıştırmayı içeren hibrit bir yöntem kullanılarak ağırlıkça %0.1, %0.3 ve %0.5 grafen nanolevhalar eklenerek elde edilen nanokompozitlerin termal özelliklerini incelemek için diferansyel taramalı kalorimetre, termogravimetrik analizleri, mekanik özelliklerini incelemek için 3 nokta eğme testi ve Shore D sertlik testi, kimyasal yapısını incelemek için fourier transform infrared spektrometresi analizi, nanokompozitlerin kesit alanından grafen nanolevhaların dağılımını incelemek için taramalı elektron mikroskobu ve grafen nanolevhaların nanokompozitlerin yüzey morfolojisine etkisini incelemek için atomsal kuvvet mikroskobu ve taramalı elektron mikroskobu analizleri yapıldı.

Anahtar Kelimeler: Şekil hafızalı polimer nanokompozit, grafen nanolevhalar, biyouyumluluk, termal ve mekanik özellikler

CONTENTS

M.Sc. THESIS EXAMINATION RESULT FORM ii
ETHICAL DECLARATION iii
ACKNOWLEDGMENTS iv
ABSTRACT v
ÖZ vi
NOMENCLATURE ix
LIST OF TABLES xi
LIST OF FIGURES xii
CHAPTER 1 - INTRODUCTION 1
CHAPTER 2 – LITERATURE REVIEW 4
2.1 Shape Memory Materials (SMMs) 4
2.2 Shape Memory Polymers (SMPs) 6
2.2.1 Definition and History of Shape Memory Polymers (SMPs) 6
2.2.2 Shape Memory Polymer (SMP) Classification 7
2.2.3 Shape Memory Cycle 9
2.3 Shape Memory Polymer (SMP) Characterizations 12
2.3.1 Differential Scanning Calorimeter (DSC) 12
2.3.2 Thermogravimetric Analysis (TGA) 13
2.3.3 Dilatometer (DIL) 13
2.3.4 Fourier Transform Infrared Spectroscopy (FTIR) 14
2.3.5 Identification of Surface Morphologies 15
2.3.6 Three-Point and Four-Point Bending Testing 15
2.3.7 Impact Testing 15
2.3.8 Shore (Durometer) Hardness Testing 16
2.4 Polyurethane Shape Memory Polymer (SMPU) 16
2.5 Shape Memory Polymer Composites (SMPCs) 18
2.6 Shape Memory Polymer Nanocomposites (SMPNs) 18
2.6.1 Particle-filled Shape Memory Polymer Nanocomposites 19
2.6.2 Graphene Based Nanocomposites 19
CHAPTER 3 - EXPERIMENTAL PROCEDURE 21
3.1 Materials 21
3.1.1 Shape Memory Polymer MP 3510 21

3.1.2 Graphene Nanoplatelets 22
3.2 Sample Preparation of SMP MP 3510 23
3.2.1 Graphene Nanoplatelets/SMP Nanocomposites Preparation 27
3.2.1.1 Graphene Nanoplatelets/SMP Nanocomposites Preparation by High Speed Mechanical Mixing Method 27
3.2.1.2 Graphene Nanoplatelets/SMP Nanocomposites Preparation by Hybrid Method Including Ultrasonic Probe Mixing - High Speed Mechanical Mixing 28
3.3 Characterization Methods 29
3.3.1 Thermal Characterization 29
3.3.2 FTIR Analysis 31
3.3.3 Microscopic Analysis 32
3.3.4 Mechanical Analysis 33
CHAPTER 4 - RESULTS AND DISCUSSION 35
4.1 DSC Analysis 35
4.2 TGA / DTA Analysis 39
4.3 FTIR Analysis 44
4.4 Mechanical Analysis 46
4.5 Microscopic Analysis 50
CHAPTER 5 - CONCLUSION AND FUTURE WORK 54
5.1 Conclusion 54
5.2 Future Work 56
REFERENCES 57
APPENDICES 63
CURRICULUM VITAE 87

NOMENCLATURE

Abbreviations

T_g	Glass transition temperature
g	gram
mm	millimeter
T_m	Melting temperature
T_{trans}	Thermal transition temperature
nm	nanometer
MPa	Megapascal
SiC	Silicon Carbide
Ni	Nickel
Fe_3O_4	Magnetite
wt	weight
µm	micrometer
S	Siemens
rpm	Revolution per minute
min	minute
mg	milligram
CO_2	Carbon dioxide
N	Nitrogen
vs.	versus

Acronyms

SMP	Shape Memory Polymer
SMM	Shape Memory Material
MHI	Mitsubishi Heavy Industries
SMPU	Shape Memory Polyurethane
PU	Polyurethane
GBM	Graphene-based Material
CNT	Carbon Nanotube
THF	Tetrahydrofuran
DMF	Dimethylformamide
GNP	Graphene Nanoplatelets

SMA	Shape Memory Alloy
PE	Polyethylene
SME	Shape Memory Effect
DSC	Differential Scanning Calorimeter
TGA	Thermogravimetric Analysis
DIL	Dilatometer
TMA	Thermal Mechanical Analyzer
FTIR	Fourier Transform Infrared Spectroscopy
IR	Infrared
XRD	X-ray Diffraction
SEM	Scanning Electron Microscopy
TEM	Transmission Electron Microscopy
AFM	Atomic Force Microscopy
SMPN	Shape Memory Polymer Nanocomposite
GO	Graphene Oxide
PLGA	Polylactic-co-glycol Acid
DTA	Differential Thermal Analysis

LIST OF TABLES

Table 4.1 T_g values of SMP and GNP/SMP Nanocomposites Produced by High Speed Mechanical Mixing Method 36

Table 4.2 T_g values of SMP and GNP/SMP Nanocomposites Produced by including Ultrasonic Mixing and High-Speed Mechanical Mixing Hybrid Method 37

LIST OF FIGURES

Figure 2.1 The position of shape memory polymers in the material family. 5

Figure 2.2 Classification of SMPs based on structure, stimulus, and shape–memory function. 8

Figure 2.3 Typical thermo-mechanical cycle for the shape-memory effect. 10

Figure 2.4 The standard thermo-mechanical cycle of a shape-memory polymer depicted by a stress-strain temperature diagram. 11

Figure 2.5 The change of mechanical properties vs. temperature for an amorphous polymer. 12

Figure 2.6 Thermal transitions in a typical DSC curve of a cross-linked polymer... 13

Figure 2.6 T_g determination through dilatometry..... 14

Figure 2.7 Example of the shape-memory effect in an SMPU. 17

Figure 2.8 Thrombectomy concept of SMPU device..... 18

Figure 3.1 Shape Memory Polymer SMP MP3510 22

Figure 3.2 Graphene Nanoplatelets..... 23

Figure 3.3 a) SMP with bubble structre b) Failed curing of SMP 24

Figure 3.4 SpeedMixer Device..... 24

Figure 3.5 Vacuum Chamber 25

Figure 3.6 a) A component of SMP MP 3510 before degassing process b) A component of SMP MP3510 after degassing process c) B component of SMP MP3510 before degassing process d) B component of SMP MP3510 after degassing process26

Figure 3.7 Mold Prepared with Teflon Bars In Teflon Mold Homogenous Mixing Component A and B with SpeedMixer without any Bubles..... 27

Figure 3.8 Ultrasonic Probe 29

Figure 3.9 Differantial Scanning Calorimeter (DSC) 30

Figure 3.10 Thermogravimetric Analysis (TGA) 31

Figure 3.11 Fourier-Transform Infrared Spectroscopy (FTIR)..... 31

Figure 3.12 Scanning Electron Microscope (SEM) 32

Figure 3.13 Atomic Force Microscope (AFM) 33

Figure 3.14 3-Point Bending Test Machine with Cooling Cabinet..... 34

Figure 3.15 Digital Durometer..... 34

Figure 4.1 DSC Results of SMP and GNP/SMP Nanocomposites Produced by High Speed Mechanical Mixing Method 36

Figure 4.2 DSC Results of SMP and SMP/GNP Nanocomposites Produced by including Ultrasonic Mixing – High Speed Mechanical Mixing Hybrid Method 37

Figure 4.3 TGA/DTA Result of Polyurethane SMP MP3510 40

Figure 4.4 TGA/DTA Result of Polyurethane SMP MM3520 41

Figure 4.5 Comparison of Degradation Temperatures of GNP/SMP Nanocomposites Produced by High Speed Mechanical Mixing Method 42

Figure 4.6 Comparison of Degradation Temperatures of GNP/SMP Nanocomposites Produced by Including Ultrasonic Mixing – High Speed Mechanical Mixing Hybrid Method 43

Figure 4.7 FTIR Result of SMP and Nanocomposites Produced with High Speed Mixing Method 45

Figure 4.8 FTIR Result of SMP and Nanocomposites Produced with Including Ultrasonic Mixing – High Speed Mechanical Mixing Hybrid Method 45

Figure 4.9 Flexural Strength Results of Nanocomposites Produced by both Methods 47

Figure 4.10 Flexural Modulus Results of Produced Nanocomposites by both Methods 47

Figure 4.11 Hardness Results of Produced Nanocomposites by both Methods 49

Figure 4.12 SEM images of (a) Pure SMP, (b) 0.1% GNP, (c) 0.3% GNP (d) 0.5% GNP produced with hybrid method involving ultrasonic mixing – high speed mechanical mixing 51

Figure 4.13 SEM images of (a) Pure SMP, (b) 0.1% GNP, (c) 0.3% GNP (d) 0.5% GNP produced with high speed mechanical mixing method 51

Figure 4.14 SEM images of nanocomposites taken from fractured surface (A) PU, (B) PU 0.1%, (C) PU 0.25%, (D) PU 0.5%, (E) PU 1% include graphene [47] 52

Figure 4.15 Surface SEM images of nanocomposites a) Pure SMP, b) 0.1% GNP, c) 0.3% GNP, d) 0.5% GNP produced with hybrid method involving ultrasonic mixing – high speed mechanical mixing e) 0.1% GNP, f) 0.3% GNP g) 0.5% GNP produced with high-speed mechanical mixing method..... 53

Figure 4.16 Surface AFM images of nanocomposites a) Pure SMP, b) 0.1%, GNP, c) 0.3% GNP, d) 0.5% GNP produced with hybrid method involving ultrasonic mixing – high speed mechanical mixing e) 0.1% GNP, f) 0.3% GNP, g) 0.5% GNP produced with high speed mechanical mixing method 53

CHAPTER 1

INTRODUCTION

Shape memory polymers (SMPs) are a kind of shape memory materials (SMMs) that, if exposed to adequate stimulation, may regenerate their shape from a distorted condition back into their permanent shape [1]. Shape memory mechanism can be briefly explained with reversible energy conversion that occurs during the movement of polymer chains. Generally, when SMP is heated and deformed and then cooled below its switch transition temperature, a significant amount of internal tension may be stored in the cross-linking structure; when the SMP is heated over its switch transition temperature, the internal tension is released and the SMP regains its permanent shape [2]. SMPs have gained widespread acceptance as smart materials due to their high deformation, low density, versatility of stimulation techniques, and strong biocompatibility. SMPs, on the other hand, have several drawbacks and shortcomings that become apparent in engineering applications such as, low mechanical strength and low thermal stability [3-5]. As a result, many reinforcing fillers are being investigated to increase the thermal and mechanical properties of pure SMPs while retaining their shape memory capabilities. Particles, fibers, sheets, and platelets are all examples of these fillers. The distribution levels of fillers and their interactions with the polymer influence several properties of the materials i.e. thermal, mechanical or shape memory characteristics of SMP composites. The homogeneous dispersion of fillers and the strong interactions between fillers and polymers result in an increase in the thermal stability, mechanical characteristics, and shape memory property of SMP composites [6].

Hayashi's (1990) polyurethane SMP is now one of the most researched polyurethane SMPs. Since the 1980s, Mitsubishi Heavy Industries (MHI) has conducted substantial research on the shape memory polyurethane (SMPU). Glass transition temperature (T_g) values spanning a large temperature range of -30 to 65 °C are part of the MHI SMPUs, making them suitable for a variety of commercial applications, including culinary equipment, textiles, automobile industries, and biomedical equipment.

Because they offer several unique features, SMPUs have been developed fast for medical device applications in recent years; biocompatibility, cheap cost, and simple synthesis techniques. PU-based SMPs show high biocompatibility, with the cytotoxicity and mutagenicity tests established. T_g of the SMPUs may be customized for shape recovery/self-assembly of a variety of medical instruments. Memory stimuli like alternating magnetic fields or light have substantially increased their usage and applications in contact-free operations [7].

Research on graphene-based materials (GBMs) with applications in areas as varied as nanoelectronics, energy technology, sensors and composites has increased in recent years. Several biological uses such as biosensing, drug delivery, cancer treatment, and antimicrobial materials have also been investigated. Moreover, techniques in biological, regenerative, and biotechnological applications are under research, which are, enhancement in the mechanical/thermal/electric characteristics of biomaterials, increased cellular adhesion and proliferation on the biomaterial surface and development of more effective biosensors are many examples of the purported benefits of GBMs [8]. It should be highlighted that current data on another carbon-based materials may not necessarily apply to GBMs because of variations in the production methodology, shape of particles or surface chemistry. For example, unlike carbon nanotubes (CNTs), metal catalysis is not often used in the production of GBMs, allowing for the avoidance of cytotoxicity and inflammation produced by residual metals [9].

The dispersion condition of graphene in the matrix is critical for the formation of epoxy/graphene nanocomposites with outstanding characteristics [10]. Graphene is incompatible with simple mixing in epoxy. This is because graphene has a high tendency of re-agglomeration in the matrix phase because of the strong Vander-Waals force and pi-stacking between individually distributed graphene nanosheets [11, 12]. Maximum enhancements in final qualities are possible only when graphene is distributed uniformly throughout the matrix. The use of solvents is widely used and is considered the easiest way of graphene dispersion. In acetone, tetrahydrofuran (THF), 1-propanol and dimethylformamide (DMF), graphene may be dispersed. It should, however, be highlighted the need for these dispersions to remove solvents before they

may be cured. This can lead to operational difficulties and unwanted lengths of processing. The remaining solvent also has an adverse influence on the composite material's ultimate characteristics. In addition, certain solvents are costly and toxic and might have consequences for the environment, the health and safety [13].

In this study, it is aimed to obtain PU nanocomposite with improved thermal and mechanical properties without losing the biocompatibility of SMP MP3510, one of the polymer series produced by MHI, which is used in biomedical applications. Graphene nanoplates from GBMs were used as additives to produce this nanocomposite, which showed successful results in biocompatibility in in vivo and in vitro tests. Firstly, PU nanocomposites prepared with different ratios of GNPs were produced by applying SpeedMixer™ (mechanical mixing) and ultrasonic mixing method to disperse GNPs in SMP MP3510 polymer without the use of solvents. Then, the thermal and mechanical properties of PU nanocomposites were characterized. In addition, the effect of the dispersion of GNPs in the polymer matrix by SpeedMixer™ and ultrasonic mixing on the mechanical properties was investigated.

CHAPTER 2

LITERATURE REVIEW

2.1 Shape Memory Materials (SMMs)

Nowadays, we can mention about the existence of many materials that we cannot count. However, with the developing technology and engineering applications, we need new materials and witness the discovery of these materials almost every day. These discoveries often emerge after long pursuits, but sometimes as a result of coincidence and sometimes by being inspired by a creature in nature. As a novel feature amongst the newly discovered materials, the materials that react by an appropriate stimulus, can change their physical and chemical properties with an external effect. We can sort of these factors as heat, stress, pressure, electric current or voltage, magnetic field, pH, changing the level of humidity, light and other factors [14, 15].

When we look at the literature, this group is called stimulus responsive materials (SRMs) (see Figure 2.1). Materials that react with external effects, especially polymeric materials, became interesting with their wide usage areas. The materials that react to the right stimulus can change their shape spontaneously and instantly when the right effect comes from the outside, these types of materials are called shape change materials. Piezoelectric materials and electroactive polymers are two typical examples. The second group is called shape memory materials and can keep their temporary shape until the external stimulus comes. When the correct stimulus comes after the semi-plastic distortion, it regains its original shape [14].

As was said before, the shape memory materials are one of the most popular topics in materials science. Under this title, it could be said that shape memory alloys (SMAs) and SMPs are the most important ones. SMAs have been studied for a long time, but with discovery of SMPs, SMAs lost that previous importance to some extent because SMPs provide several benefits than SMAs [14,15].

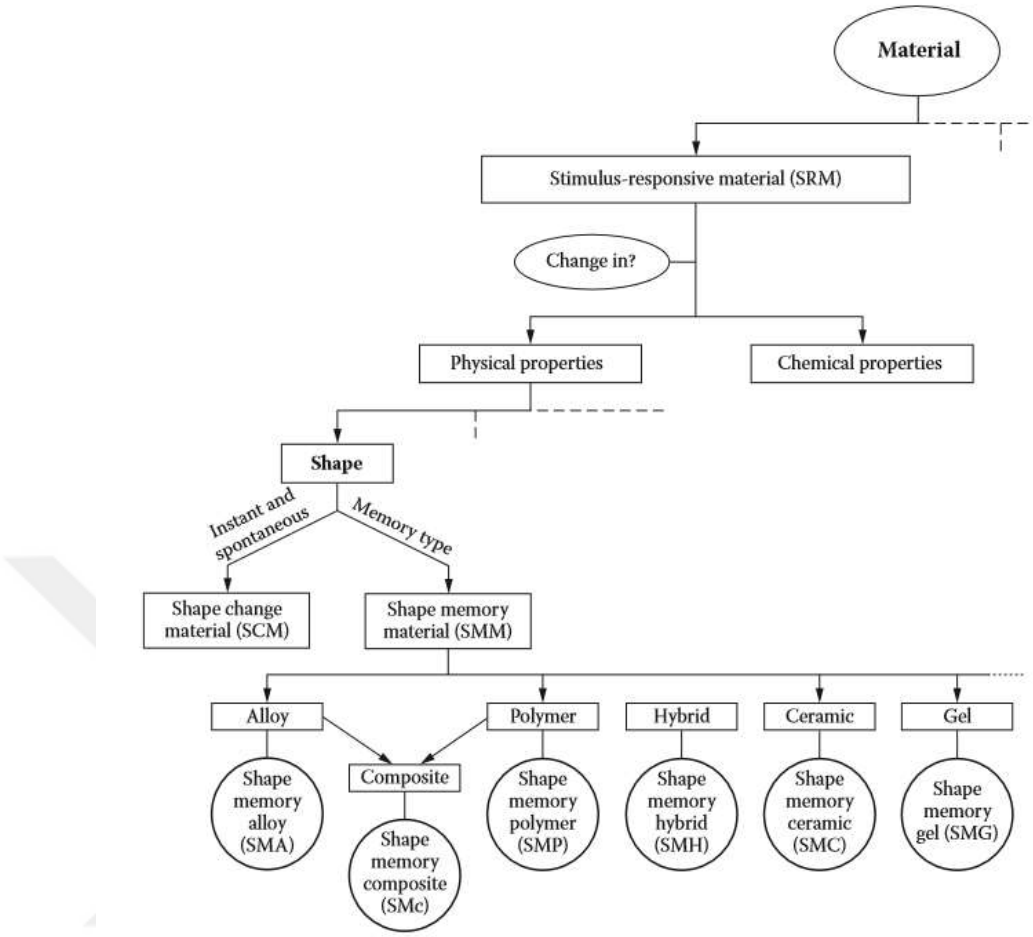


Figure 2.1 The position of shape memory polymers in the material family [14].

The advantages of SMPs can be listed as follows:

1. Their low density and low cost are important advantages for shape memory polymers. As an example, the density of polyurethane SMP is 1.25 g/mm^3, while that of the NiTi SMA is 6.4 g/mm^3. Shape memory polymers (SMPs) have a slightly less density than five times of the SMAs [14,15].

2. It is an important advantage that the raw material is easily accessible, the manufacturing methods and easy processing reduce the costs of SMPs [14].

3. SMPs have highly recoverable strain, this strain is 100% for solids and 95% for foams. When we look at the traditional SMAs, this rate is below 10% [14].

4. We can easily design thermomechanical properties. It is possible to do this by mixing it with various nano powders in different proportions [14].

5. Shape memory polymers have glassy transition temperature in wide variety (from -20 ºC to +150 ºC) [14].

6. Shape memory polymers have high chemical stability. In addition, they are biocompatible and even biodegradable [14].

7. While a variety of stimulating methods can be cited for shape memory polymers, these stimulation methods for shape memory alloys are limited. For shape memory polymers, stimulants such as temperature, light, change in pH value, adding solvent can be counted; while for shape memory alloys, we can only mention heat and magnetic field [14].

2.2 Shape Memory Polymers (SMPs)

2.2.1 Definition and History of Shape Memory Polymers (SMPs)

Materials which can form a different shape when subjected to different external stimuli are called SMPs. They are capable of reversing the strain caused by the mechanical force. Molecular chains allow the material to alter its shape and movement. Numerous stimuli may be used to activate SMPs. These include heat, light, magnetic field, electrical field, humidity, infrared light, and so on. In both, heat stimulation is still mostly used. An SMP is divided into two parts. One section is flexible, and the other is rigid. The hard segments have a high degree of elasticity, while the soft segments have a lower degree of elasticity. At elevated temperatures, the micro-Brownian motion of soft segments accelerates and the total material's elasticity decreases. These flexible segments become calm and frozen upon cooling. Thus, the content is repositioned. When an appropriate stimulus is applied to the material, the soft segments rapidly react, their micro-Brownian motion increases, and the material returns to its original state, a process known as shape recovery [4].

The first SMP, a poly(norbornene)-based polymer, was produced in 1984 by CdF-Chimie Company in France and commercialized the same year under the trade name Norsorex by Nippon Zeon Company in Japan [16]. Since this polymer has a T_g of between 35 ºC and 40 ºC, its processability has restricted its applications. In 1987, Japan's Kurare Corporation produced a second commercial SMP, the Kurare TP-301. It is composed of poly(trans-isoprene), has a glass transition temperature (T_g) of -68 ºC and a melting point (T_m) of 67 ºC, however, like poly(norbornene) exhibits reduced processability. MHI produced diisocyanate/polyol based polyurethane SMPs in the late 1980s. SMPs based on poly(urethane) are marketed under a variety of trade names, including Diary MM-4510, which is a polyester polyol-based poly(urethane), and Diary MM-4520, which is a polyether polyol-based poly(urethane). The benefit of poly(urethane) SMPs is the versatility provided by the polyurethane chemistry in designing materials with a variety of T_gs and thus temperatures capable of inducing the shape memory effect. Additionally, this poly(urethane) is thermoplastic polymers, which improves processability significantly [17].

2.2.2 Shape Memory Polymer (SMP) Classification

Classification of SMPs have been extensively addressed in the literature. According to their external stimuli, SMPs are specified as light and thermally induced, electroactive, water/moisture/solvent-induced, pH/magnetically sensitive. According to the essence of their net points, Ratna and Karger-Kocsis, as well as Liu and coworkers, classified SMPs into physically and chemically crosslinked. Also, biodegradable SMPs are distinct forms of SMPs. Occasionally, SMPs may be subdivided into glass transition temperature-style SMPs with an amorphous phase and T_m-type SMPs with a crystalline phase depending on their transform type. However, Behl and Lendlein classified polymers based on their aggressive movement between shape-memory and shape-changing polymers. These classifications will not be universally agreed since they illustrate just a portion of the SMP concept [18].

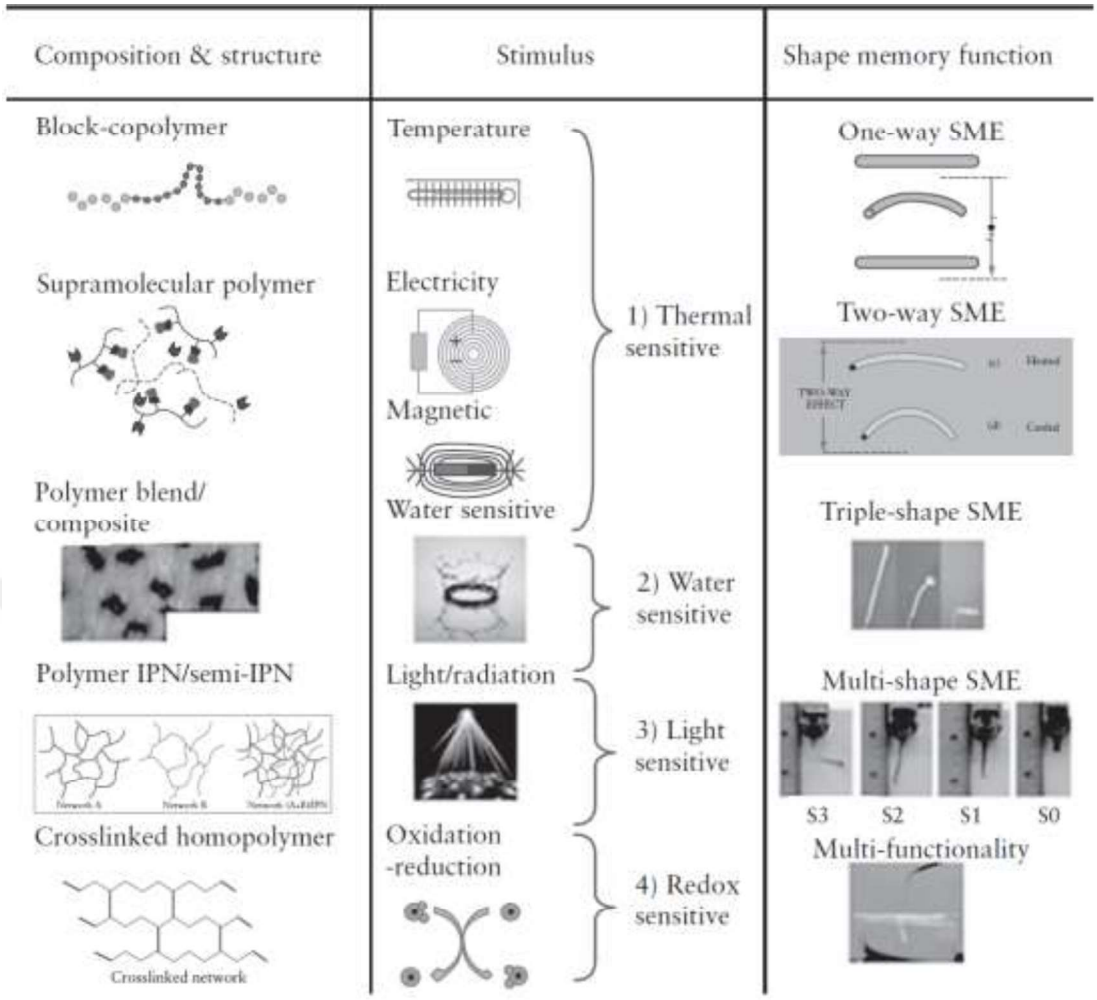


Figure 2.2 Classification of SMPs based on structure, stimulus, and shape–memory function [18].

Figure 2.2 illustrates the grouping of SMPs according to their polymerization, form, stimulus, and shape-memory features. SMPs may be block/segmented copolymers, chemically crosslinked polymers, interpenetrating/semi-interpenetrating polymers, polymer blends, polymer composites, and supramolecular polymer networks. Thus, SMPs can be synthesized by virtually any polymerization method: addition, condensation, free-radical and photochemical polymerization, radiation reaction, acyclic diene metathesis polymerization, and even ring-opening polymerization. Condensation polymerization is generally used to synthesize SMPU and ethylene oxide-ethylene terephthalate segmented copolymers. A radiation reaction is used to establish crosslinked PE. Additionally, such SMP products may be synthesized by

combining two polymers or by incorporating non-woven textile composites into an elastomer matrix [18].

The structure and chemistry/polymerization of SMPs can be regulated to create different shapes memory functions (including the SME and other functionality). The SMEs of SMPs have been transformed into two-way, three-way, and also several SMEs from traditional single-way SMEs. Multifunctionality can be obtained in SMP, as Behl and colleagues discussed, in addition (e.g., permeable, optical, biodegradability, and thermal chromic properties). To achieve SMEs, external stimuli (e.g., heating, light and humidity) are used to cause pressure recovery. Heating, such as electrically induced, magnetic, and infrared light heaters may be accomplished by direct or indirect heating. In addition, redox conditions will cause SMEs. SMP can thus be categorized into four categories with their stimulus: thermally induced; athermally sensitive to water(molecule), athermally sensitive to light and redox sensitive [18].

2.2.3 Shape Memory Cycle

After major deformations, when the SMPs are exposed to an exterior stimulus such as heating, light, magnetism, or humidity; they may regain their original shape. Thermo-reactive SMPs are the most frequent of these SMPs. The standard thermo-mechanical cycle of a thermo-responsive SMPs at a macro-level, as shown below in Figure 2.3, is as follows:

(1) SMP manufacturing in the initial form,

(2) Heat SMP above the temperature of thermal transition (T_{trans}),

(3) SMP deformation for the use of an external force — far below T_{trans} cooling,

(4) Removing the restriction of obtaining the pre-deformed form temporarily and heating the pre-deformed SMPs over T_{trans} again, which results in the recovery of the SMP into its original shape known as its recovered form [19].

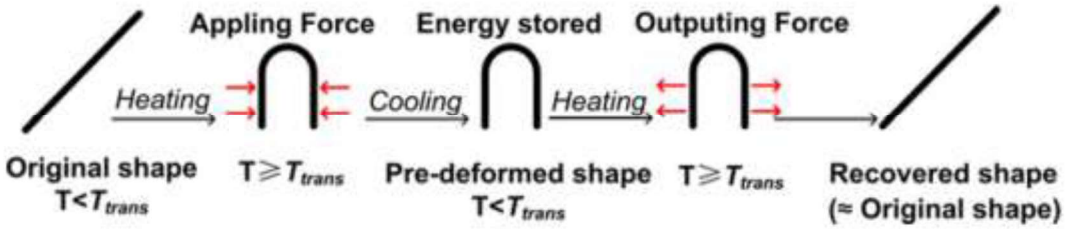


Figure 2.3 Typical thermo-mechanical cycle for the shape-memory effect [19].

Figure 2.4 clearly shows the three-dimensional view (stress, strain, and temperature) of the SMP cycle. The thermo-mechanical cycle begins with the substance being brought above its T_g by a higher temperature. Step 1 (path 1–2) indicates that the substance is deformed in rubber condition to a peculiar deformation. F_{max} indicates the stress value at point 2. Step 2 (path 2–3) reveals that this deformation is maintained when the material is cooling below T_g at temperature. The pressure in the substance is stored here. Step 3 (Path 3-4) is a mechanism that results in random spring-back unloading at a lower temperature. Stress is loosened and stress becomes zero. The fixed displacement usually amounts to less than 100%. Displacement number fixed (d_F) in the material is the resulting pressure at unload. The transient form is set at point 4. The last step is to split the recovery step into 2 paths: path (4-5a) and path (4-5b), depending on the boundaries. The route (4-5b) is the restricted recovery obtained when the substance is heated by fixing the location temporary or fixed. This step tracks the forces produced during the recovery step and the curve approaches point 2 very nearby. In the same way, direction (4-5a) is the uncontrolled recovery obtained when the substance is enabled and re-established. Most of the displacement is restored, and the remaining displacement used to assess the recovery of the form is removed. The curve is very similar to point 1 during unconstructed recovery, the original material state [20].

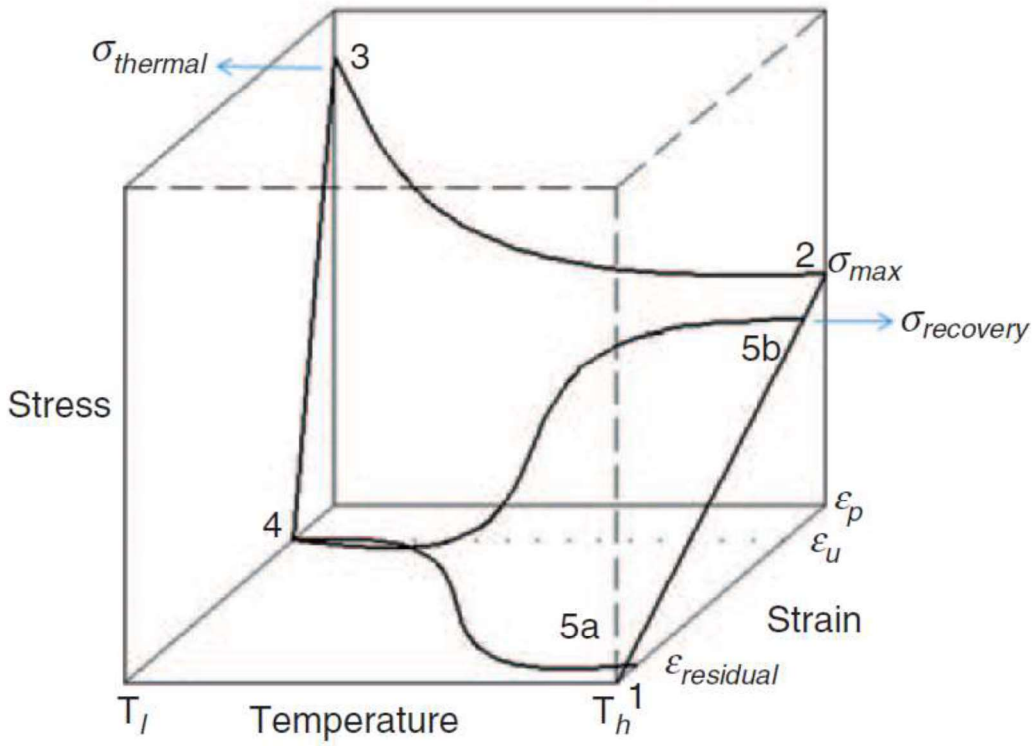


Figure 2.4 The standard thermo-mechanical cycle of a shape-memory polymer depicted by a stress-strain temperature diagram [20].

Figure 2.5 illustrates what happens to molecular chains throughout the SM cycle. The molecular chains above T_g (rubbery state) micro-Brown movement are decreased and the polymer material elastic module decreases. With the use of external force, the polymer may rapidly deform in the rubber state and molecular chains may be guided towards the application force. When the temperature was below T_g, the micro-Brownian motions are frozen and chain alignment, and deformation are rectified. Movement starts again once the material heats up over T_g, molecular chains lose their alignment and the material reverts to its original shape [21].

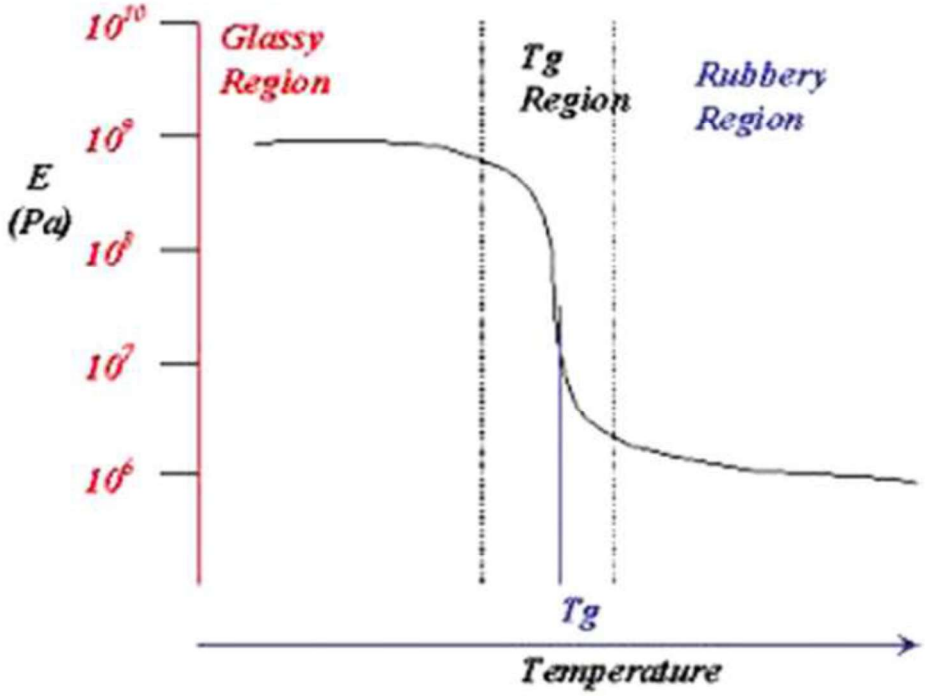


Figure 2.5 The change of mechanical properties vs. temperature for an amorphous polymer [21].

2.3 Shape Memory Polymer (SMP) Characterizations

2.3.1 Differential Scanning Calorimeter (DSC)

A DSC analyzer detects the energy changes that occur in combination with the heating, cooling, or holding of a sample and its temperatures. Generally, DSC is used to describe materials such as specific heat, percentage crystallinity and kinetic reactions, for their temperature of transition from glass, melting point and other material reactions [22]. While DSC is effective for determining melting temperatures (T_m) and glass transition temperatures (T_g), sub-T_g thermal transitions are typically too faint or widespread to be detected by DSC. Figure 2.6 illustrates a typical DSC curve representing heat flow as a function of temperature [23].

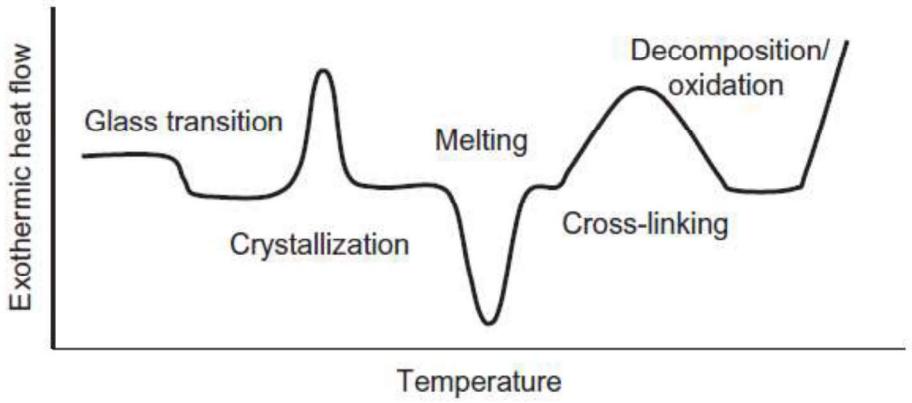


Figure 2.6 Thermal transitions in a typical DSC curve of a cross-linked polymer [23].

2.3.2 Thermogravimetric Analysis (TGA)

TGA determines the rate and degree of mass change in a material as a function of temperature or time in a controlled environment. It is possible to assess the qualities of selected materials that exhibit mass loss or gain because of degradation, oxidation, dehydration, or other fluid component loss. These characteristics include the composition (multi-component polymer systems), thermal and oxidative stability, kinetic decomposition, and humidity and volatile component levels [23].

2.3.3 Dilatometer (DIL)

Dilatometers are instruments for measuring changes in volume. This includes a controlled temperature change mechanism that might be a furnace for high temperature readings (up to 2000 ^{o}C or more) or a cryostat for temperatures below room temperatures. They can be applied in many applications, such as metal alloys, refractory compounds crushed and sintered, glasses, ceramics, composites, or polymers [24]. The glass transition relates to an intersection in the dimensional variation in the dilatometer (DIL) and the thermal mechanical analyzer (TMA) [25]. T_g determination through dilatometry is shown in Figure 2.6.

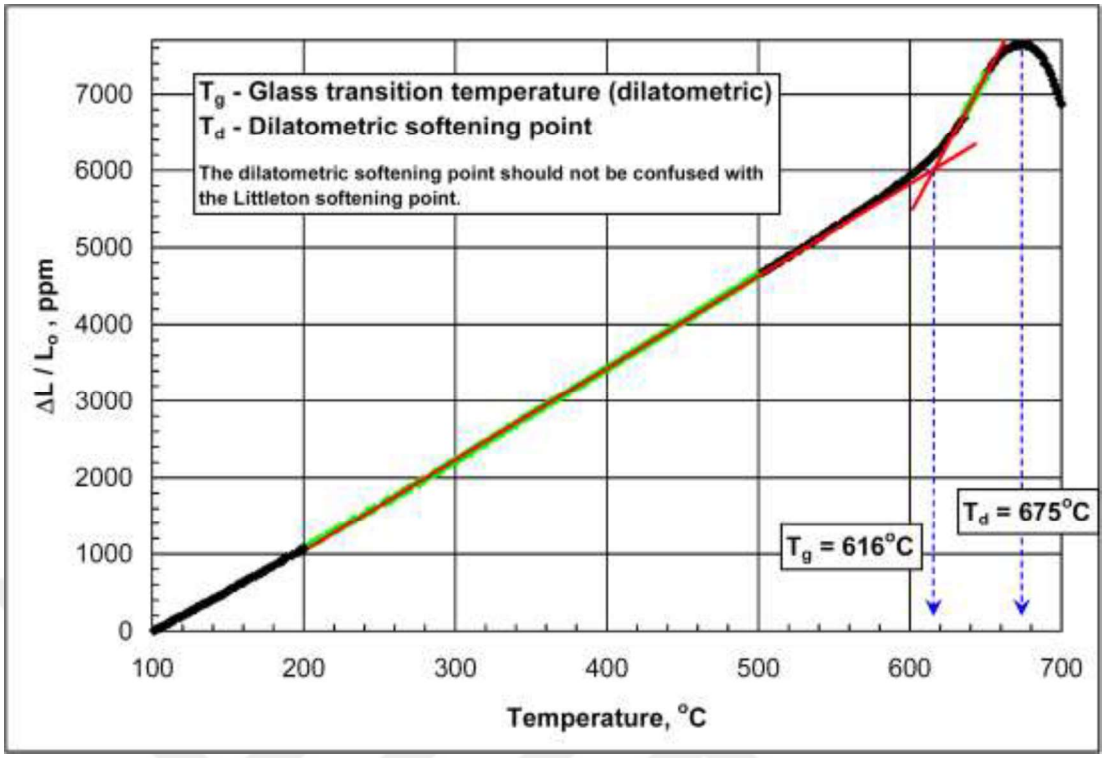


Figure 2.6 T_g determination through dilatometry [25].

The below and above T_g linear sections have a green mark; T_g is at the point of cross-section of the respective red regression lines [25].

2.3.4 Fourier Transform Infrared Spectroscopy (FTIR)

FTIR is the primary technique of infrared (IR) spectroscopy, Fourier Transform Infra-Red. IR radiation is transmitted through a sample in IR spectroscopy. The sample absorbs certain of the IR radiation, and transmits part of it (transmitted). The spectrum produced represents molecule absorption and transmission and creates a molecular sample fingerprint. No two single chemical configurations create the same IR spectrum, as with a fingerprint. For certain analytical kinds, this makes IR spectroscopy valuable. In addition, unknown materials can be identified, the quality or coherence of a specimen determined and the number of components in a mixture established [26]. The chemical structures are also determined by Raman spectroscopy and X-ray diffraction (XRD).

2.3.5 Identification of Surface Morphologies

The SMPs or their composites may be seen by optical microscopy, electron scanning (SEM) and electron transmission microscopy (TEM). The optical microscope magnifies pictures of tiny objects using visible light and a lens system. SEM produces images 300–600 times finer than those produced by optical microscopes due to the scattered electrons. TEM is a type of microscopy in which an electron beam is delivered through an ultra-thin object and interacts with it. TEM is capable of providing information down to a magnitude of roughly 1 nm [19]. Atomic force microscopy (AFM) fulfills this goal by giving a nanoscale-resolution map of the surface topography of SMPs. Indeed, current AFM devices frequently have a resolution of less than a nanometer. They are simply a sharp point attached to a cantilever. When the tip is brought into proximity to a surface, the tip deflects due to the contact of the tip and the surface. Changes in voltage (where piezoelectric devices are included into the cantilever) or laser beam deflection or optical interferometry are used to measure this deflection [23].

2.3.6 Three-Point and Four-Point Bending Testing

Flexural strength, also known as bend strength, is the capacity of a material to withstand deformation under force. Flexural strength is a measure of the maximum stress encountered within a material at the point of rupture. It is quantified in terms of perceived stress. Three and four-point bending tests are frequently used to measure a specimen's flexural strength [27].

2.3.7 Impact Testing

The impact test establishes the quantity of energy absorbed during fracture by a material. This absorbed energy is an indication for the toughness of a material and may be used to investigate the temperature-dependent brittle-ductile transitions. It is used to determine if a material is naturally brittle or ductile. Impact testing is performed to examine the material's behavior under conditions of rapid deformation. By measuring the height of the pendulum hammer after impact, traditional pendulum impact tests calculate the impact energy received by a standardized specimen up to failure. There

are two fundamental types of impact testing: pendulum testing and drop weight testing. The most often used pendulum tests are the Izod, Charpy, and tensile impact [28].

2.3.8 Shore (Durometer) Hardness Testing

Plastic hardness is mostly determined by the Shore® (Durometer) test or Rockwell durability test. Both methods assess plastic resistance to indentation and offer an empirical hardness value which does not correspond well necessary with other qualities or basic features. Shore Hardness is the recommended approach for rubbers/elastomers and is also used in softeners such as polyolefins, fluoropolymers and vinyls using either the Shore A or Shore D Scale. For 'softer' rubber, the Shore A scale is utilized whereas the Shore D scale is for 'harder' rubber. Many more Shore hardness scales exist, such as Shore O and Shore H hardness, however the majority of the plastic sector seldom find themselves [29].

2.4 Polyurethane Shape Memory Polymer (SMPU)

Polyurethanes (PUs) are a polymer category including lengthy and entangled polymer chains exhibiting shape memory effect (SME). SMPU is made up of soft and hard segments; immiscibility between these two segments causes phase separation, resulting in an outstanding shape-memory material. Some soft and hard segments remain mixed together after manufacture of the SMPU. Hard portions serve as pivots for form recovery, and soft portions operate as shock absorbers for the SMPU. In the glass state, T_g, the soft segments do not have enough kinetic energy to provide movement; hence, SMPUs are difficult to bend. Above T_g SMPU turns into a rubber state and then is readily distorted (See Figure 2.7). The soft and hard sections reposition themselves toward external force, becoming stressed. Cooling SMPUs below T_g while applying force deforms the soft segments, which reduces mobility and maintains the distortion after removal of the restrictions. As the soft segments return to their previous coiled configuration, the SMPU is able to restore to its original form [7].

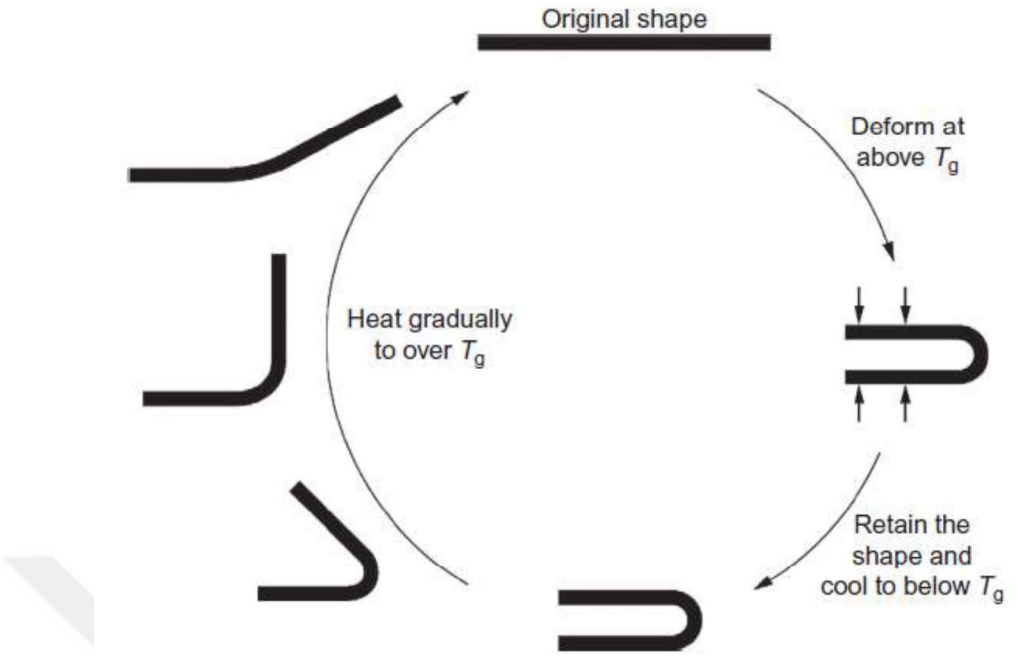


Figure 2.7 Example of the shape-memory effect in an SMPU [7].

PU-based SMPs have many advantages over other kinds of SMPs, including easy processing, low material cost, low manufacture cost, large recovery loads of up to 1000%, large adjustable form-recovery temperature range, excellent chemical properties, and biocompatibility for most of the SMPUs. SMPU features like elasticity, temperature range for crystallization, melting point, thermal behavior, etc. may readily be adjusted to alter the ratio of hard and soft segments [7].

Due to its superior biocompatibility, SMPUs may be used for several possible medical applications. Baer et al. [30] described a photothermally actuated self-expanding polyurethane stent. The SMPU stent is crimped onto the end of an optical fiber connected to an infrared diode laser. The optical fiber acts as both a conveyance for light energy and a conduit for its delivery to the stent. Additionally, Baer et al. detailed the device's design and construction, as well as laser actuator in a water-filled in vitro vascular model.

Small et al. [31] design a device using SMPU to mechanically remove the blood clot formed after a stroke and restore the blood flow. This innovative material based on polyurethane may retain a steady secondary form and will recover to its primary form

after appropriate heating. The primary shape of this gadget is conical corkscrew, while the secondary form is a straight rod. Thrombectomy concept is shown in Figure 2.8. Small et al. discuss the manufacturing procedures and device's optical photothermal and thermal characteristics. An in vitro thrombotic vascular occlusive model is also demonstrated by the clinical deployment of the device.

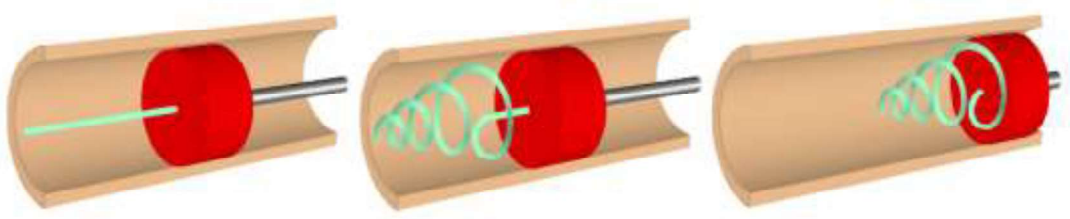


Figure 2.8 Thrombectomy concept of SMPU device [31].

2.5 Shape Memory Polymer Composites (SMPCs)

Due to their low weight, cheap cost, simplicity of manufacture, and extraordinarily high recoverable strain (several hundred percent) as compared to SMAs (maximum 8%), SMPs are well-suited for a range of potential applications. The downside of SMPs is that they have a lower stress recovery (3±2MPa) than SMAs (0.50±.25GPa), which restricts their usage in some applications under constraint circumstances. The invention of SMPCs resolves this issue by making them robust enough to generate bigger recovery strains. As a result, much research effort has been directed into enhancing SMPs' inherent low stiffness and low recovery stress through the creation of composites including shape memory polymer as the polymer matrix. Reinforcement in any kind enhances the composite structure's stiffness, strength, and actuation stress [2, 32, 33].

2.6 Shape Memory Polymer Nanocomposites (SMPNs)

Originally, in engineering, the term composites described the indicate when two or more materials were joined to alter the weaknesses of one component. Nanocomposite polymer is typically characterized as the combination of a polymer matrix and nanometer additive with at least one dimension. Additives can either be 1-D (e.g., nanotubes, fiber), 2-D (e.g., layered clay minerals), or 3-D (for example, spherical

particles). Due to its exceptional significance in mechanical features like elastic modulus and strength with only a little number of nanoscale additions, Polymer nanocomposites have gained great interest in both academia and the industry throughout the past decade. This is caused by nano additives in relation to micro and macro-additives' huge surface ratio to their volumes. Other very advanced qualities of nanocomposite polymers include barrier resistance to inflammation, scratch/wear strength, and optical and magnetic characteristics and electrical capabilities. To increase the mechanical characteristics, satisfy the realistic trigger requirements and diversify applications of SMPs, the addition of reinforcement fillers has been studied [34–36].

2.6.1 Particle-filled Shape Memory Polymer Nanocomposites

This group includes the SMPs full of particles or short fibers. The particles that have been filled may consist of black carbon, nano-carbon nanotubes, carbon nano-fivers, SiC, Ni, Fe_3O_4, clay and short fibers etc. With these fillers, the elastic modulus or rigidity of SMPs are improved, hence raising the composite recovery stresses. However, the SMPs are employed as functional materials and not as structural materials with particles or short fibers. For example, electro-active SMPs are included electrically conducting carbon black, carbon nanotubes, and cut carbon fibers amongst the SMPs [19].

2.6.2 Graphene Based Nanocomposites

Graphene is a two-dimensional (2-D) honeycomb lattice made up of two interconnected triangular sub-lattices. Graphene sheets have unique and highly powerful electrical characteristics, thanks to their extremely large 2-D conductivity, wide surface area and inexpensive cost. Graphene is a suitable material for electrochemistry; it is also a suitable material for the manufacture of nanocomposites based on polymer and has numerous distinguishing benefits over nanocomposites based on CNT [14, 37]

Graphene is a biocompatible material with low metallic impurities; in comparison, CNTs have been linked to substantial toxicological consequences, primarily due to their metallic impurities [14].

In order to improve the required characteristics, in other words mechanical, thermal and electrical; GBMs can be introduced into different polymer matrices. In biomedical applications, biocompatibility should not be reduced by including GBMs and bacterial surface growth would be dissuaded as appropriate and thrombogenicity would be reduced [8].

Pinto et al. [38] demonstrated a considerable improvement in the tensile strength and the Young's modulus by including tiny volumes of GO and GNP in PLA (0.4 wt. percent). This class of composites hence has the potential to make advantage of better mechanical performance surgical implants. However, it is important to ensure that there are no toxicity concerns with these biomaterials. The work surface characteristics of thin films PLA/GO, and PLA/GNP are investigated and show that modest quantities of GO, and GNP may safely be added into the PLA in order to improve its biomedical mechanical characteristics. In addition, the effect of GO on cell adhesion and proliferation appears to be beneficial and leads to quicker tissue regeneration. On the other hand, GNP inclusion diminishes the thrombogenicity that can lessen the complications of surgery caused by the development of blood clots.

Yoon et al. [39] selected GO nanosheets in nanocomposite scaffolds in their investigation, as better surface-level chemical property such as hydrophilicity and enhancement of the mechanical characteristics of biopolymer nanofiber were predicted from carboxylic acid and carbonyl grouping on GO nanosheet surfaces. In their study, they investigated nanofibrous nanosheets, made by the electrospinning of PLGA and GO (1, 2 wt. percent) nanosheets, morphological, surface-chemical, and thermomechanical characteristics and biocompatibility of nanofibrous nanotubes. It has been shown that nano composite PLGA/GO (2 wt. percent) has better thermomechanical characteristics than pure PLGA nanofibers and nanofibers PLGA/GO (1 wt. percent). The good biocompatibility of PLGA/GO (2 wt. percent) nanocomposite nanofibers due to increased chemical characteristics of the surface has been proven by viability tests on PC 12 cultivated nanocomposite scaffolds.

CHAPTER 3

EXPERIMENTAL PROCEDURE

The production processes of polymer nanocomposites used in this study were carried out in Ankara Yıldırım Beyazıt University Materials Process Laboratory. Characterization tests of produced polymer nanocomposites; DSC, TGA and FTIR analysis in Gebze Technical University Chemistry Department Chromatography Laboratory, AFM examination in Gebze Technical University Materials Engineering Thermal Analysis Research Laboratory, 3-Point Bending Test in cooling cabinet and Shore D Test in Bursa Technology Coordination and R&D Center, SEM examination in Gebze Technical University Materials Engineering Department Scanning Electron Microscope Laboratory was carried out.

In this study, MHI company's SMP MP3510 polymer, which shows biocompatibility is investigated in terms of thermal and mechanical properties by producing polymer nanocomposites formed by mixing graphene nano-platelets in different proportions from graphene-based materials with the aim of maintaining the biocompatibility of this polymer. The differences in thermal and mechanical properties between polymer nanocomposites formed by two different methods were also discussed by using a hybrid method including ultrasonic mixing – high speed mechanical mixing method and high speed mechanical mixing method and investigated dispersion of GNP in SMP matrix.

3.1 Materials

3.1.1 Shape Memory Polymer MP 3510

Shape memory polymer used in this study was supplied from MHI, a subsidiary of Diaplex Company. Consisting of two parts, resin (Solution A) and hardener (Solution B), this shape memory polymer has displayed thermoset properties (can be seen in Figure 3.1). The two digits after the first two letters represent the glass transition temperature specified by the manufacturer in degrees Celsius. It is known that this

shape memory polymer with proprietary compositions is polyurethane-based. This polymer, which has a light yellow appearance, has incorporation ratio of 1:1 in mass. In the data supplied by the manufacturer, while resin and hardener viscosity is 300-600 mPa.s, 200-1200 mPa.s, respectively specific gravity values are given as 1.066, 1.216. In the glassy state, strength values of the polymer is 63 MPa, bending modulus is 1550 MPa, tensile strength is 53 MPa, and the hardness value is 78 on the Shore D scale. This polymer with a glass transition temperature of 35 °C has the characteristics of pot life of 270 seconds and curing in 2 hours at 70 °C [40].



Figure 3.1 Shape Memory Polymer SMP MP3510

3.1.2 Graphene Nanoplatelets

The graphene nanoplatelets used in this study were obtained from the company Nanografi (Shown in Figure 3.2). These graphene nanoplatelets used have technical properties such as 99.9% purity, 3 nm thickness, 1.5 μm diameter, 800 m^2/g specific surface area and 1500-1980 S/m conductivity value [41].



Figure 3.2 Graphene Nanoplatelets

3.2 Sample Preparation of SMP MP 3510

In general, the steps in the MHI's guidebook to produce thermoset SMP MP3510 polymer were followed. The first step in this process was to keep A and B components separately at 70 °C for 1 hour under vacuum at a pressure not exceeding 50 torr, then mixing the A and B components in a ratio of 1:1 by mass and keeping them under vacuum for 60 seconds at a pressure not exceeding 50 torr. It is observed in this step that when this process included in the company's guide book, is applied, air bubbles in the A and B components decrease in size and increase in number with the effect of vacuum and in the vacuum process applied after mixing the A and B components in a 1:1 ratio, these air bubbles in the mixture cannot get out and it still survives in the mixture. This situation caused the sample obtained after curing to have a hollow structure. (Shown in Figure 3.3 a)). Also, when trying to extend the vacuum time to get rid of air bubbles. It was observed that although the polymer used approached the pot life time, there were still bubbles and curing problem is observed when the pot life period is exceeded (Shown in Figure 3.3 b)).



Figure 3.3 a) SMP with bubble structre b) Failed curing of SMP

SpeedMixer device with a double asymmetrical rotation mechanism shown in Figure 3.4 was used rather than keeping under vacuum to remove the air bubbles in the A and B components in this step. Thanks to this device, air bubbles in A and B components were completely eliminated and since the mixing process is faster than the vacuum method, pot life time of 270 seconds was used more effectively and no problem was observed in the polymer curing. Pot life time of 270 seconds is a limiting factor both for removing the air bubbles of the A and B components and for the vacuum process applied after mixing the A and B components.



Figure 3.4 SpeedMixer Device

As a solution to the above-mentioned problems in all samples to be produced for the tests instead of a vacuum chamber (See Figure 3.5) for the degassing process in the polymer and its hardener, an alternative method for degassing, SpeedMixer device with a double asymmetrical rotation mechanism at high-speed (3500 rpm) was used (Can be seen in Figure 3.5).



Figure 3.5 Vacuum Chamber

The process of removing air bubbles in the polymer has been realized with SpeedMixer device. Air bubble images present in the A component and B components of the polymer is shown in Figure 3.6 before and after degassing process.

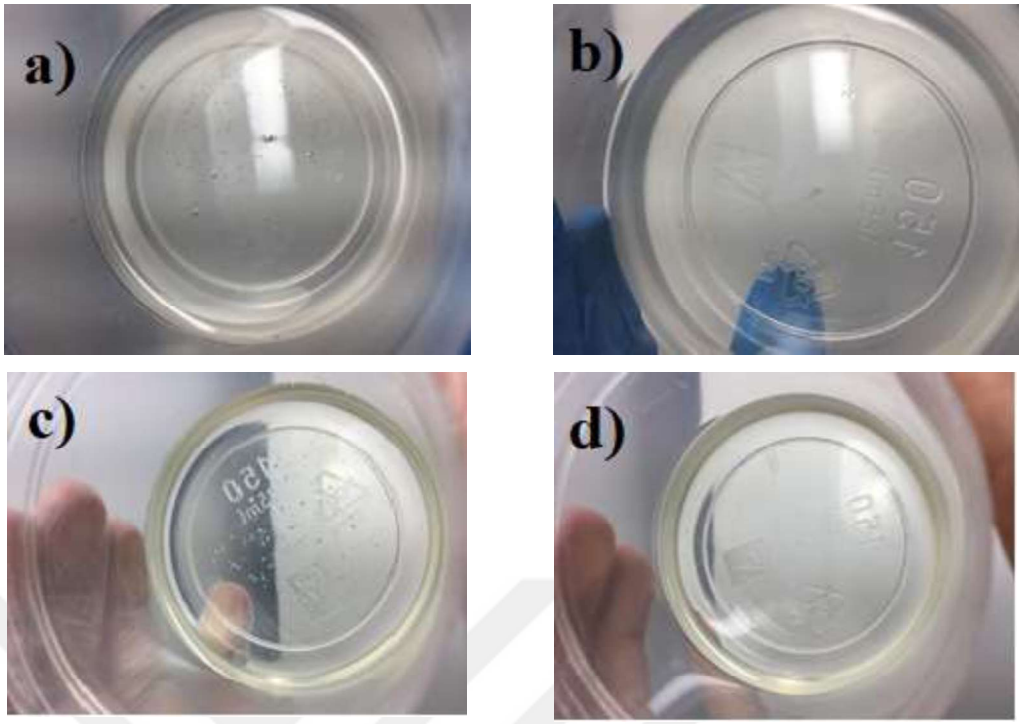


Figure 3.6 a) A component of SMP MP 3510 before degassing process b) A component of SMP MP3510 after degassing process c) B component of SMP MP3510 before degassing process d) B component of SMP MP3510 after degassing process

After removing the air bubbles in the polymer and its hardener, as in the manual homogeneous mixture obtained by weighing 1:1 by mass and mixing at 3500 rpm for 1 minute was poured into the mold prepared using teflon bars (as shown in Figure 3.7) and cured at 70 °C for 2 hours.

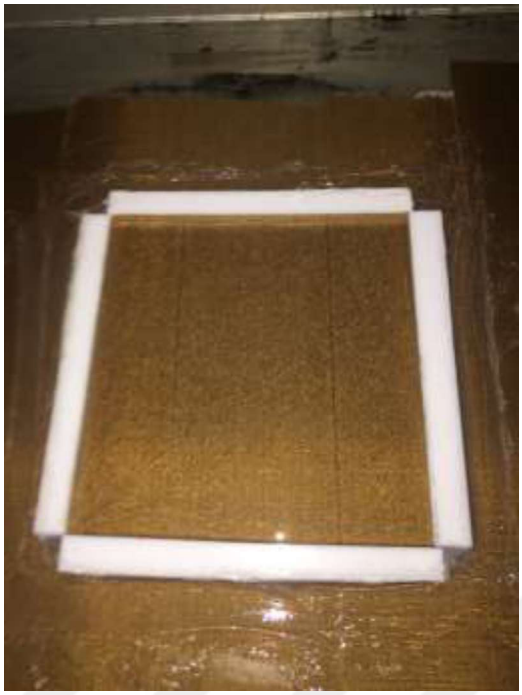


Figure 3.7 Mold Prepared with Teflon Bars In Teflon Mold Homogenous Mixing Component A and B with SpeedMixer without any Bubles

3.2.1 Graphene Nanoplatelets/SMP Nanocomposites Preparation

Polyurethane-based SMP MP3510 polymer supplied from MHI was combined with graphene nano-platelets at 0.1%, 0.3%, 0.5% by weight, and nanocomposites were formed. These nanocomposites were produced two different methods which are with a hybrid method including ultrasonic mixing – high speed mechanical mixing and and high speed mechanical mixing method.

3.2.1.1 Graphene Nanoplatelets/SMP Nanocomposites Preparation by High Speed Mechanical Mixing Method

Ready to use resin after removing the air bubbles; resin (solution A) and hardener (solution B) has been mixed for 1 minute at 3500 rpm 0.1%, 0.3%, 0.5% by weight of graphene nano-platelets in previously calculated amounts by using SpeedMixer with high speed mechanical mixing method. Then the resin and hardener containing calculated amounts of graphene nano-platelets was mixed for 1 minute at 3500 rpm by using a high speed mixer again in a 1:1 ratio by mass. Afterwards, this homogeneous

mixture was poured into the mold prepared using Teflon bars and left to cure for 2 hours in the oven at 70 °C.

3.2.1.2 Graphene Nanoplatelets/SMP Nanocomposites Preparation by Hybrid Method Including Ultrasonic Probe Mixing - High Speed Mechanical Mixing

Just as in the previous method, resin and hardener having their air bubbles removed were combined with the calculated graphese nano-platelets as to be 0.1%, 0.3% and 0.5% by weight. In this method, half of the graphene nano-platelets calculated in the first step were mixed in the resin and the other half in the hardener with a high speed mixer at 3500 rpm for 1 minute. Then, the calculated amounts of graphene nanoplatelets in the mechanically mixed resin and hardener were disaggregated with an ultrasonic probe (Ultrasonics, Ultrasonic Processor, see Figure 3.8) for 10 minutes. After this process, the resin and hardener were mixed separately with a high speed mixer at 3500 rpm for 1 minute. Then resin and hardener cured in an oven at 70 °C for 2 hours, speed mixer is mixed at 3500 rpm for 1 minute to be 1:1 by mass and then this homogeneous mixture is poured into the mold prepared with teflon bars.



Figure 3.8 Ultrasonic Probe

3.3 Characterization Methods

3.3.1 Thermal Characterization

DSC (Mettler Toledo DSC822e see Figure 3.9) analysis was used to determine the vitreous transition temperature of the produced polymer and the effect of graphene nano-platelets to T_g temperature of polymer nanocomposite in nanocomposites produced by adding calculated amounts of graphene nano-platelets. DSC measurement was carried out by increasing from -40 °C to 250 °C with a heating rate of 10 °C/min. Samples weighing 10 ± 3mg were used for measurement.



Figure 3.9 Differantial Scanning Calorimeter (DSC)

TGA (Mettler Toledo TGA/SDTA851e see Figure 3.10) analysis was applied to identify decomposition temperature of the produced polymer and polymer nanocomposites and to observe change in mass of polymer and polymer nanocomposite with increase in temperature and temperature. TGA measurement was carried out by increasing from 25 °C to 700 °C with a heating rate of 10 °C/min. Samples in the range of 5-20mg were used for measurement.



Figure 3.10 Thermogravimetric Analysis (TGA)

3.3.2 FTIR Analysis

Perkin Elmer Spectrum 100 device, shown in Figure 3.11, was used in the wavelength range of 650 to 4000 cm^{-1} for observing FTIR spectra of pure SMP and SMP nanocomposites and the chemical structure of SMP and nanocomposites and especially the changes in C=O bond regions in composites.



Figure 3.11 Fourier-Transform Infrared Spectroscopy (FTIR)

3.3.3 Microscopic Analysis

SEM images of sections of pure SMP and GNP/SMP nanocomposites were taken. The samples were crushed in solid carbon dioxide (CO_2) and coated with gold. Images were taken with the Philips XL30S scanning electron microscope, seen in Figure 3.12 below. AFM and SEM images were analyzed to assess surface morphology of pure SMP and SMP nanocomposites. Digital Instrument NanoScope IV AFM device given in Figure 3.13 was used.



Figure 3.12 Scanning Electron Microscope (SEM)

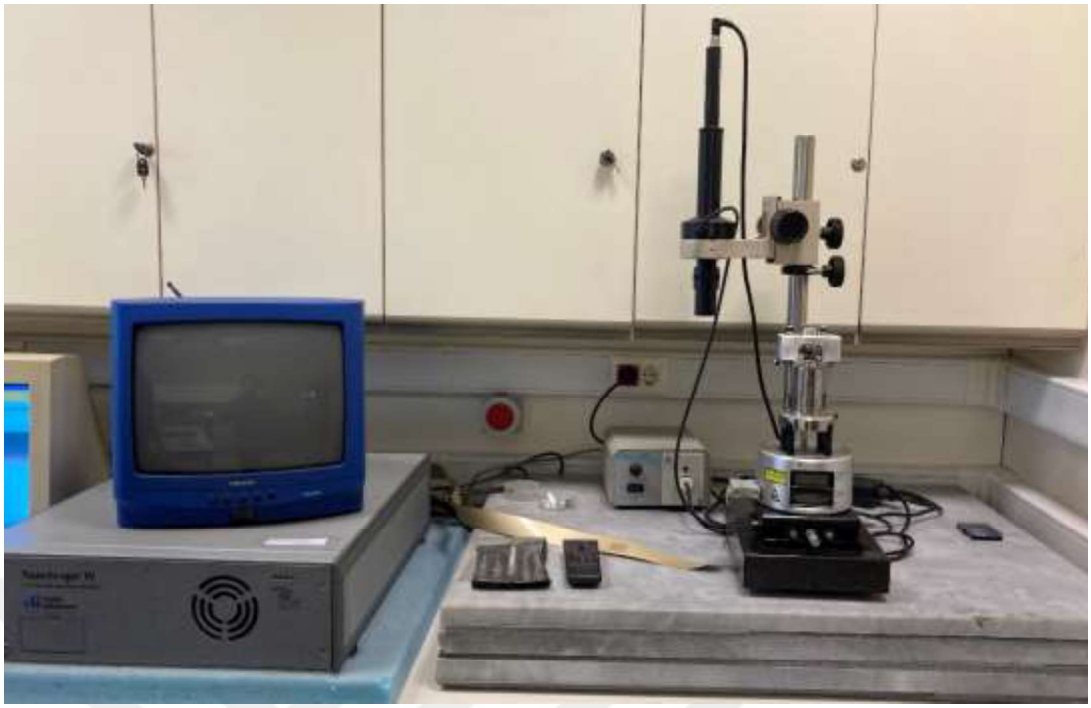


Figure 3.13 Atomic Force Microscope (AFM)

3.3.4 Mechanical Analysis

3-Point Bending Test at 0 °C was performed to determine the mechanical properties of pure SMP and SMP nanocomposites. Samples were produced in dimensions of 80mm x 10mm x 4mm for the 3-point bending test. The 3-point bending test was performed on 3 samples for each parameter. For this test, the Shimadzu AGS-X device with cooling cabinet for setting the temperature at 0 ºC seen in Figure 3.14 was used. In order to observe samples' hardness values, the samples kept at 0 °C were removed from 0 °C respectively, and the hardness was taken from 3 different points to the Shore D hardness value within 1 minute. Shore D test was performed with the Hildebrang digital durometer device seen in Figure 3.15.

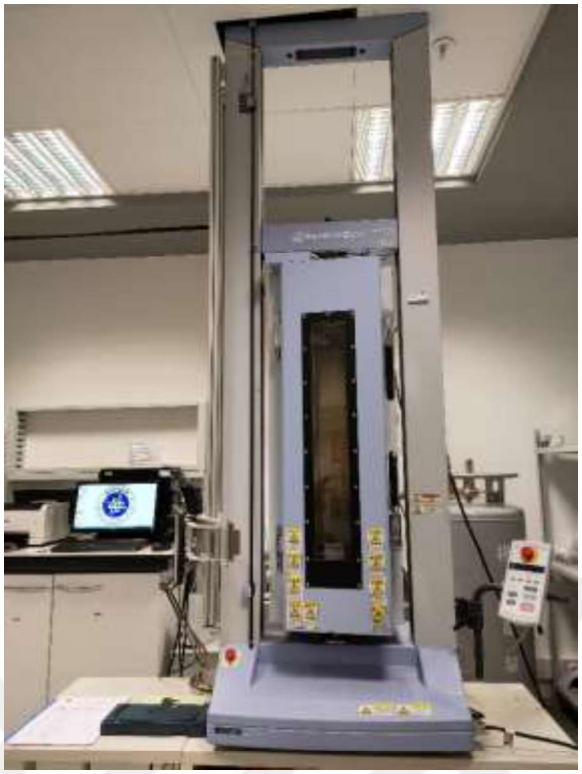


Figure 3.14 3-Point Bending Test Machine with Cooling Cabinet



Figure 3.15 Digital Durometer

CHAPTER 4

RESULTS AND DISCUSSION

4.1 DSC Analysis

T_g reflects both the temperature of the glass transition and the temperature of the form recovery at which the SME is triggered for the SMP. This SMP is in a glass state at a temperature below T_g and is stiff and difficult to distort (with high modulus). The soft section in the SMP is in this situation frozen. It can mildly vibrate, but there is no major segmental movement. It is rather difficult to distort the bulk material in this condition. When the SMP is heated progressively, it enters a transitional glass area. The transition does not start or end immediately but takes place across a temperature range gradually. Soft segments tread in this region and the thermal capacity of the SMP rises by a certain amount. Differential scanning calorimeter (DSC) testing may be employed as one of the standard techniques to identify increases in heat capacity step by step for the determination of the T_g as defined as the average point in the glass transition ramp [14].

In this study, DSC analysis was applied as thermal analysis to identify glass transition temperature of the samples. The analysis was carried out by heating from -40 °C to 250 °C in N atmosphere. Glass transition temperature of SMP MP3510 polymer is given as 35 °C in MHI company datasheet. SMP MP3510 polymer used in this study and 0.1%, 0.3%, 0.5% by weight graphene nano-platelets to these polymer glass transition temperatures of polymer nanocomposites formed by adding two different methods: high speed mechanical mixing method and a hybrid method including ultrasonic mixing - high speed mechanical mixing compared to the value given by the company and the effect of the added graphene nano-platelets on the glass transition temperature was investigated. DSC analysis results of the pure SMP produced and the nanocomposites produced using a high speed mechanical mixer is shown in Figure 4.1.

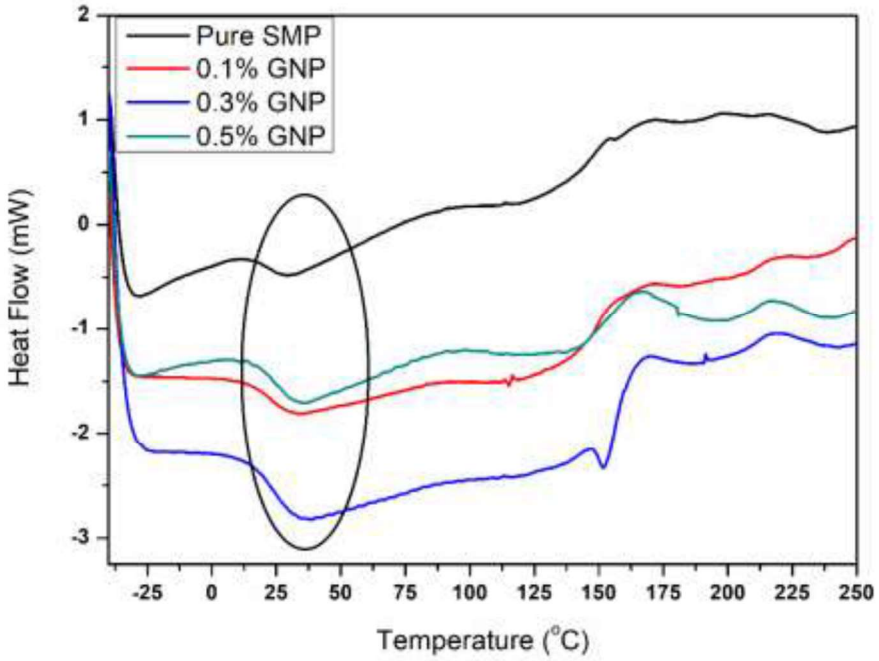


Figure 4.1 DSC Results of SMP and GNP/SMP Nanocomposites Produced by High Speed Mechanical Mixing Method

Polymer produced by adding pure SMP and graphene nano-platelets as seen in Figure 4.1. polymer nanocomposites produced by adding pure SMP and graphene nanoplatelets caused minor changes in the glass transition temperature zone. Small amounts of graphene nano-platelets disaggregated in the SMP caused a small increase in the T_g temperatures of the polymer nanocomposites as seen in Table 4.1 in the glass transition temperature.

Table 4.1 T_g values of SMP and GNP/SMP Nanocomposites Produced by High Speed Mechanical Mixing Method

Sample	T_g (°C)
Pure SMP	33
0.1% GNP/SMP Nanocomposite	33
0.3% GNP/SMP Nanocomposite	35
0.5% GNP/SMP Nanocomposite	35

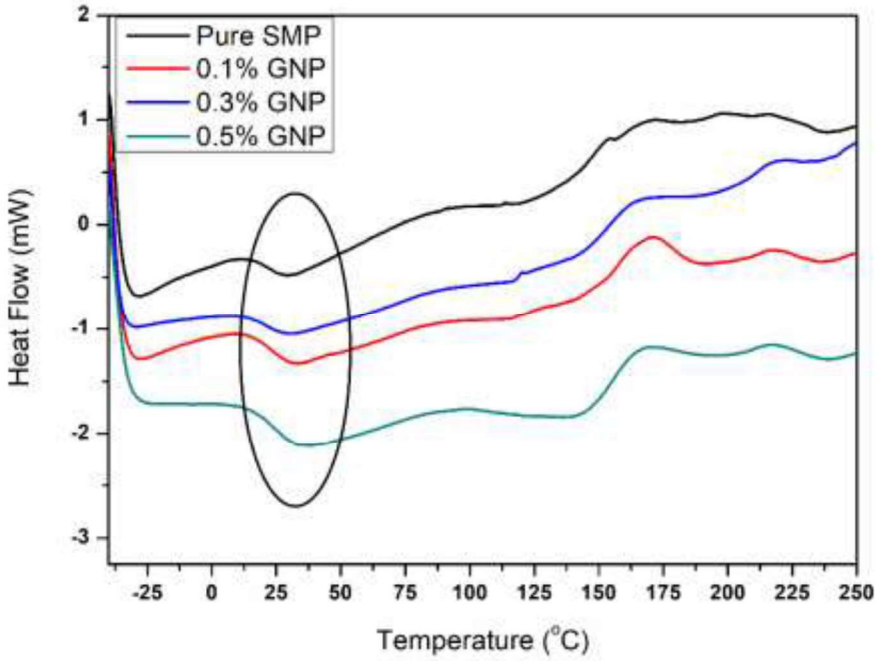


Figure 4.2 DSC Results of SMP and SMP/GNP Nanocomposites Produced by including Ultrasonic Mixing – High Speed Mechanical Mixing Hybrid Method

In Figure 4.2, when DSC analysis results of nanocomposites produced using a hybrid method including ultrasonic mixing - high speed mechanical mixer are examined no significant changes were observed in the glass transition temperature zone. Graphene nano-platelets disaggregated in a small amount of polymer did not cause a significant change in T_g temperature, but were almost identical.

Table 4.2 T_g values of SMP and GNP/SMP Nanocomposites Produced by including Ultrasonic Mixing – High Speed Mechanical Mixing Hybrid Method

Sample	T_g (°C)
Pure SMP	33
0.1% GNP/SMP Nanocomposite	33
0.3% GNP/SMP Nanocomposite	33
0.5% GNP/SMP Nanocomposite	34

When the glass transition temperatures among the thermal properties of nano-composites produced with either method investigated, GNP added at the glass transition temperature of pure SMP had no effect. An increase of 2 °C in T_g temperature was observed for the nanocomposite obtained from pure SMP with 0.5% GNP additive by high speed mechanical mixing method. T_g temperature increased by only 1 °C with the addition of 0.5% GNP from pure SMP for the hybrid method including ultrasonic mixing - high speed mechanical mixing. No increase in T_g temperature was observed for the intermediate values of 0.1% and 0.3%. It is shown that DSC curves glass transition temperatures for GNP/SMP nanocomposites are between 33-35 °C for high speed mechanical mixing method, 33-34 °C for hybrid method including ultrasonic mixing - high speed mechanical mixing. In this polyurethane-based SMP, disaggregation of small amounts of GNP in volume does not have a significant effect to change the T_g of the obtained nanocomposites pure SMP.

Bear et al. [42] investigated the thermal properties and shape memory behavior of thermoset and thermoplastic polymer series with T_g temperatures ranging from 35 to 75 °C produced by MHI in their studies. They identified T_g temperature of the SMP MP3510 polymer of MHI, which we also used in our study, by DSC analysis. They determined the T_g temperature as 31 °C. In our study, the Tg temperature of the SMP MP3510 polymer was fixed by the same method DSC analysis and was measured as 33 °C. Baer et al., in their study, cured the polymer's curing temperature at 80 °C, different from what is written in the company's datasheet and realized curing period suggested as 2 hours as 4 hours. The difference in T_g, however small, could be due to this change in the manufacturing process. Although small amounts of additives made to the polymer to produce nanocomposites provide homogeneous disaggregation and significant increases in thermal stability and mechanical properties it was observed that most of the time it did not have a significant effect on the T_g temperature. Thuc et al. [43] showed that the small additive had no effect on T_g temperatures in the nanocomposites they designed in their study.

The glass transition temperature of the SMP used in this study being 35 °C, having a value close to or just below the human body temperature, also thanks to its biocompatibility properties and being non-toxic, it has a very important advantage as it is a material that can be used in in-body biomedical applications. As the aim of this study, GNP was used among the graphene-based materials that do not impair the biocompatibility of the material with a significant advantage. As can be seen from the DSC results, it has been observed that the T_g temperatures of the nanocomposites produced with different ratios of GNP additives made to pure SMP have almost the same T_g value. Thanks to these results, when the nanocomposites produced are combined with GNP, one of the graphene-based materials showing biocompatibility has ensured that it can still be used in in-body applications.

4.2 TGA / DTA Analysis

To determine thermal stability of polyurethanes SMP, a thermogravimetric analysis (TGA) was carried out. The analysis was carried out by heating from 25 °C to 700 °C at a rate of 10 °C/min. Graphene nano-platelets/SMP nanocomposites formed by adding 0.1%, 0.3% and 0.5% by weight graphene nano-platelets using the high speed mechanical mixing method and nanocomposites formed by adding 0.1%, 0.3% and 0.5% by weight graphene nano-platelets using a hiybrit method including ultrasonic mixing - high speed mechanical mixing metod, their weight loss percentages up to 700 ^oC and the effect of adding the rate of addition of graphene nano-platelets to their degradation were investigated. When the TGA / DTA analysis result of the initially produced SMP is examined, (See Figure 4.3) endothermic peak is at 337 °C. It is seen that the temperature at which pure SMP starts to lose mass is around 260 °C. As seen in the DTA/TGA graph after this temperature, the material decomposes and loses 92% of its mass. As a result of the test, which started with 22.02 mg, the amount of substance remaining after this temperature is exceeded is 1.67 mg.

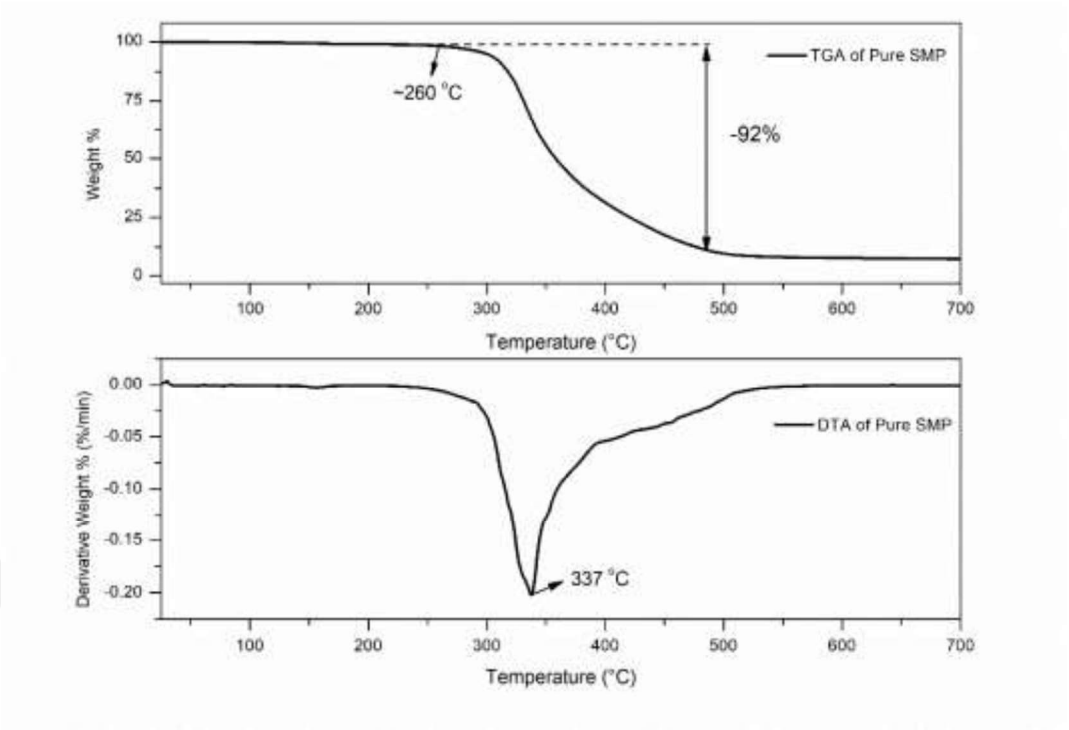


Figure 4.3 TGA/DTA Result of Polyurethane SMP MP3510

When we consider the literature, Yang Bin studied [44] the effect of moisture on SMP MP3510 polymer obtained from MHI company and electrically conductive composites in his master's thesis. In his study, the TGA/DTA result of SMP MP3510 polymer, which is the resin version of the polymer used in this study, and SMP MP3520 polymer, which is the pellet version is shown in Figure 4.4. According to this result, the temperature at which SMP started to decompose was determined as 260 °C and endothermic peak was determined as approximately 350 °C. These results show almost one-to-one agreement with the results of the type SMP we used.

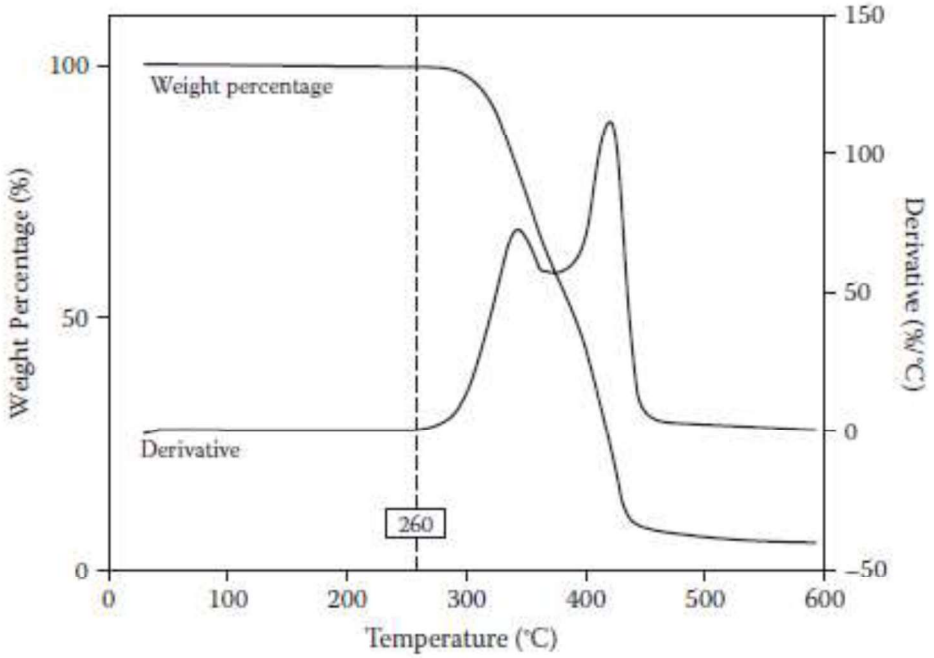


Figure 4.4 TGA/DTA Result of Polyurethane SMP MM3520 [45]

DTA/TGA results of GNP/SMP nanocomposites produced using high speed mechanical mixing method were examined. The effect of the increase in the amount of graphene nano-platelets in these nanocomposites containing 0.1%, 0.3% and 0.5% graphene nanoplatelets on the degradation temperature of the nanocomposites is shown in Figure 4.5.

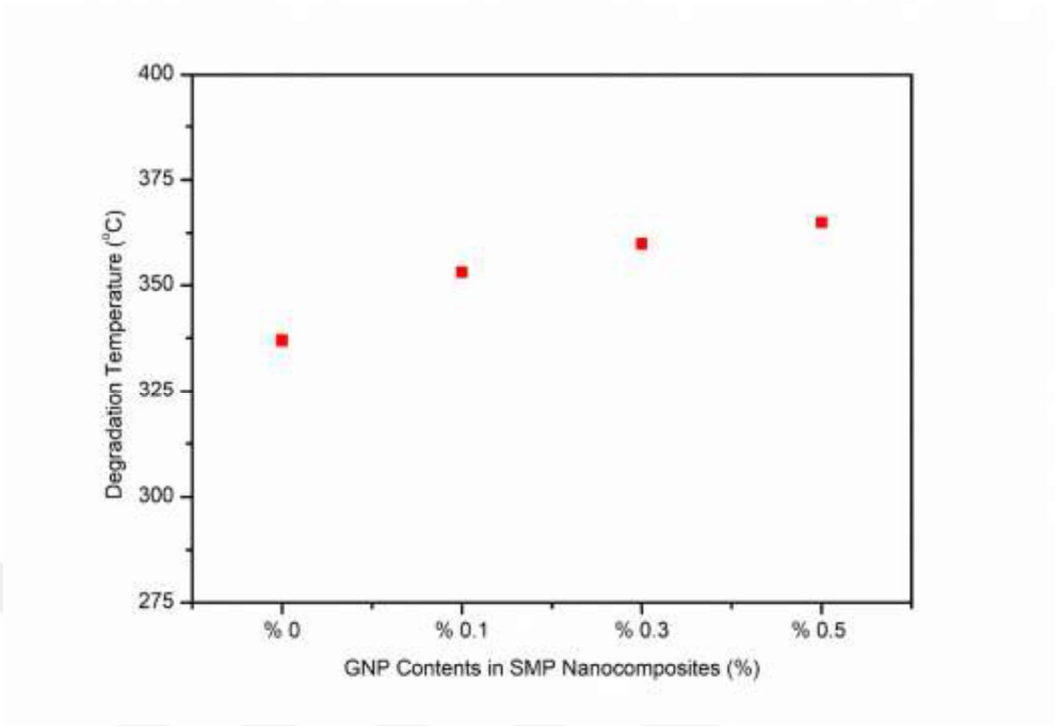


Figure 4.5 Comparison of Degradation Temperatures of GNP/SMP Nanocomposites Produced by High Speed Mechanical Mixing Method

As seen in Figure 4.5, GNP/SMP nanocomposite's thermal stability increased by 4.5% from 337 °C to the decomposition temperature of the GNP/SMP nanocomposite, with the contribution of 0.1% by weight of GNP. When this additive rises to 0.3 % GNP, decomposition temperature becomes 354 °C. Between 0.1% and 0.3%, an increase of only 1 °C was seen. For 0.5% GNP additive, decomposition temperature of the nanocomposite increased to 365 °C, and its thermal stability showed an increase of 7.7% compared to pure SMP.

DTA/TGA analysis results of GNP/SMP nanocomposites produced utilizing hybrid method including ultrasonic mixing - high speed mechanical mixing were examined. The effect of the increase in the amount of GNP on the degradation temperatures of nanocomposites is shown in Figure 4.6.

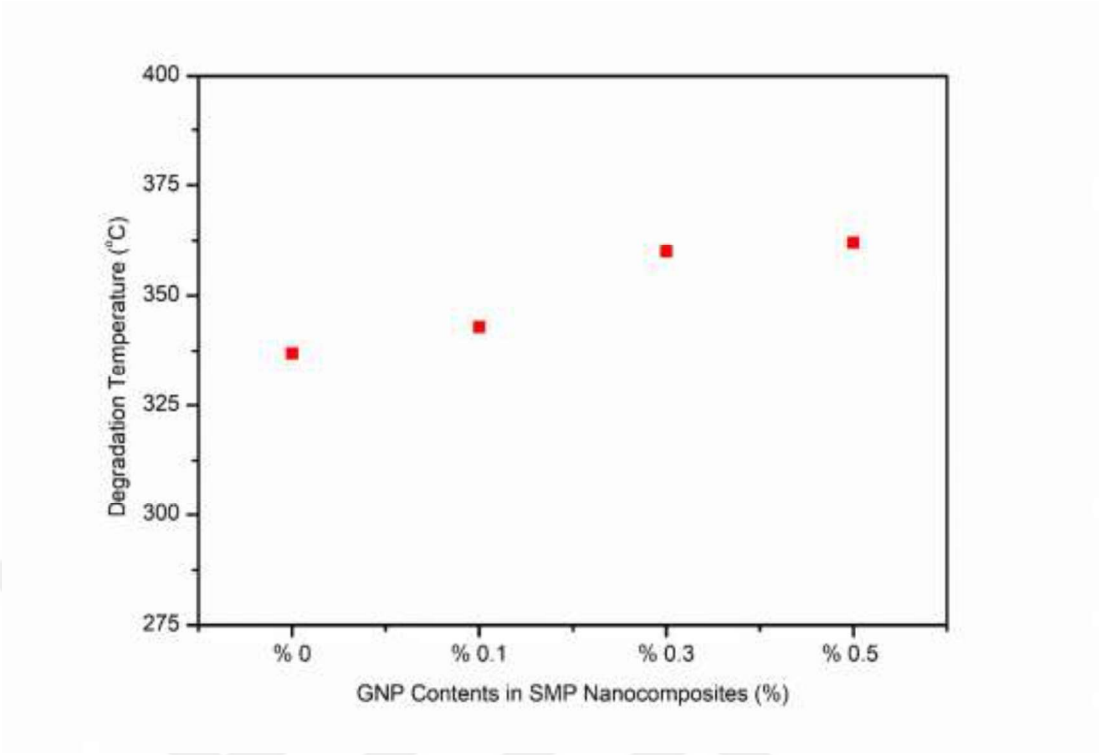


Figure 4.6 Comparison of Degradation Temperatures of GNP/SMP Nanocomposites Produced by Including Ultrasonic Mixing – High Speed Mechanical Mixing Hybrid Method

As can be seen in Figure 4.6; 0.1% GNP addition to the pure SMP increased polymer degradation temperature to 343 °C. Addition of 0.1% to SMP increased the thermal stability of the polymer by 1.7%. 0.3% GNP addition to SMP increased the degradation temperature of the GNP/SMP nanocomposite to 360 °C. With this ratio, thermal stability of the polymer nanocomposite showed an increase of 6.4%. When the GNP additive increased to 0.5% by weight, it increased to 362 °C at the decomposition temperature. A 7% increase in thermal stability was observed over pure SMP, but only a 2 °C increase over 0.3% GNP additive.

Chieng et al. [46] investigated the effect on the tensile strength and thermal properties of the polymer nanocomposite they obtained by adding graphene nano-platelets to the polylactic acid/polyethylene glycol polymer. Degradation temperature of the pure polymer as a result of TGA/DTA analysis of the nanocomposite obtained by adding 0.5% GNP with pure polymer in their thermal studies was increased from 291 ºC to 344 ºC and increased the thermal stability of the obtained nanocomposite by 15%. Al-Saleh et al. [47] investigated the mechanical and thermal effects of adding GNP to the

polypropylene polymer in their study. They investigated the effect on the degradation temperature by adding up to 5% GNP to the pure polypropylene polymer. They increased the degradation temperature from 317 ºC to 322 ºC by adding 1% GNP to the pure polymer. It increased the stability of the produced nanocomposite polymer by 1.5%. When the GNP also was increased to 5%, an 8% increase in thermal stability was observed. When the results and literature are examined, it is seen that GNP added to the polymer improves the thermal stability of the polymer. This is because GNPs act as barriers and increase the thermal resistance of the polymer material, preventing the material from oxygen. High speed mechanical mixing method and the hybrid method including ultrasonic mixing - high speed mechanical mixing, which we used as the method of disaggregating GNP into the nanocomposites in the study, ensured an increase of 7.7% and 7%, respectively for elevating thermal stability of the nanocomposite.

4.3 FTIR Analysis

The chemical structure of pure polyurethane SMP and nanocomposites as shown in Figure 4.7 for high speed mechanical mixing method and Figure 4.8 for hybrid method including ultrasonic mixing - high speed mechanical mixing is examined with FTIR. The characteristic peaks for pure SMP were also observed for nanocomposites obtained by adding GNP to the polymer by both methods. Addition of GNP to polyurethane-based SMP did not display any change in the expected C=O bond absorption values, especially between 1650 and 1718 cm^{-1} [48]. It confirms that the added GNP does not affect the chemical structure of the polyurethane-based polymer and that there is no reaction between functional groups. Dehaghani et al. [49] investigated the nanocomposites and polyurethane, which they formed by adding graphene to the polyurethane they synthesized, with FTIR and added graphene did not react with the polyurethane and they did not recognize a change in its chemical structure.

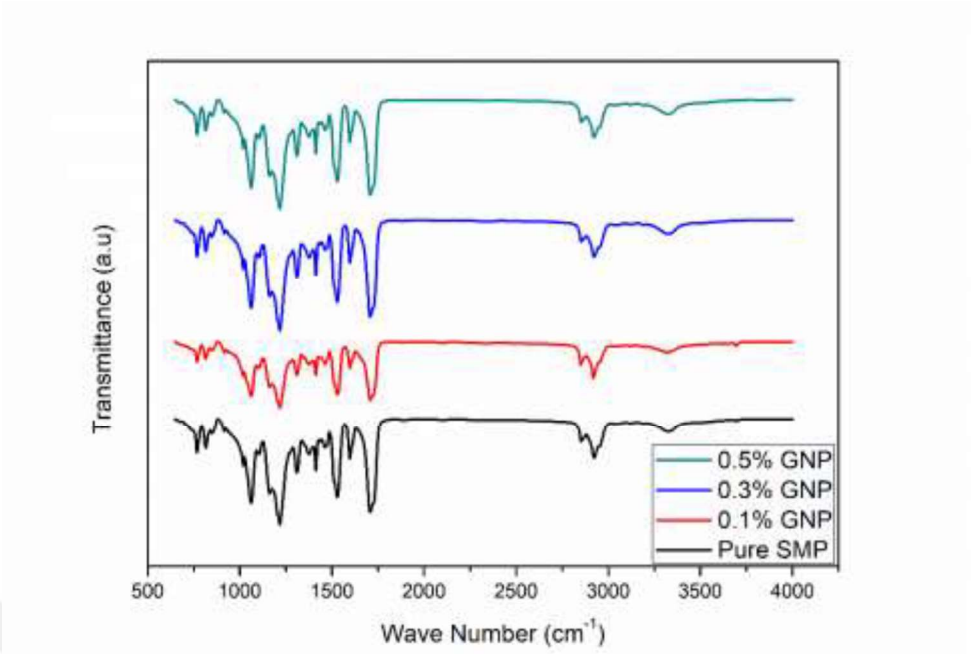


Figure 4.7 FTIR Result of SMP and Nanocomposites Produced with High Speed Mixing Method

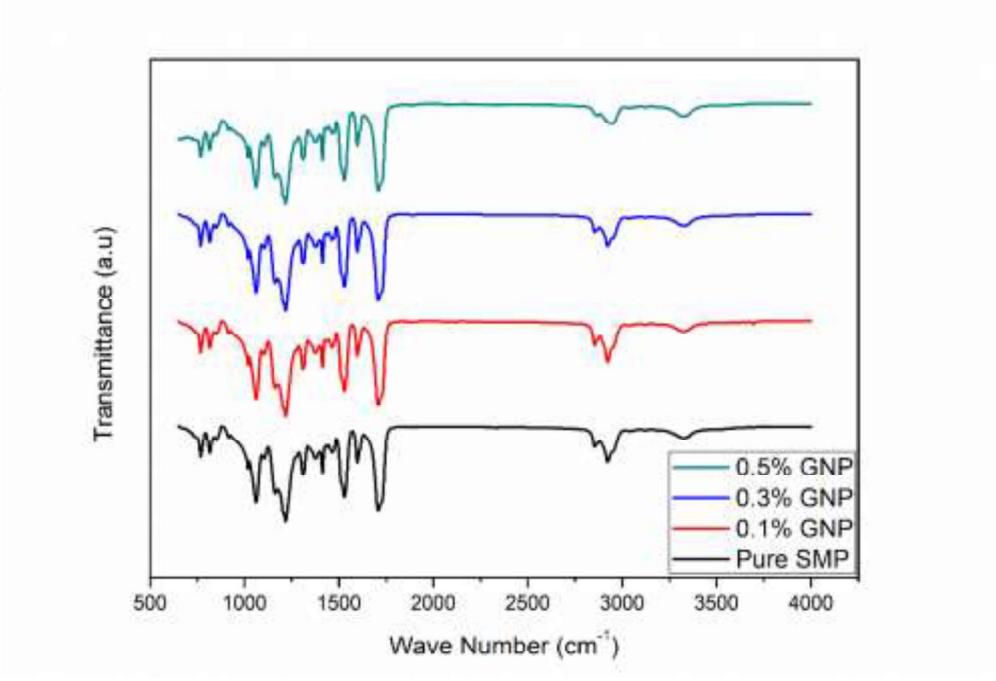


Figure 4.8 FTIR Result of SMP and Nanocomposites Produced with Including Ultrasonic Mixing – High Speed Mechanical Mixing Hybrid Method

4.4 Mechanical Analysis

3-point bending test was realized to determine the mechanical properties of the produced SMP and GNP/SMP nanocomposite samples and to examine the effect of the amount of GNP added to the pure SMP on the mechanical properties. With this test, bending modulus and bending strength values of the samples produced by both methods were gained. Flexural strength and flexural modulus values of the nanocomposites produced with a hybrid method containing ultrasonic mixing – high speed mechanical mixing of GNP/SMP nanocomposites produced with different GNP additive rate are given in Figure 4.9 and Figure 4.10.

In a hybrid method involving ultrasonic mixing - high speed mechanical mixing, a 18.4% increase was observed by elevating nanocomposite's flexural strength value to 38 MPa which was obtained with 0.1% GNP additive to pure SMP which its flexural strength value obtained as 31 MPa. When this addition increased to 0.3%, the flexural strength increased to 48 MPa. Compared to the pure polymer, an increase of 35.4% was achieved, while an increase of 21% was observed compared to the 0.1% GNP additive. Flexural strength value increased to 54 MPa for 0.5% GNP added nanocomposite and a 42.5% increase in flexural strength compared to pure SMP exhibited an 11.1% increase compared to 0.3% SMP. In hybrid method involving ultrasonic mixing – high speed mechanical mixing, GNP additive to the pure SMP increased in direct proportion to the amount of additive to the mechanical properties of the produced GNP/SMP nanocomposites.

In nanocomposites obtained via high speed mechanical mixing method, 0.1% GNP addition increased its flexural strength value from 31 MPa to 51 MPa. GNP addition of 0.1% by weight showed a 39.2% increase in flexural strength. This increase almost corresponds to the flexural strength value obtained by adding 0.5% GNP in the nanocomposite obtained using the other method. In this significant increase it was observed that addition of 0.3% and 0.5% GNP was 54 MPa for 0.3% and 51 MPa for 0.5%.

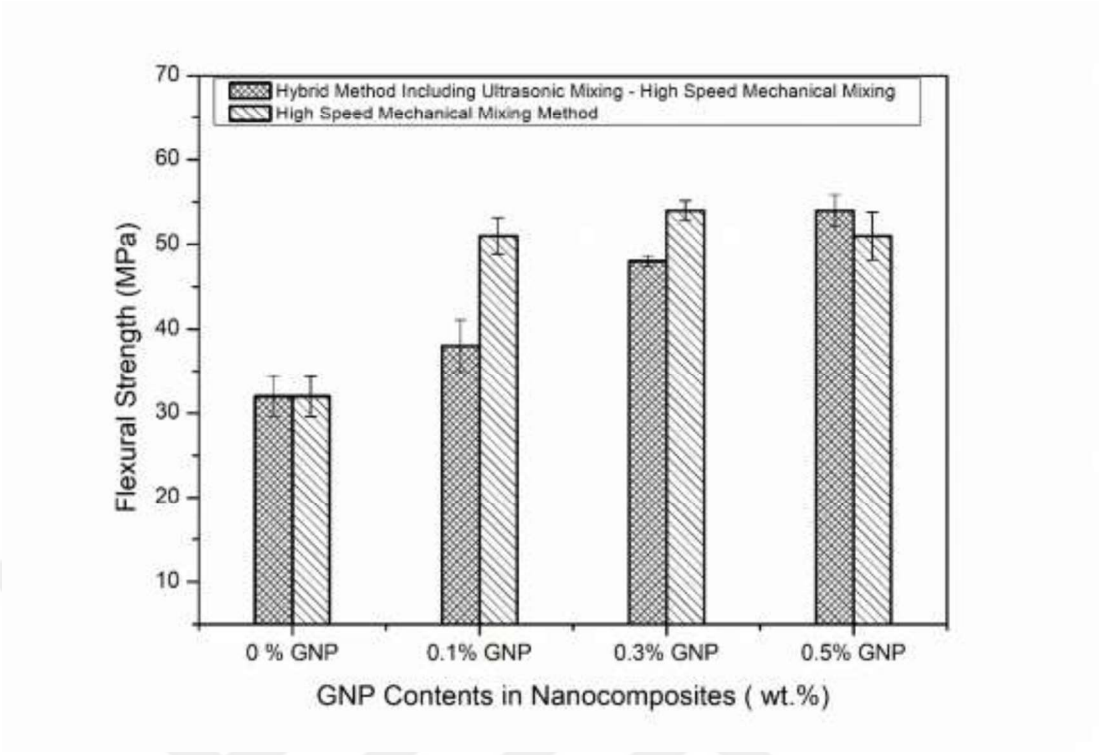


Figure 4.9 Flexural Strength Results of Nanocomposites Produced by both Methods

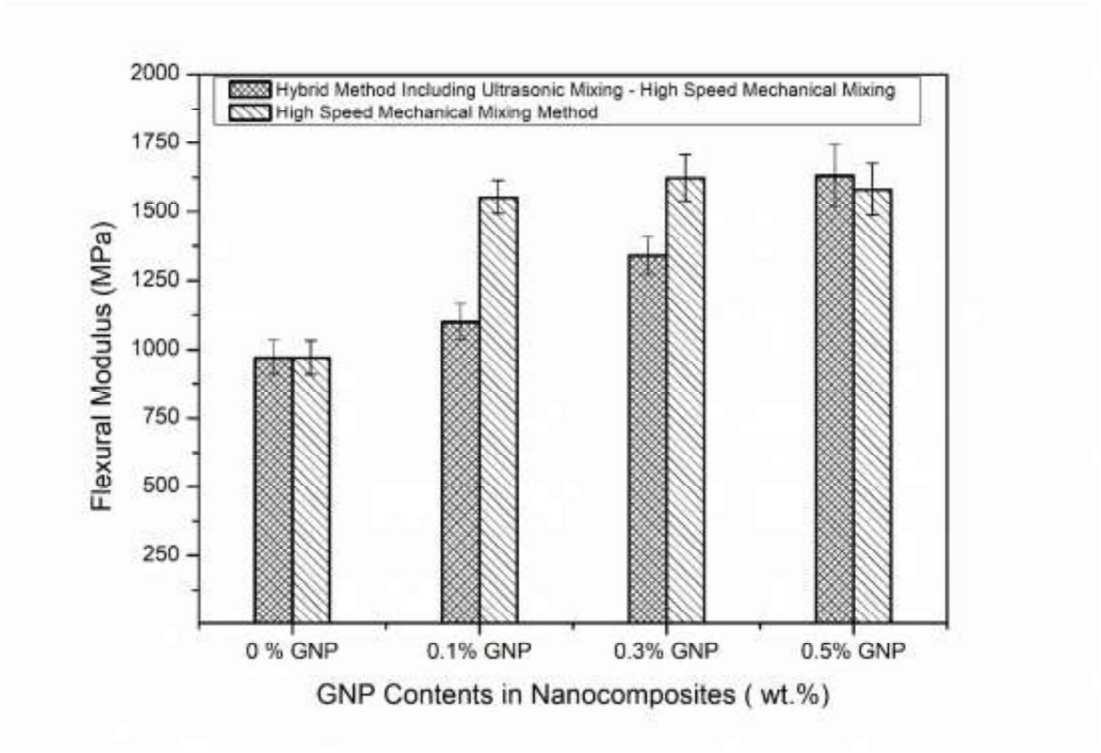


Figure 4.10 Flexural Modulus Results of Produced Nanocomposites by both Methods

It is aimed in this study to examine the effect of GNPs on their thermal properties by providing homogeneous distribution in the polymer and also to ensure increase with its mechanical properties. When these two methods are compared, the high speed mechanical mixing method and the hybrid method including ultrasonic mixing – high speed mechanical mixing exhibited increase with the mechanical property of the pure polymer however in the hybrid method involving ultrasonic mixing – high speed mechanical mixing with GNP effect, the increase in flexural strength has been in the direction of continuous increase. For high speed mechanical mixing, this is achieved with only 0.1% GNP additive a slight decrease in the 0.5% GNP contribution was observed. Result obtained with hybrid method involving ultrasonic mixing – high speed mechanical mixing shows that GNPs are more homogeneously disaggregated in the polymer. For the high speed mechanical mixing method, GNPs did not increase with the addition of GNP due to aggregation, but even a decrease was observed for the 0.5% GNP contribution. Increase of flexural strength with GNP additive in hybrid method was due to a good interface interaction between GNP and epoxy type SMP [50]. In addition, when the surface area of nano-sized materials increases, the materials tend to aggregate due to the surface loads it becomes a factor prohibiting its homogenous distribution. With ultrasonic mixing, solid fragmentation in GNPs, both by removing the GNPs from each other and preventing aggregation, and by decreasing the particle size with solid aggregation, increasing the surface that will be in contact between the GNPs and the polymer made an affirmative effect with the mechanical properties [51].

When the flexural modulus values in Figure 4.10 are examined flexural strength values and increasing trends were found to be the same. In the method involving ultrasonic mixing – high speed mechanical mixing flexural modulus of the polymer was increased from 972 MPa for pure SMP to 1100 MPa with 1% GNP additive and exhibited an increase by 11.6%. 0.3% GNP contribution increased the flexural modulus value to 1340 MPa and the 0.5% GNP contribution to 1631 MPa. A 40.4 % increase was exhibited with 0.5% GNP addition when compared to pure SMP. When we considered high speed mechanical mixing method flexural modulus value was increase to 1554 MPa with 0.1% GNP additive and to 1623 MPa with 0.3% GNP additive and 0.5% GNP addition was dropped to 1581 MPa with a decrease of 2.5%.

The reason for this increase in flexural modulus is that GNPs restrict the mobility in polymer chains and cause them to become more brittle. In Bao et al. [52], 0.8% by weight graphene nano-sheets and 0.8% by weight graphite oxide (GO) strength values increased by 46% for graphene nano-sheets and 58% for graphite oxide, respectively, 35% increase for nano-sheet n modulus value and 40% increase for graphite oxide was observed. Increase in these studies shows that graphene aggregation in the polymer with the right method has a positive effect on the mechanical properties.

Hardness values of SMP and produced nanocomposites within the scope of determining mechanical properties were taken in Shore D scale. Hardness values of nano-composites produced with both methods are shown in Figure 4.11.

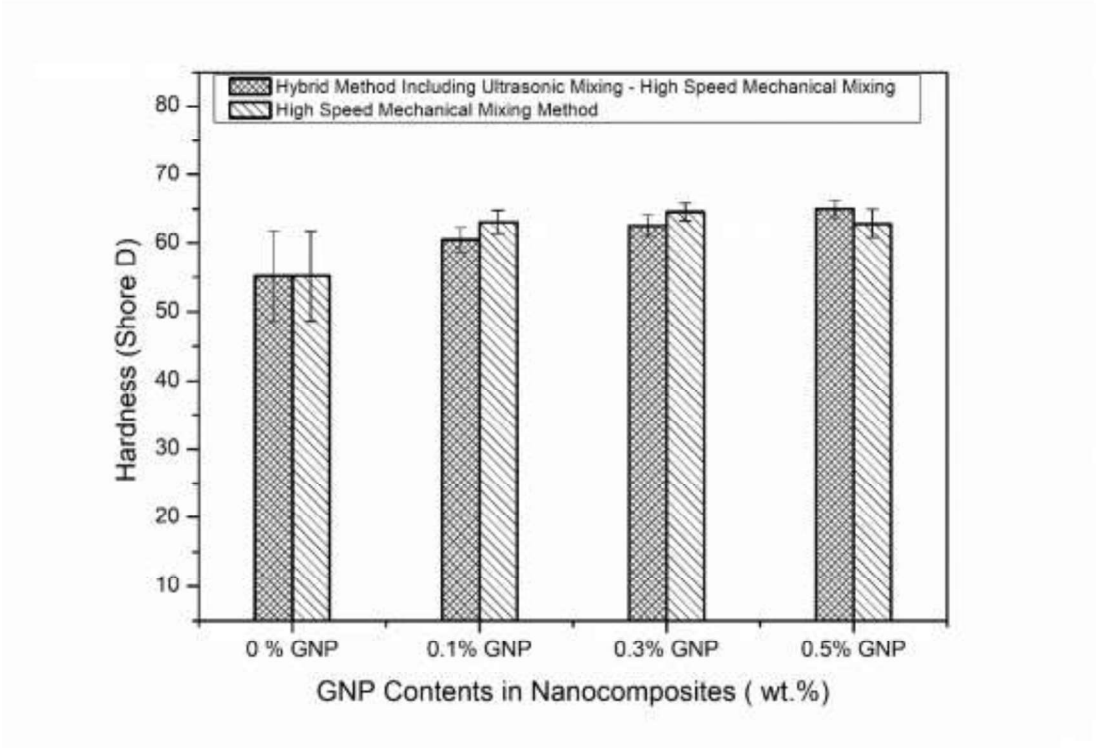


Figure 4.11 Hardness Results of Produced Nanocomposites by both Methods

In the hardness value for pure SMP in hybrid method involving ultrasonic mixing - high speed mechanical mixing the hardness value from 55.2 increased to 60.5 with 0.1% GNP addition to 62.6 with 0.3% GNP addition and to 65 with 0.5% GNP addition. Hardness values for the high speed mechanical mixing method are 63.1 for 0.1% GNP additive, 64.6 for 0.3% GNP additive and 62.9 for 0.5% GNP additive.

Hardness values obtained showed parallel trends with the strength values. Hardness values in samples produced by hybrid method including ultrasonic mixing – high speed mechanical mixing was observed to be aggregated in a more controlled trend in SMPs of GMP's with a stable increase.

4.5 Microscopic Analysis

In order to see the distributions of GNPs in the GNP/SMP nanocomposites produced in this study, the samples produced were crushed after being waited in solid CO_2. Scanning electron microscope was used to examine the GNPs dispersed through the polymer on the fractured surfaces. Nanocomposites produced with two different methods by SEM were examined. In general, a homogeneous structure is observed on the fracture surfaces in the hybrid method involving ultrasonic mixing – high speed mechanical mixing (See Figure 4.12) and the high speed mechanical mixing method (See Figure 4.13). When the fracture surfaces were examined, homogeneously dispersed GNPs changed the fracture directions of SMP nanocomposites compared to pure SMP and formed a rougher image. By looking at the images, we can interpret the increase in roughness as an increase in resistance to fracture because the sample showing the highest strength values in the hybrid method, the nanocomposite with 0.5% GNP content has a rougher fracture surface. It can be seen that the other method, the fracture surface has an intensely rough appearance from the sample with 0.1% GNP content and 0.3% GNP content. Compared with the mechanical data obtained, we get the highest mechanical value for the nanocomposite containing 0.5% GNP for the hybrid method, and for the sample with 0.3% GNP content for the high speed mechanical mixing method. It matches well with the mechanical data and SEM images about the distributions of the GNPs.

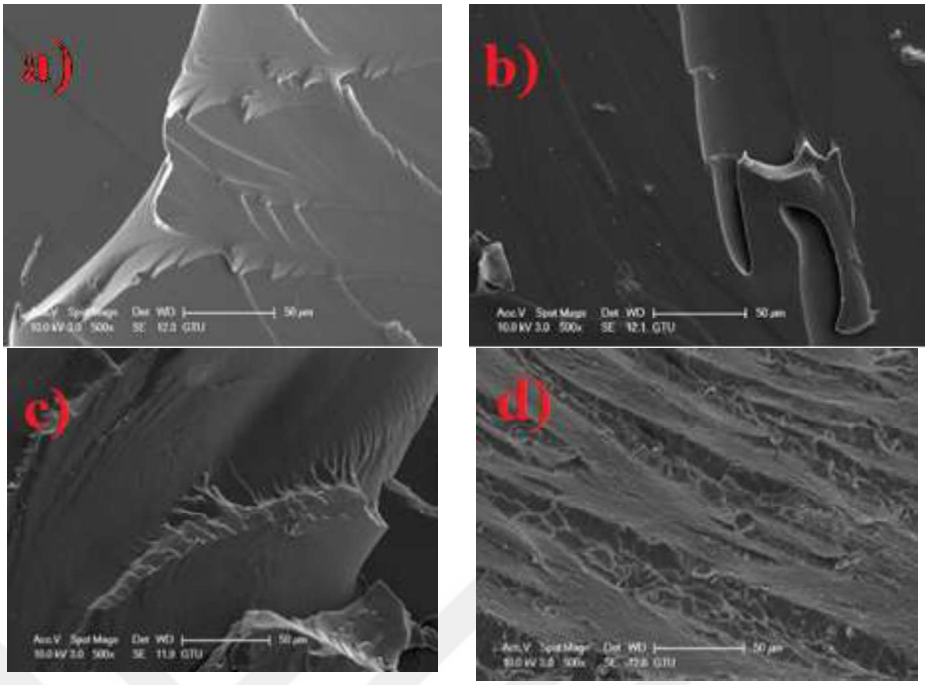


Figure 4.12 SEM images of (a) Pure SMP, (b) 0.1% GNP, (c) 0.3% GNP (d) 0.5% GNP produced with hybrid method involving ultrasonic mixing – high speed mechanical mixing

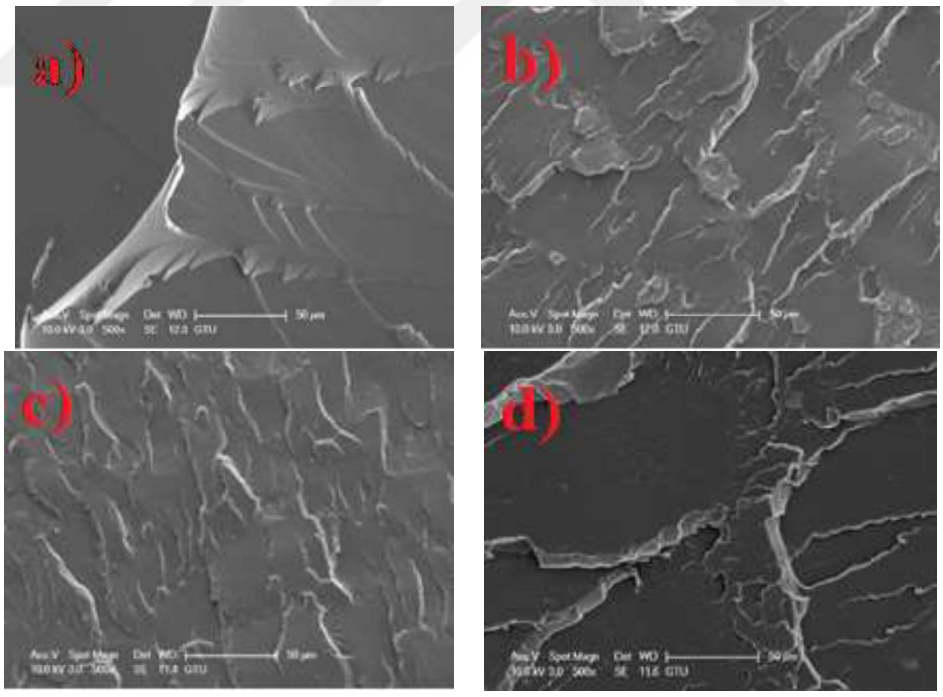


Figure 4.13 SEM images of (a) Pure SMP, (b) 0.1% GNP, (c) 0.3% GNP (d) 0.5% GNP produced with high speed mechanical mixing method

Dehaghani et al. [49] in their study, the graphene distributions in the polyurethane nanocomposites they produced were examined with SEM images taken from the fracture surfaces. They obtained similar images (See Figure 4.14) with the images we obtained in our study and the roughness on the fracture surface progressed in proportion to the mechanical data.

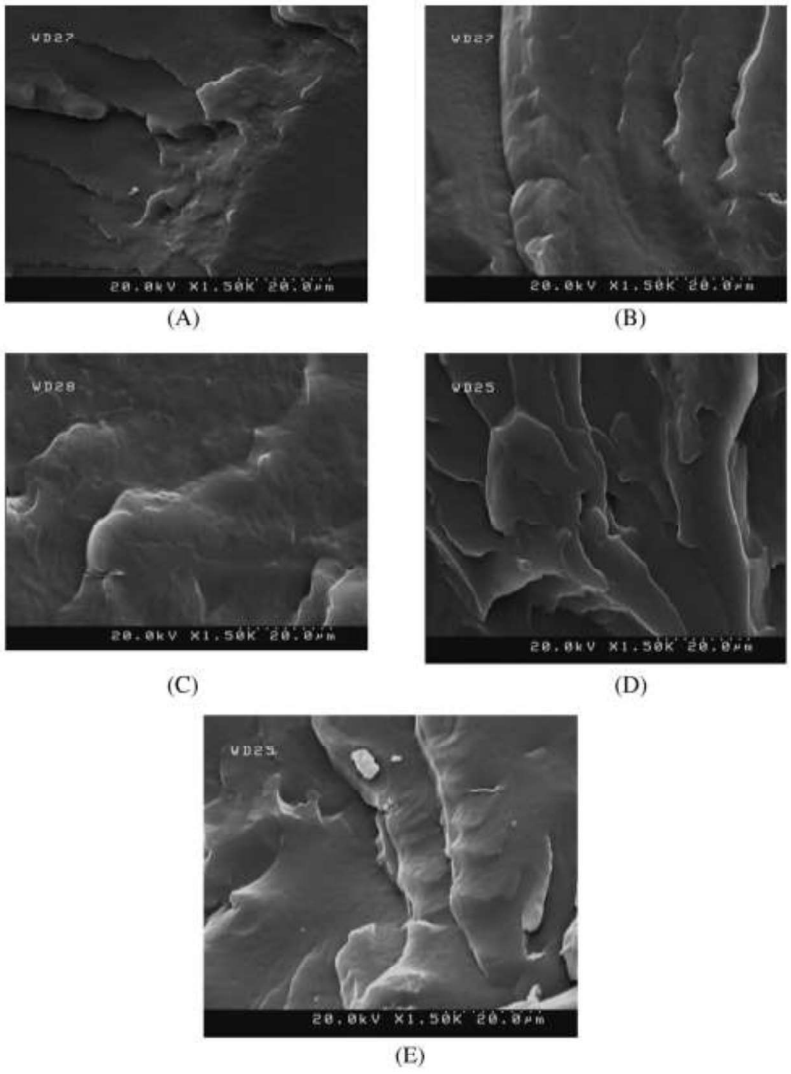


Figure 4.14 SEM images of nanocomposites taken from fractured surface (A) PU, (B) PU 0.1%, (C) PU 0.25%, (D) PU 0.5%, (E) PU 1% include graphene [49]

Then, GNPs added without any treatment on the surfaces of the polymer were used to observe whether the produced GNP/SMP nanocomposites cause a change in the surface morphology samples' surfaces were examined in contact mode with atomic force microscopy. In the images obtained, it was seen that the GNPs added in both methods did not affect the surface morphology because the GNPs were coated with SMP, they could not be detected on the surface of the SMP . In addition, SEM images were taken from the surface from which the AFM images were taken, no GNP effect was observed on the surface morphology in the AFM images and SEM images (See Figures 4.15 and 4.16).

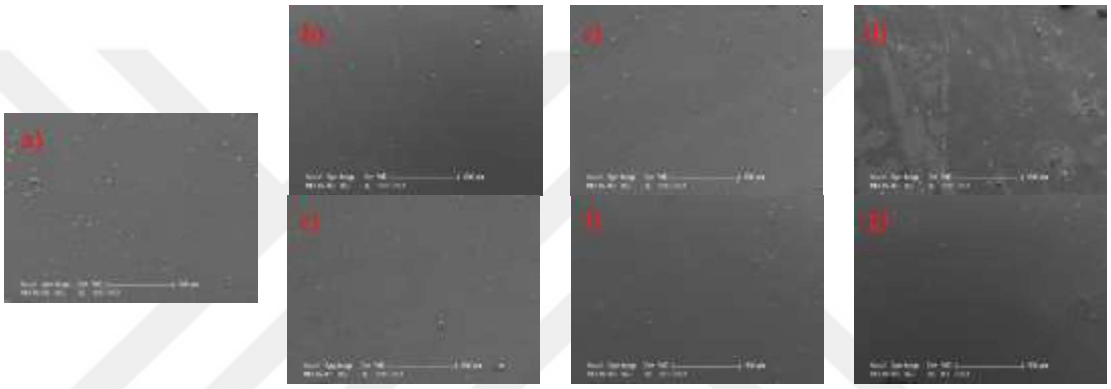


Figure 4.15 Surface SEM images of nanocomposites a) Pure SMP, b) 0.1% GNP, c) 0.3% GNP, d) 0.5% GNP produced with hybrid method involving ultrasonic mixing – high speed mechanical mixing e) 0.1% GNP, f) 0.3% GNP g) 0.5% GNP produced with high-speed mechanical mixing method

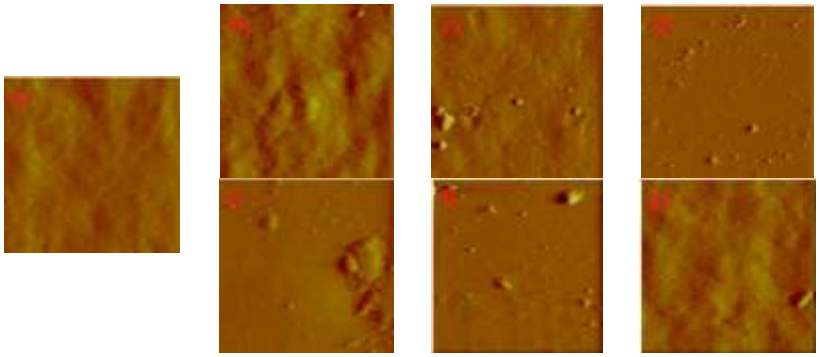


Figure 4.16 Surface AFM images of nanocomposites a) Pure SMP, b) 0.1%, GNP, c) 0.3% GNP, d) 0.5% GNP produced with hybrid method involving ultrasonic mixing – high speed mechanical mixing e) 0.1% GNP, f) 0.3% GNP, g) 0.5% GNP produced with high speed mechanical mixing method

CHAPTER 5

CONCLUSION AND FUTURE WORK

5.1 Conclusion

The thermal and mechanical properties of nanocomposites containing 0.1%, 0.3% and 0.5% by weight GNPs were investigated using a high speed mechanical mixing method and a hybrid method involving ultrasonic mixing - high speed mechanical mixing. The results obtained from the study are as follows:

1. The effect of graphene added to the pure polymer in DSC analysis on the T_g value in the produced nanocomposites was investigated. The T_g value of the pure polymer was obtained as 33 ^oC. T_g value did not change with 0.1% GNP contribution in nanocomposites produced by high speed mechanical mixing method. It increased by 2 ^oC to 35 ^oC with 0.3% GNP contribution. The 0.5% GNP contribution unchanged compared to 0.3%. In the hybrid method, the T_g value for 0.1% and 0.3% GNP additives remained constant at 33 ^oC and did not change, for 0.5% GNP additives it was determined as 34 ^oC with an increase of 1 ^oC. The small amount of additive did not have a significant effect on the T_g value for both production methods.

2. The change in decomposition temperatures with the effect of added GNPs in nanocomposites produced by TGA analysis was investigated. The endothermic peak for pure SMP was at 337 ^oC. In the high-speed mechanical mixing method, the decomposition temperature increased to 365 ^oC with 0.5% GNP contribution. The thermal stability of the obtained nanocomposite increased by 7.7%. In the hybrid method, decomposition temperature increased to 362 ^oC with 0.5% GNP contribution. The thermal stability of the obtained nanocomposite increased by 7%. In the samples produced by the two methods, GNPs formed a barrier and increased their thermal stability by preventing contact with oxygen.

3. It was investigated whether the added GNPs by FTIR analysis caused a change in the chemical structure in the SMP. No change in chemical structure was observed in the produced nanocomposites.

4. Three-point bending tests were conducted to assess the mechanical characteristics of the SMP and GNP/SMP nanocomposite samples, as well as the influence of the amount of GNP added to the pure SMP on the mechanical properties. In the high speed mechanical mixing method, a significant increase in mechanical properties was observed with the addition of 0.1% GNP. A small increase in contribution was observed with 0.3% GNP compared to 0.1% GNP contribution. There was a slight decrease with 0.5% GNP contribution. In the hybrid method, on the other hand, mechanical properties showed an increasing trend proportionally with the contribution of GNP. In the high-speed mechanical mixing method, there was no increase in mechanical properties after 0.3% GNP, but on the contrary, a decrease was observed in 0.5% GNP. This is probably due to agglomeration of GNPs. In the hybrid method, it can be said that the increase in the GNP content, the increase in the mechanical properties prevent aggregation and provide a homogeneous distribution of GNPs.

When the hardness values were examined, it showed a slight decrease with 0.5% GNP additive after an increase up to 0.3% GNP additive in high-speed mechanical mixing method. In the hybrid method, the hardness value increased directly proportional with the increase in the GNP ratio. The hardness values showed parallel results with the mechanical properties.

5. In microscopic examination, the distribution of GNPs on the fracture surfaces of the samples was examined. While a smooth surface is observed on the fracture surface of the pure SMP, a rougher structure is observed for the nanocomposite containing 0.1% GNP and 0.3% GNP in the high-speed mechanical mixing method, where good results are obtained in the mechanical properties, and for the nanocomposite containing 0.5% GNP in the hybrid method. The GNPs in it changed their fracture directions and formed a rougher fracture surface. In addition, when the SEM and AFM images taken from the surface of the sample were examined, it was seen that the added GNPs did not cause a change in the surface morphology.

5.2 Future Work

- The effect of GNP added to pure SMP on the electrical properties of the nanocomposite can be studied.
- By adding GNP, the threshold value can be determined and a material that can change shape not only with heat but also with electricity can be obtained.
- The shape memory properties of pure SMP and produced nanocomposites can be studied.
- Biocompatibility tests of pure SMP and produced nanocomposites can be performed.

REFERENCES

[1] Xia, Y., He, Y., Zhang, F., Lui, Y. & Leng, J. A review of shape memory polymers and composites: mechanisms, materials, and applications. Advanced materials, 33 (1), 2000713, 2021.

[2] Behl, M. & Lendlein, A. Shape-memory polymers. Materials today. 10 (4), 20-28. 2007.

[3] Mu, T., Liu, L., Lan, X., Liu, Y. & Leng, J. Shape memory polymers for composites. Composite science and technology, 160, 169-198. 2018.

[4] Chen, L., Li, W., Liu, Y. & Leng, J. Nanocomposites of epoxy-based shape memory polymer and thermally reduced graphite oxide: mechanical, thermal and shape memory characterizations. Composites part B: engineering, 91, 72-82. 2016.

[5] Zhao, W., Liu, L., Zhang, F., Leng, J. & Liu, Y. Shape memory polymers and their composites in biomedical applications. Materials science & engineering C, Materials for biological applications, 97, 864-883. 2019.

[6] Rana, S., Karak, N., Cho, J.W. & Kim, J.H. Enhanced dispersion of carbon nanotubes in hyperbranched polyurethane and properties of nanocomposites. Nanotechnology, 19 (49), 495707. 2008.

[7] Fu, Y.Q., Huang, W.M., Luo, J.K. & Lu, H. Polyurethane shape-memory polymers for biomedical applications. L. Yahia, (Ed.). Shape memory polymers for biomedical applications (1st ed.) (167-195). Woodhead Publishing. 2015.

[8] Pinto, A.M., Gonçalves, I.C. & Magalhaes, F.D. Graphene-based materials biocompatibility: a review. Colloids and surfaces B: biointerfaces, 111, 188-202. 2013.

[9] Tjong, S.C. Editorial corner – a personal view graphene and its derivatives: novel materials for forming functional polymer nanocomposites. Express polymer letters, 6 (6). 2012.

[10] Qi, B., Yuan, Z., Lu, S., Liu, K., Li, S., Yang, L., et al. Mechanical and thermal properties of epoxy composites containing graphene oxide and liquid crystalline epoxy. Fibers and polymers, 15, 326-333. 2014.

[11] Wei, J., Vo, T. & Inam, F. Epoxy/graphene nanocomposites-processing and properties: a review. RSC advances, 90 (5), 73510-73524. 2015.

[12] Inam, F. & Peijs, T. Re-aggregation of carbon nanotubes in two-component epoxy system. Journal of nanostructured polymers and nanocomposites, 2 (3), 87-95. 2006.

[13] Wei, J., Atif, R., Vo, T. & Inam, F. Graphene nanoplatelets in epoxy system: dispersion, reaggregation, and mechanical properties of nanocomposites. Journal of nanomaterials, 2015, 12. 2015.

[14] Huang, W.M., Yang, B. & Fu, Y.Q. Shape memory materials and shape memory polymers. Polyurethane shape memory polymers (1st ed) (1-13). Boca Raton: CRC Press. 2012.

[15] Huang, W.M., Ding, Z., Wong, C.C., Wei, J., Zhao, V. & Purnawali, H. Shape memory materials. Materials today, 13 (7-8). 2010.

[16] Liang, C., Rogers, C.A. & Malafeew, E. Investigation of shape memory polymers and their hybrid composites. Journal of intelligent material systems and structures, 8 (4), 380-386. 1997.

[17] Defence Research and Development Canada. Shape memory polymers – literature review. (TM 2002-127). Canada: DRDC Atlantic. 2002.

[18] Hu, J., Zhu, Y., Huang, H. & Lu, J. Recent advances in shape-memory polymers: structure, mechanism, functionality, modeling and applications. Progress in polymer science, 37 (12), 1720-1763. 2012.

[19] Leng, J., Lan, X., Liu, Y. & Du, S. Shape-memory polymers and their composites: stimulus methods and applications. Progress in materials science, 56 (7), 1077-1135. 2011.

[20] Tandon, G.P., Goecke, K., Cable, K. & Baur, J. Durability assessment of styrene- and epoxy-based shape-memory polymer resins. Journal of intelligent material systems and structures, 20 (17), 2127-2143. 2009.

[21] Solowski, W., Metcalfe, A., Hayashi, S., Yahia, L. & Raymond, J. Medical applications of shape memory polymers. Biomedical materials, 2 (1), 23. 2007.

[22] Gabbott, P. A practical introduction to differential scanning calorimetry. P. Gabbott (Ed.) Principle and applications of thermal analysis (1st ed.) (1-50). Blackwell Publishing. 2008.

[23] Dyamenahalli, K., Famili, A. & Shandas, R. Characterization of shape-memory polymers for biomedical applications. L. Yahia, (Ed.) Shape memory polymers for biomedical applications (1st ed.) (35-63). Woodhead Publishing. 2015.

[24] Rocha, J.G., Correia, V.M.G., Martins, M. & Cobral, J.M. Dilatometer for characterization of thermal expansion of ceramic samples. International electronics conference proceedings. 2009.

[25] Measurement of the glass transition temperature Tg. Retrieved July 1, 2021, from http://glassproperties.com/tg/. 2021.

[26] Introduction to FTIR spectroscopy. Retrieved July 1, 2021, from https://www.thermofisher.com/tr/en/home/industrial/spectroscopy-elemental-isotope-analysis/spectroscopy-elemental-isotope-analysis-learning-center/molecular-spectroscopy-information/ftir-information/ftir-basics.html. 2021.

[27] Three point and four point bending. Retrieved July 1, 2021, from http://www.med.upenn.edu/pcmd/3pt-4pt-bending.html. 2021.

[28] Hayward, N. Impact testing. Advanced materials and processes, 162, 31-32. 2004.

[29] Shore (durometer) hardness testing of plastics. Retrieved July 1, 2021, from http://www.matweb.com/reference/shore-hardness.aspx. 2021.

[30] Baer, G.M., Small, W., Wilson, T.S., Benett, W.J., Matthews, D.L., Hartman, J., et al. Fabrication an in vitro deployment of a laser-activated shape memory polymer vascular stent. Biomedical engineering online, 6, 43. 2007.

[31] Small, W., Wilson, T.S., Benett, W.J., Loge, J.M. & Maitland, D.J. Laser-activated shape memory polymer intravascular thrombectomy device. Optics express, 13, 8204-8213. 2005.

[32] Ratna, D. & Karger-Kocsis, J. Recent advances in shape memory polymers and composites: a review. Journal of materials science, 43, 254-269. 2008.

[33] Meng, Q. & Hu, J. A review of shape memory polymer composites and blends. Composites part A: applied science and manufacturing, 40(11), 1661-1672. 2009.

[34] Leng, J., Wu, X. & Liu, Y. Infrared light-active shape memory polymer filled with nanocarbon particles. Journal of applied polymer science, 114, 2455-2460. 2009.

[35] Jin, X., Ni, Q. & Natsuki, T. Composites of multi-walled carbon nanotubes and shape memory polyurethane for electromagnetic interference shielding. Journal of composite materials, 45 (24), 2547-2554. 2011.

[36] Vialle, G., Prima, M.D., Hacking, E., Gall, K., Garmestani, H., Sanderson, T., et al. Remote activation of nanomagnetite reinforced shape memory polymer foam. Smart materials and structures, 18 (11), 115014. 2009.

[37] Aydas, B., Design, production and fire characterization of flax fiber reinforced shape memory composites with flame retardant property. Unpublished master thesis, Ankara Yıldırım Beyazıt University. 2020.

[38] Pinto, A.M., Moreira, S., Gonçalves, I.C., Gama, F.M., Mendes, A.M. & Magalhaes, F.D. Biocompatibility of poly(lactic acid) with incorporated graphene-based materials. Colloids and surfaces. B, biointerfaces, 104, 229-238. 2013.

[39] Yoon, O.J., Jung, C.Y., Sohn, I.Y., Kim, H.J., Hong, B., Jhon, M.S., et al. Nanocomposite nanofibers of poly(D, L-lactic-co-glycolic acid) and graphene oxide nanosheets. Composites part A: applied science and manufacturing, 42 (12), 1978-1984. 2011.

[40] Shape memory polymer. Retrieved July 1, 2021, from http://www2.smptechno.com/en/smp/. 2021.

[41] Graphene nanoplatelet. Retrieved July 1, 2021, from https://nanografi.com/graphene/graphene-nanoplatelet-purity-99-9-size-3-nm-s-a-800-m2-g-dia-1-5-m/. 2021.

[42] Baer, G., Wilson, T.S., Matthews, D.L. & Maitland, D.J. Shape-memory behavior of thermally stimulated polyurethane for medical applications. Journal of applied polymer science, 103 (6), 3882-3892. 2007.

[43] Thuc, C.N.H., Cao, H.T., Nguyen, D.M., Tron, M.A., Duclaux, A.-C., et al. Preparation and characterization of polyurethane nanocomposites using vietnamese montmorillonite modified by polyol surfactants. Journal of nanomaterials, 2014, 11. 2014.

[44] Yang, B. Influence of moisture in polyurethane shape memory polymers and their electrically conductive composites. Unpublished doctoral thesis, Nanyang Technological University. 2007.

[45] Yang, B., Huang, W.M., Li, C., & Chor, J.H. Effects of moisture on the glass transition temperature of polyurethane shape memory polymer filled with nano-carbon powder. European polymer journal, 41 (5), 1123-1128. 2005.

[46] Chieng, B.W., Azowa, I.N., Yunus, W.MD.Z.W., & Hussein, Z. Effects of graphene nanoplatelets on poly (lactic acid)/poly (ethylene glycol) polymer nanocomposites. Advanced materials research, 1024, 136-139. 2014.

[47] Al-Saleh, M.A., Yussuf, A.A., Al-Enezi, S., Kazemi, R., Wahit, M.U., Al-Shammari, T., et al. Polypropylene/graphene nanocomposites: effects of GNP loading and compatibilizers on the mechanical and thermal properties. Materials, 12 (23), 3924. 2019.

[48] IR Spectrum table & chart. Retrieved July 1, 2021, from https://www.sigmaaldrich.com/TR/en/technical-documents/technical-article/analytical-chemistry/photometry-and-reflectometry/ir-spectrum-table. 2021.

[49] Dehaghani, M.Z., Kaffashi, B., Haponiuk, J.T., & Piszczyk, L. Shape memory thin films of polyurethane: does graphene content affect the recovery behavior of polyurethane nanocomposites?. Polymer composites, 41, 3376-3388. 2020.

[50] Halder, S., Ghosh, P.K., & Goyat, M.S. Influence of ultrasonic dual mode mixing on morphology and mechanical properties of ZrO2-epoxy nanocomposite. High performance polymers, 24 (4), 331-341. 2012.

[51] Santos, H.M., Lodeiro, C., & Capelo, J.L. The power of sound. Capelo, J.L., (Ed.) Ultrasound in chemistry: analytical applications (1st ed.) (1-16). Wiley-VCH. 2008.

[52] Bao, C., Guo, V., Song, L., & Hu, Y., Poly (vinyl alcohol) nanocomposites based on graphene and graphite oxide: a comparative investigation of property and mechanism. Journal of materials chemistry, 21, 13942-13950. 2011.

APPENDICES

Appendix A1: Differential Scanning Calorimeter Results – Pure SMP

Appendix A2: Differential Scanning Calorimeter Results – 0.1% GNP/SMP Nanocomposite produced by high speed mechanical mixing method

Appendix A3: Differential Scanning Calorimeter Results – 0.3% GNP/SMP Nanocomposite produced by high speed mechanical mixing method

Appendix A4: Differential Scanning Calorimeter Results – 0.5% GNP/SMP Nanocomposite produced by high speed mechanical mixing method

Appendix A5: Differential Scanning Calorimeter Results – 0.1% GNP/SMP Nanocomposite produced by hybrid method including ultrasonic mixing-high speed mechanical mixing

Appendix A6: Differential Scanning Calorimeter Results – 0.3% GNP/SMP Nanocomposite produced by hybrid method including ultrasonic mixing-high speed mechanical mixing

Appendix A7: Differential Scanning Calorimeter Results – 0.5% GNP/SMP Nanocomposite produced by hybrid method including ultrasonic mixing-high speed mechanical mixing

Appendix B1: Thermogravimetric Analysis Results – Pure SMP

Appendix B2: Thermogravimetric Analysis Results – 0.1% GNP/SMP Nanocomposite produced by high speed mechanical mixing method

Appendix B3: Thermogravimetric Analysis Results – 0.3% GNP/SMP Nanocomposite produced by high speed mechanical mixing method

Appendix B4: Thermogravimetric Analysis Results – 0.5% GNP/SMP Nanocomposite produced by high speed mechanical mixing method

Appendix B5: Thermogravimetric Analysis Results – 0.1% GNP/SMP Nanocomposite produced by hybrid method including ultrasonic mixing-high speed mechanical mixing

Appendix B6: Thermogravimetric Analysis Results – 0.3% GNP/SMP Nanocomposite produced by hybrid method including ultrasonic mixing-high speed mechanical mixing

Appendix B7: Thermogravimetric Analysis Results – 0.5% GNP/SMP Nanocomposite produced by hybrid method including ultrasonic mixing-high speed mechanical mixing

Appendix C1: 3-Point Bending Test Results – Pure SMP

Appendix C2: 3-Point Bending Test Results – 0.1% GNP/SMP Nanocomposite produced by high speed mechanical mixing method

Appendix C3: 3-Point Bending Test Results – 0.3% GNP/SMP Nanocomposite produced by high speed mechanical mixing method

Appendix C4: 3-Point Bending Test Results – 0.5% GNP/SMP Nanocomposite produced by high speed mechanical mixing method

Appendix C5: 3-Point Bending Test Results – 0.1% GNP/SMP Nanocomposite produced by hybrid method including ultrasonic mixing-high speed mechanical mixing

Appendix C6: 3-Point Bending Test Results – 0.3% GNP/SMP Nanocomposite produced by hybrid method including ultrasonic mixing-high speed mechanical mixing

Appendix C7: 3-Point Bending Test Results – 0.5% GNP/SMP Nanocomposite produced by hybrid method including ultrasonic mixing-high speed mechanical mixing

Appendix D: Hardness (Shore D) Test Results Table

Appendix A1 - Differential Scanning Calorimeter Results – Pure SMP

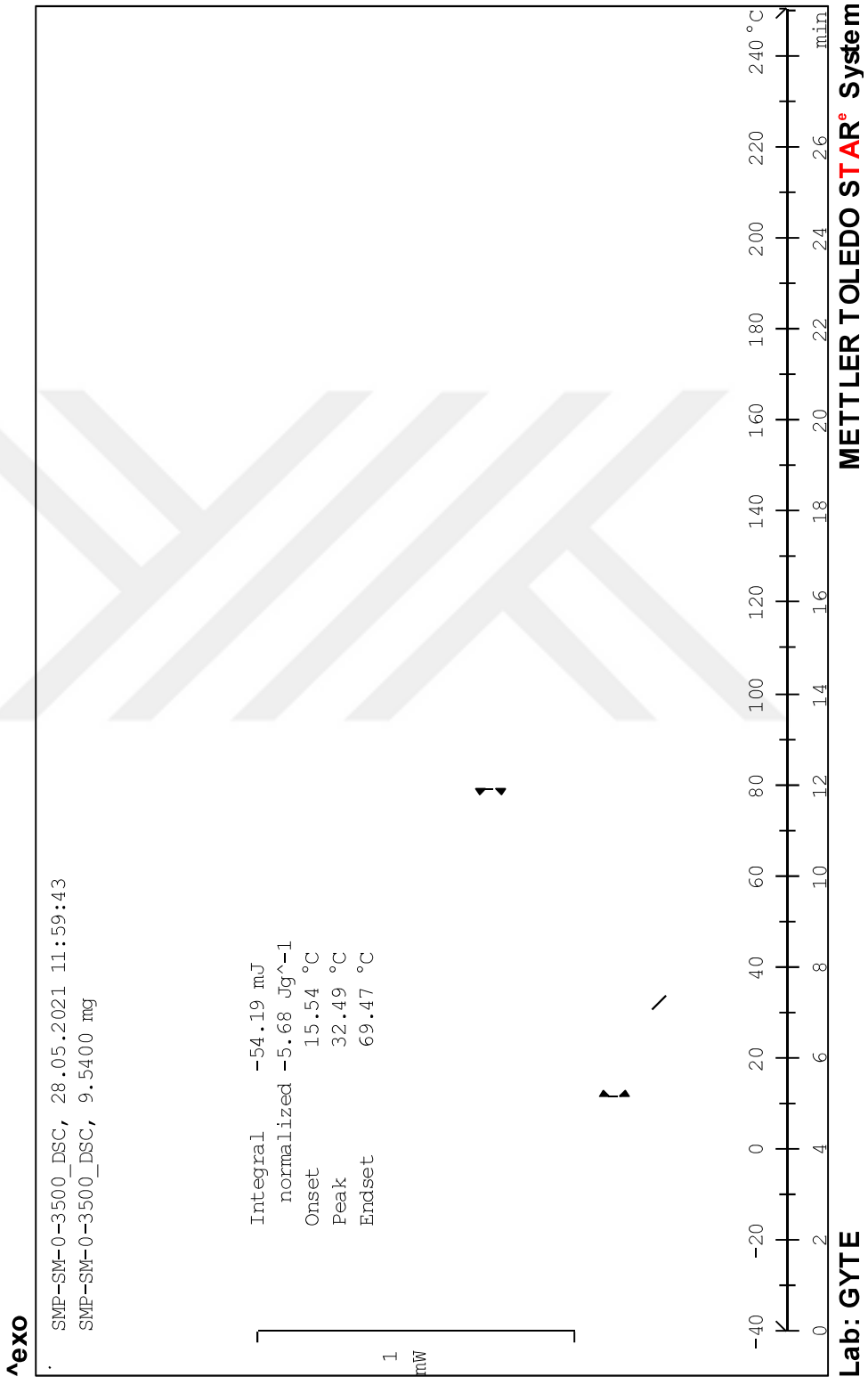


Figure A.1 Differential Scanning Calorimeter Results – Pure SMP

Appendix A2 - Differential Scanning Calorimeter Results – 0.1% GNP/SMP Nanocomposite produced by high speed mechanical mixing method

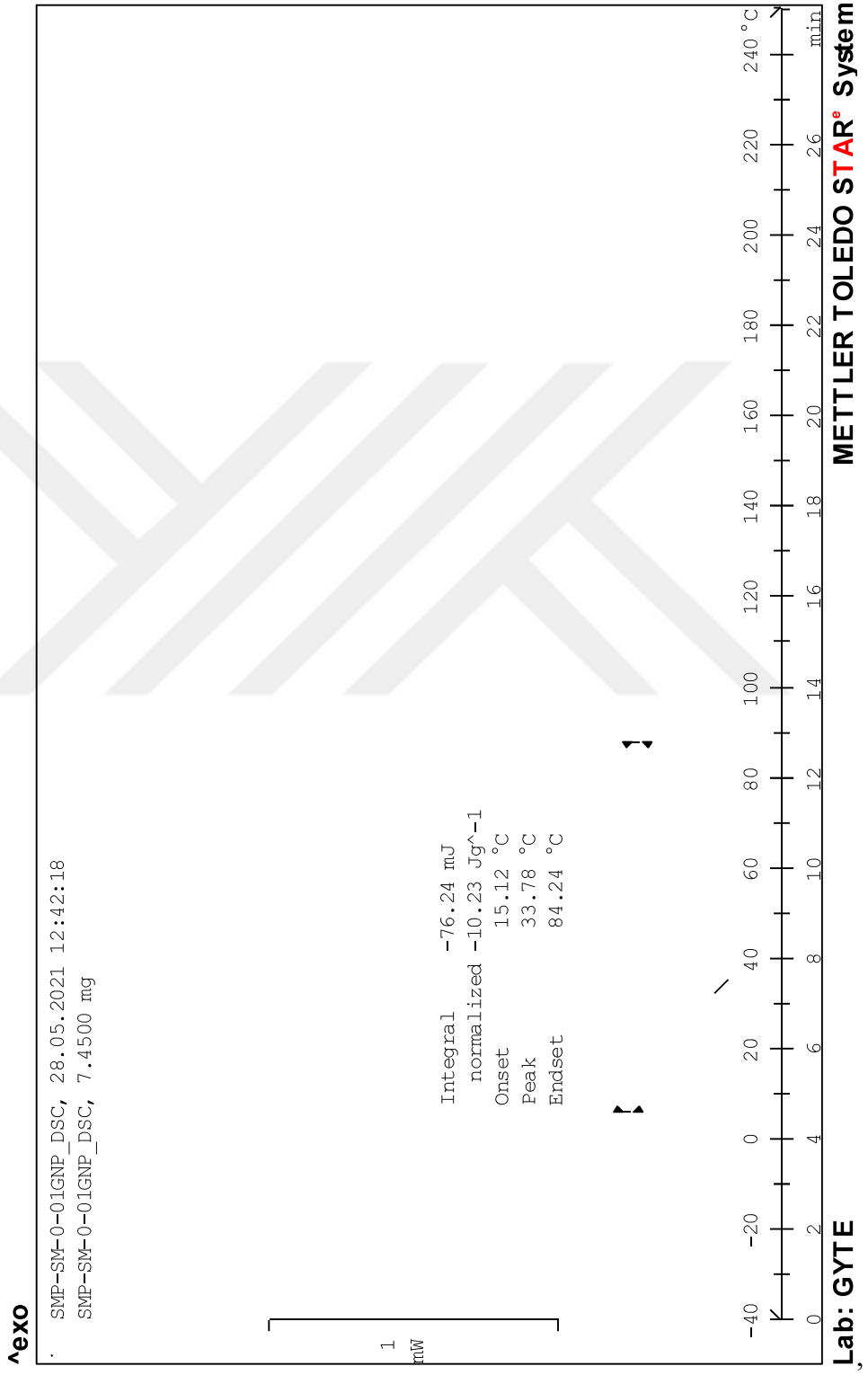


Figure A.2 Differential Scanning Calorimeter Results – 0.1% GNP/SMP Nanocomposite produced by high speed mechanical mixing method

Appendix A3 - Differential Scanning Calorimeter Results – 0.3% GNP/SMP Nanocomposite produced by high speed mechanical mixing method

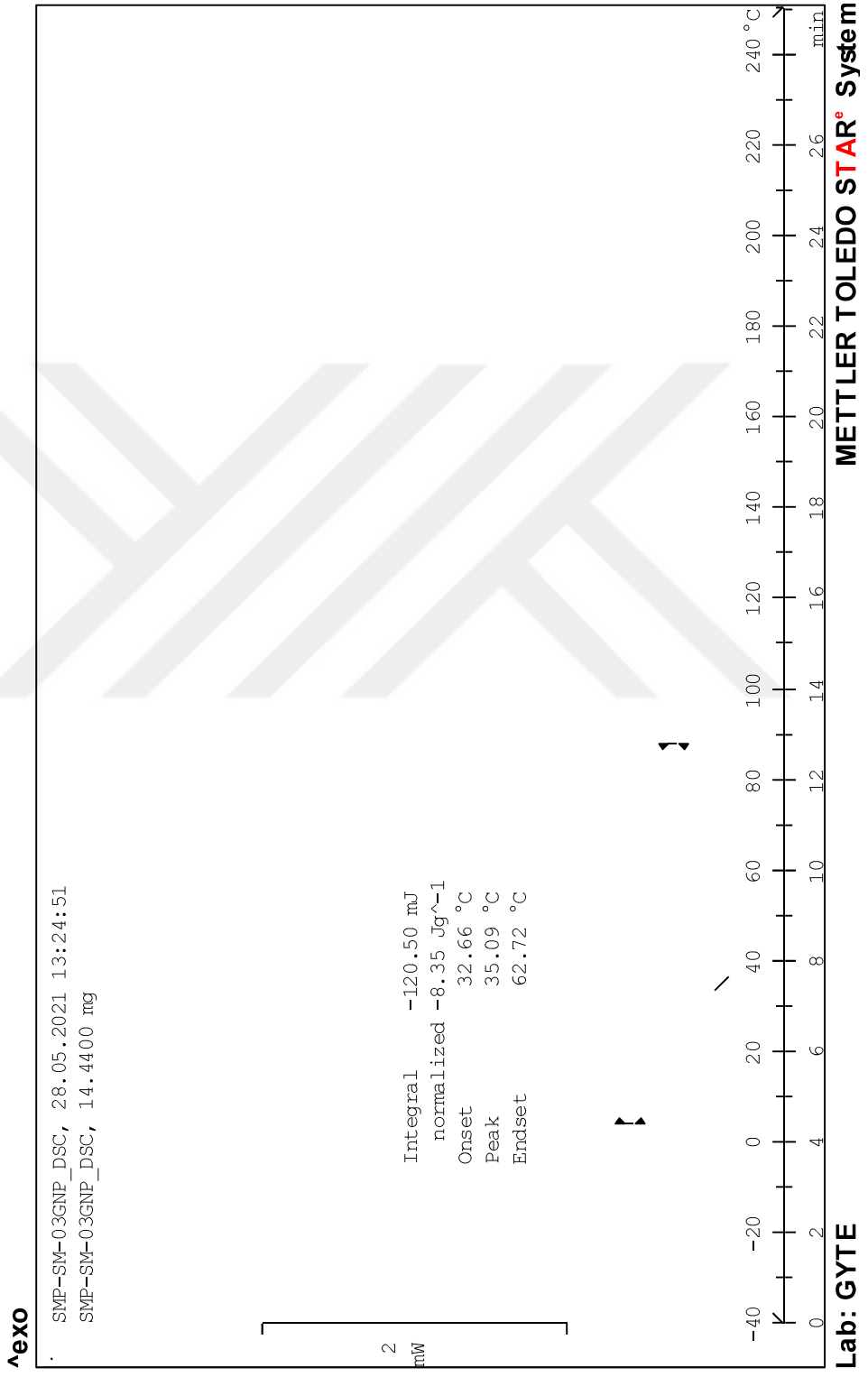


Figure A.3 Differential Scanning Calorimeter Results – 0.3% GNP/SMP Nanocomposite produced by high speed mechanical mixing method

Appendix A4 - Differential Scanning Calorimeter Results – 0.5% GNP/SMP Nanocomposite produced by high speed mechanical mixing method

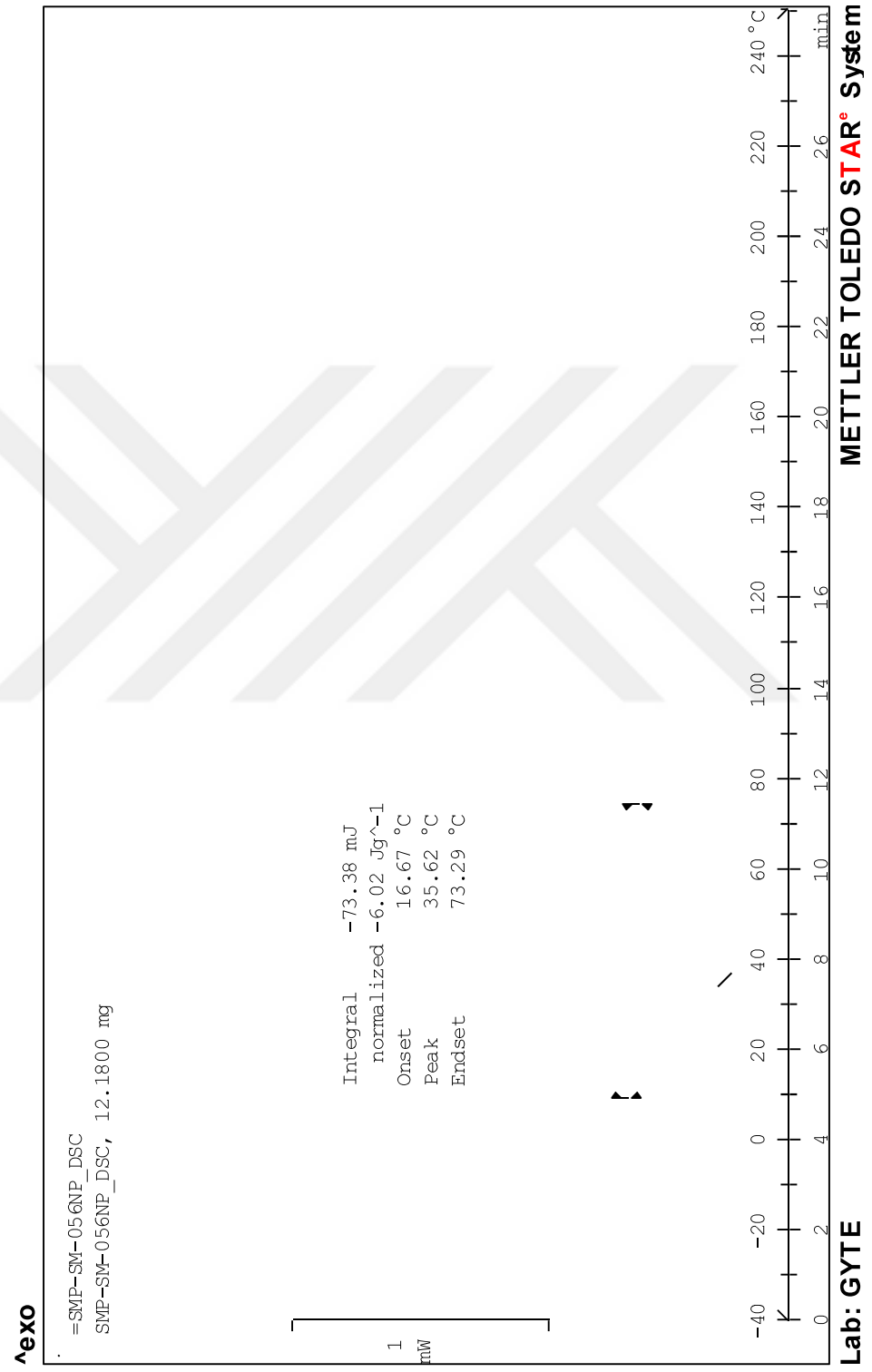


Figure A.4 Differential Scanning Calorimeter Results – 0.5% GNP/SMP Nanocomposite produced by high speed mechanical mixing method

Appendix A5 - Differential Scanning Calorimeter Results – 0.1% GNP/SMP Nanocomposite produced by hybrid method including ultrasonic mixing-high speed mechanical mixing

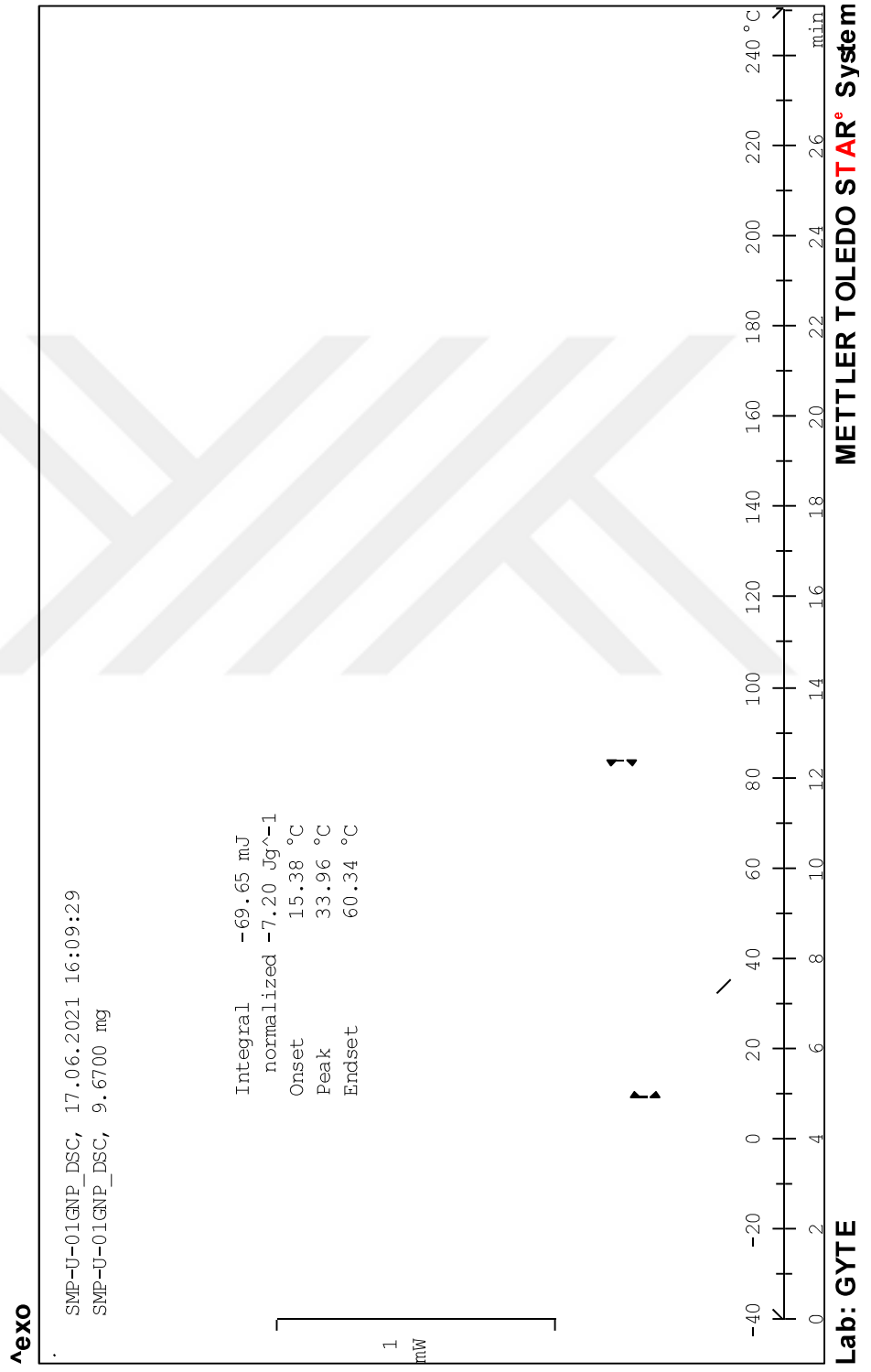


Figure A.5 Differential Scanning Calorimeter Results – 0.1% GNP/SMP Nanocomposite produced by hybrid method including ultrasonic mixing-high speed mechanical mixing

Appendix A6 - Differential Scanning Calorimeter Results – 0.3% GNP/SMP Nanocomposite produced by hybrid method including ultrasonic mixing-high speed mechanical mixing

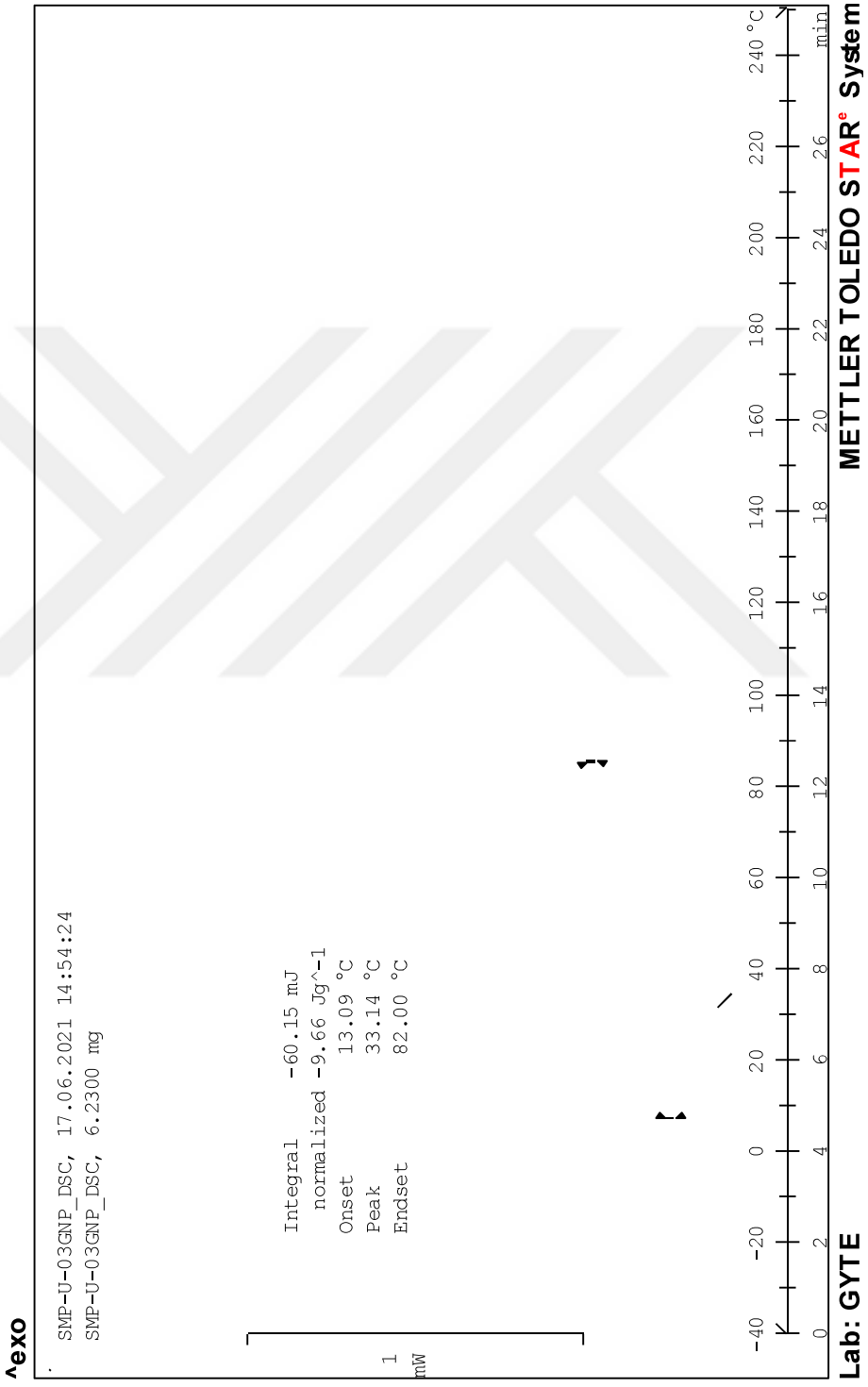


Figure A.6 Differential Scanning Calorimeter Results – 0.3% GNP/SMP Nanocomposite produced by hybrid method including ultrasonic mixing-high speed mechanical mixing

Appendix A7 - Differential Scanning Calorimeter Results – 0.5% GNP/SMP Nanocomposite produced by hybrid method including ultrasonic mixing-high speed mechanical mixing

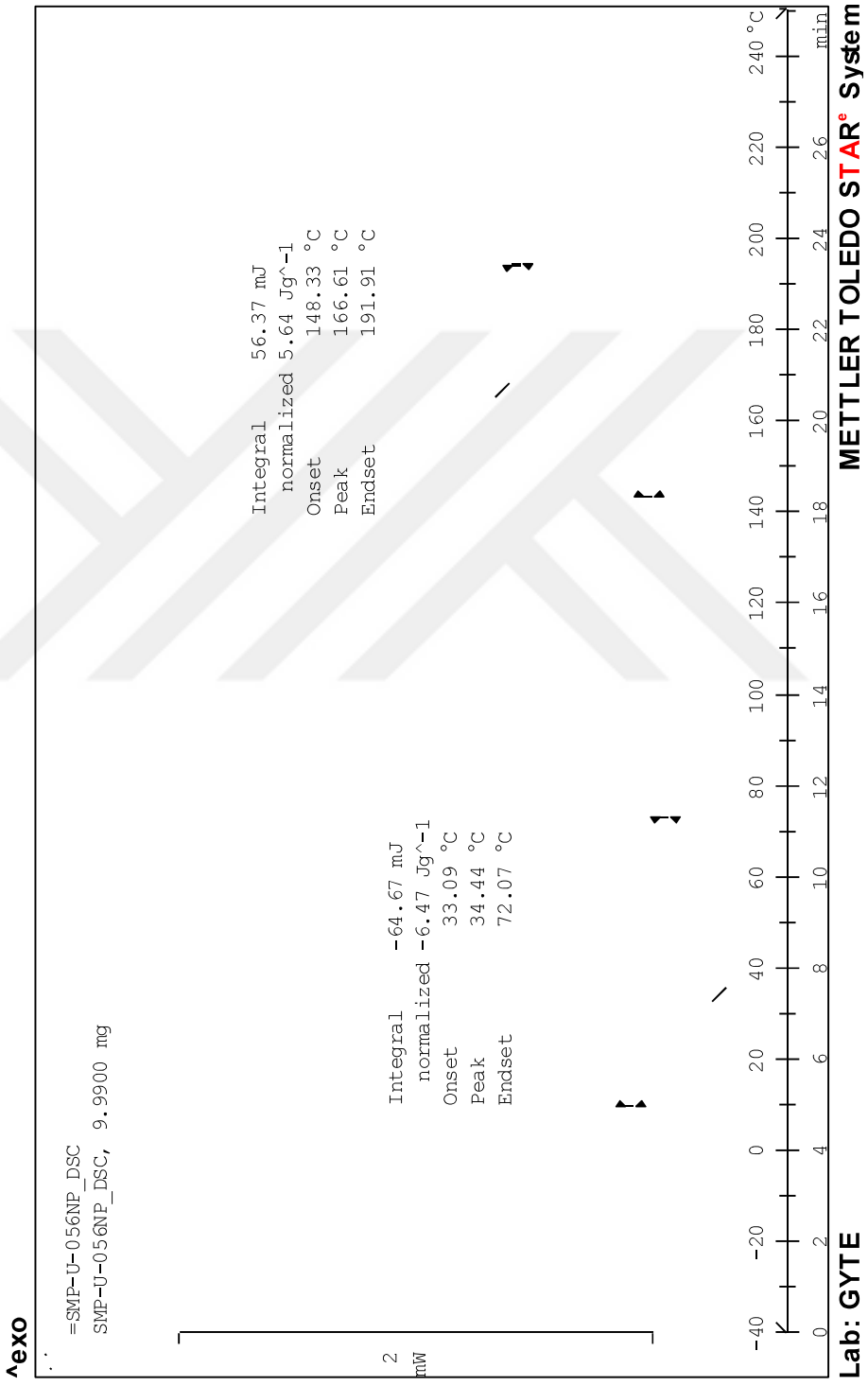


Figure A.7 Differential Scanning Calorimeter Results – 0.5% GNP/SMP Nanocomposite produced by hybrid method including ultrasonic mixing-high speed mechanical mixing

Appendix B1 - Thermogravimetric Analysis Results – Pure SMP

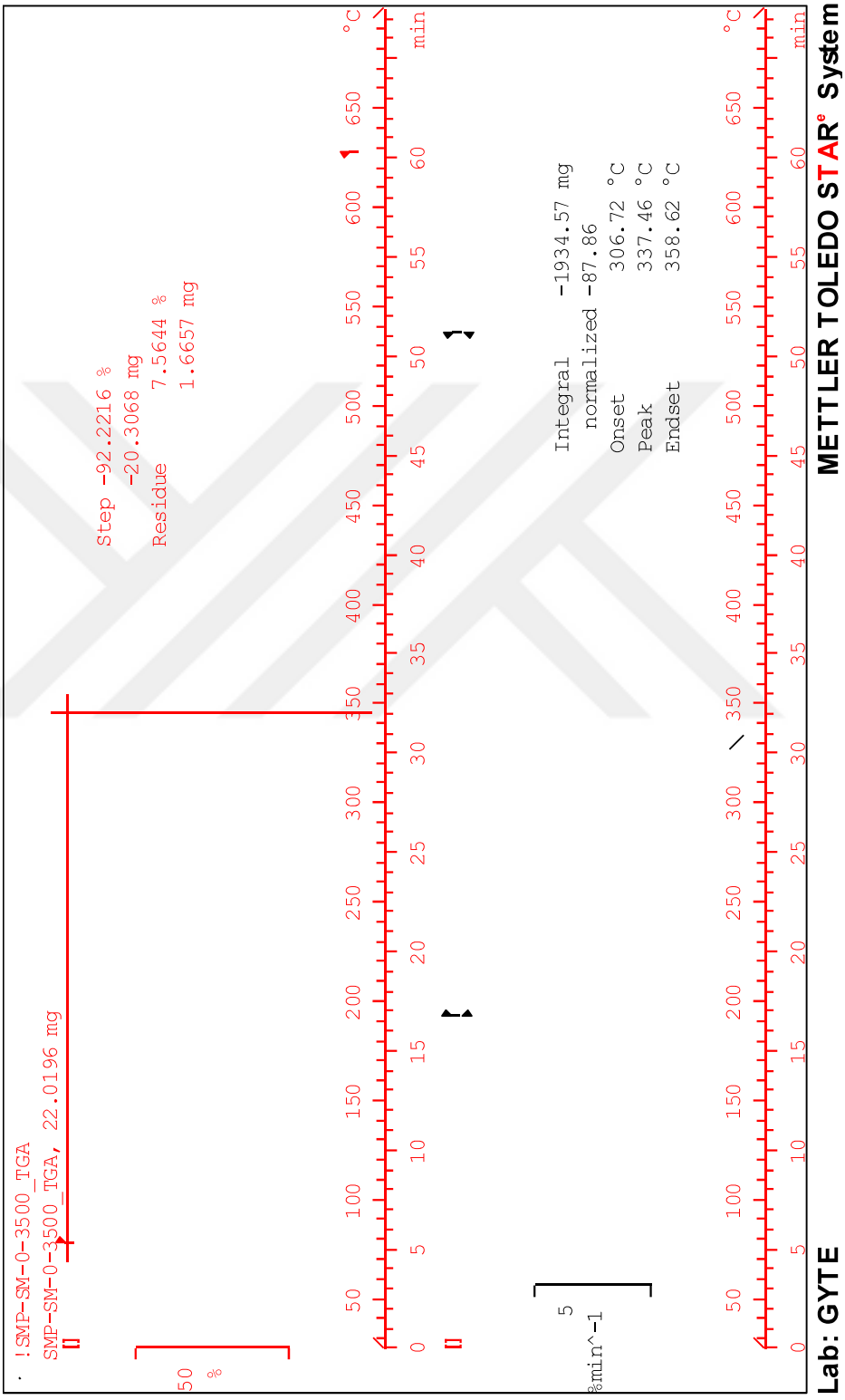


Figure B.1 Thermogravimetric Analysis Results – Pure SMP

Appendix B2 - Thermogravimetric Analysis Results – 0.1% GNP/SMP Nanocomposite produced by high speed mechanical mixing method

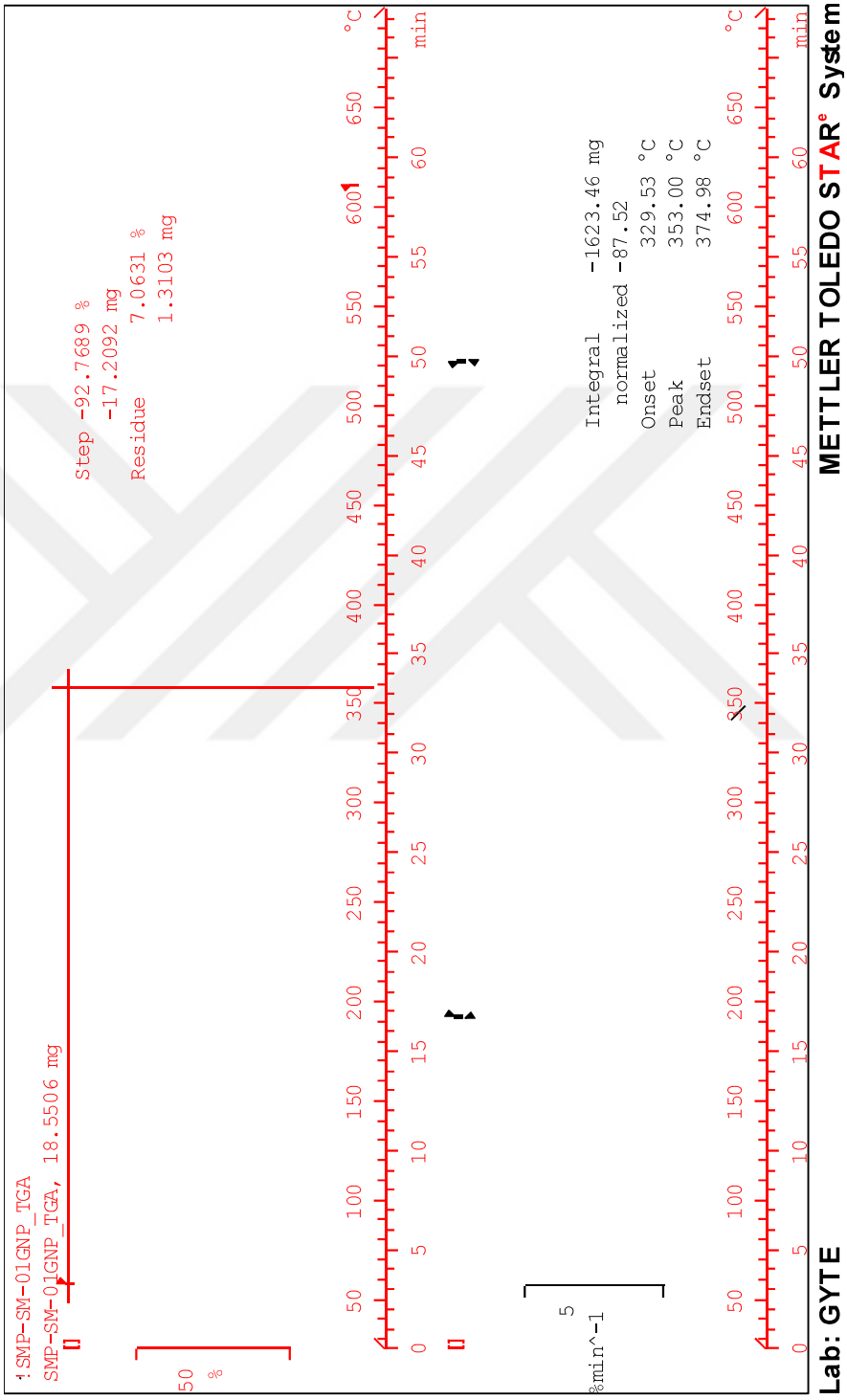


Figure B.2 Thermogravimetric Analysis Results – 0.1% GNP/SMP Nanocomposite produced by high speed mechanical mixing method

Appendix B3 - Thermogravimetric Analysis Results – 0.3% GNP/SMP Nanocomposite produced by high speed mechanical mixing method

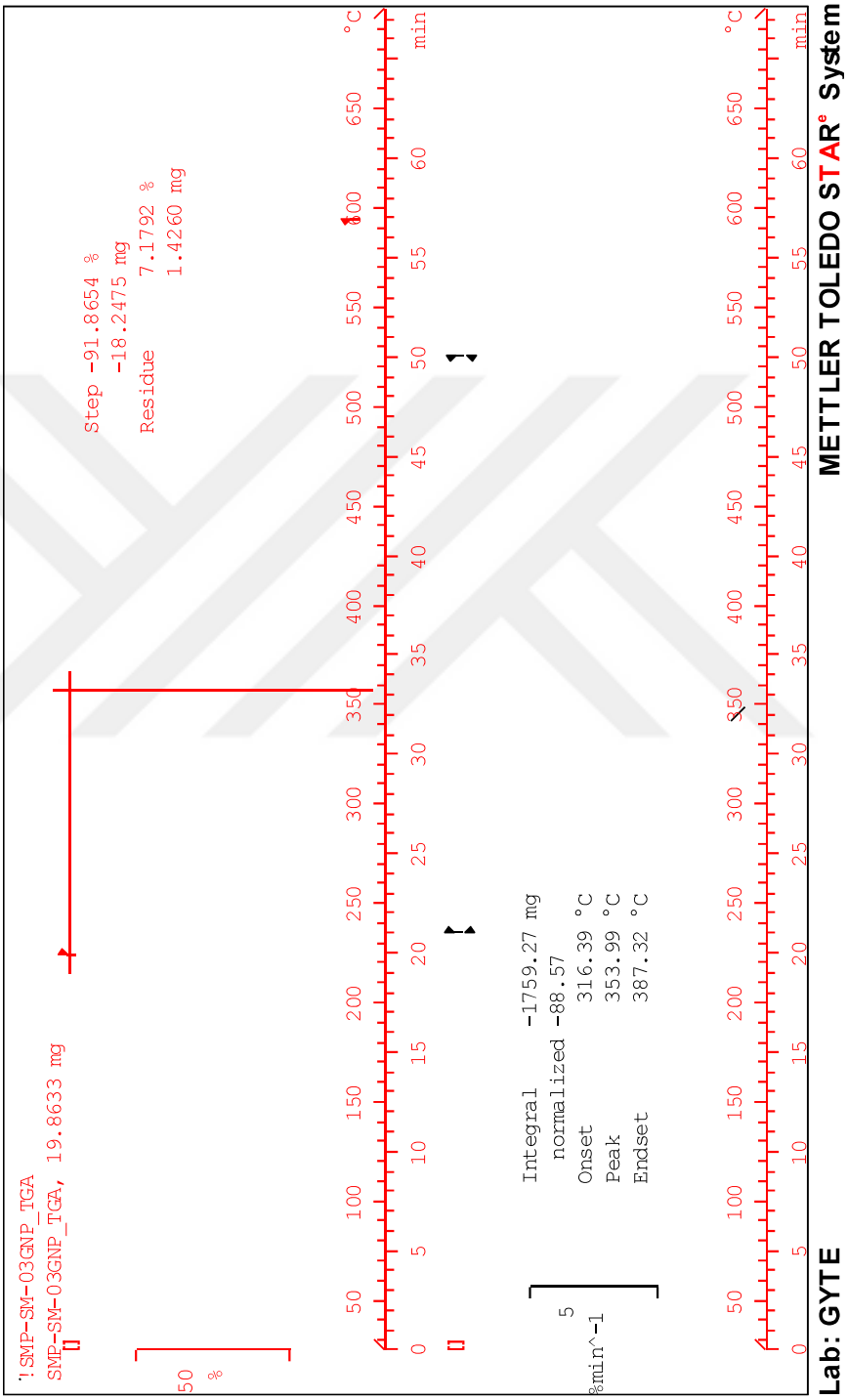


Figure B.3 Thermogravimetric Analysis Results – 0.3% GNP/SMP Nanocomposite produced by high speed mechanical mixing method

Appendix B4 - Thermogravimetric Analysis Results – 0.5% GNP/SMP Nanocomposite produced by high speed mechanical mixing method

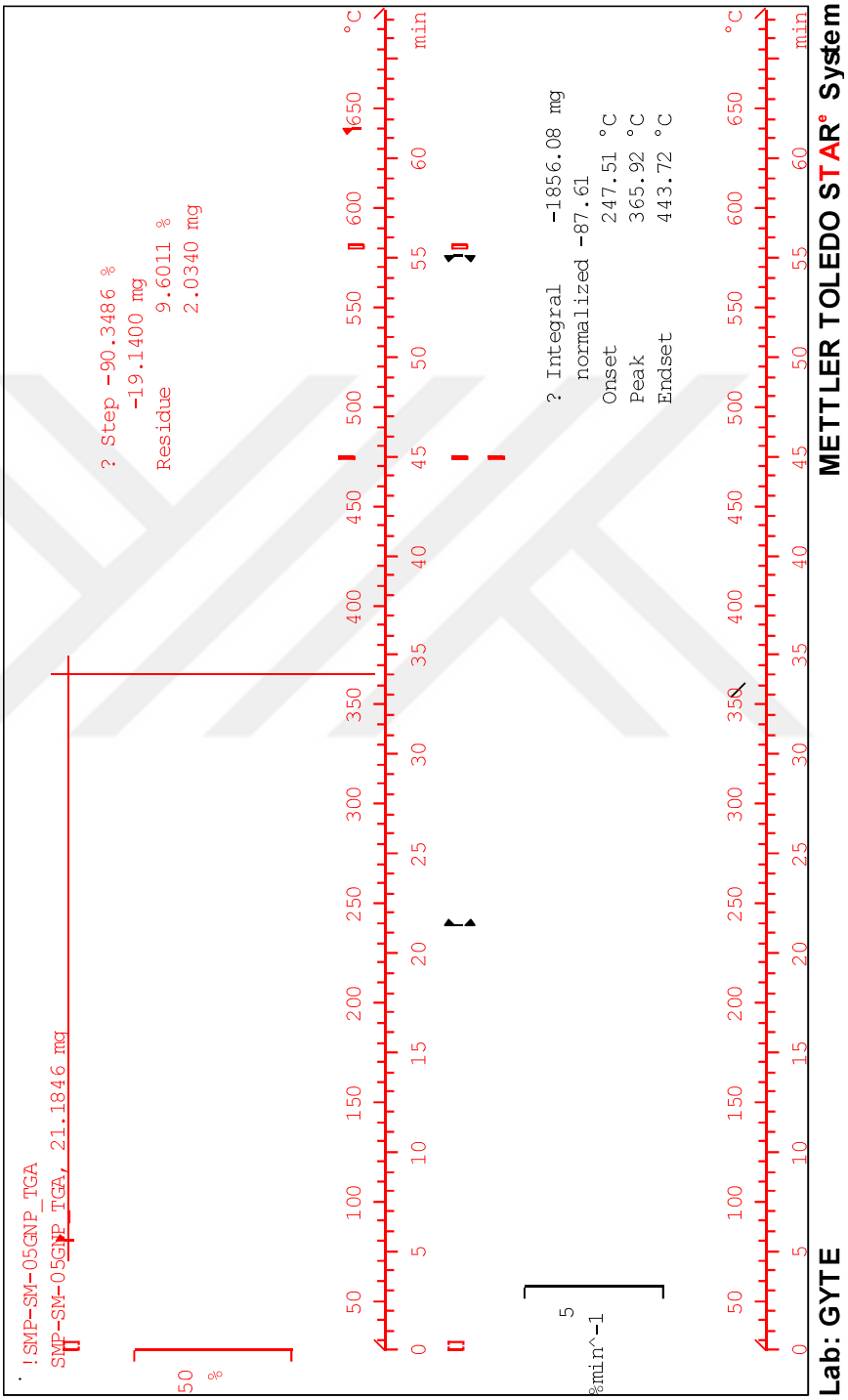


Figure B.4 Thermogravimetric Analysis Results – 0.5% GNP/SMP Nanocomposite produced by high speed mechanical mixing method

Appendix B5 - Thermogravimetric Analysis Results – 0.1% GNP/SMP Nanocomposite produced by hybrid method including ultrasonic mixing-high speed mechanical mixing

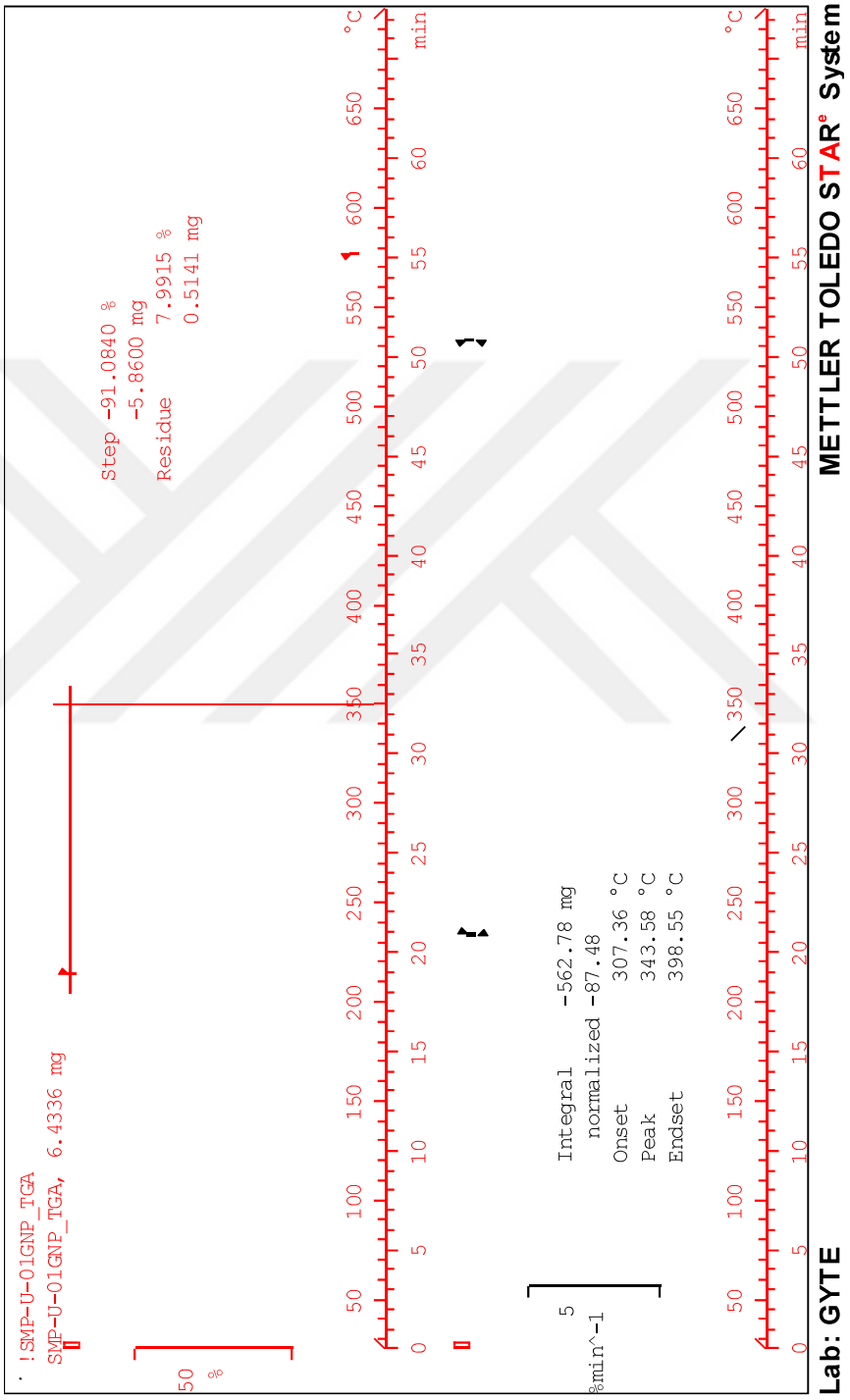


Figure B.5 Thermogravimetric Analysis Results – 0.1% GNP/SMP Nanocomposite produced by hybrid method including ultrasonic mixing-high speed mechanical mixing

Appendix B6 - Thermogravimetric Analysis Results – 0.3% GNP/SMP Nanocomposite produced by hybrid method including ultrasonic mixing-high speed mechanical mixing

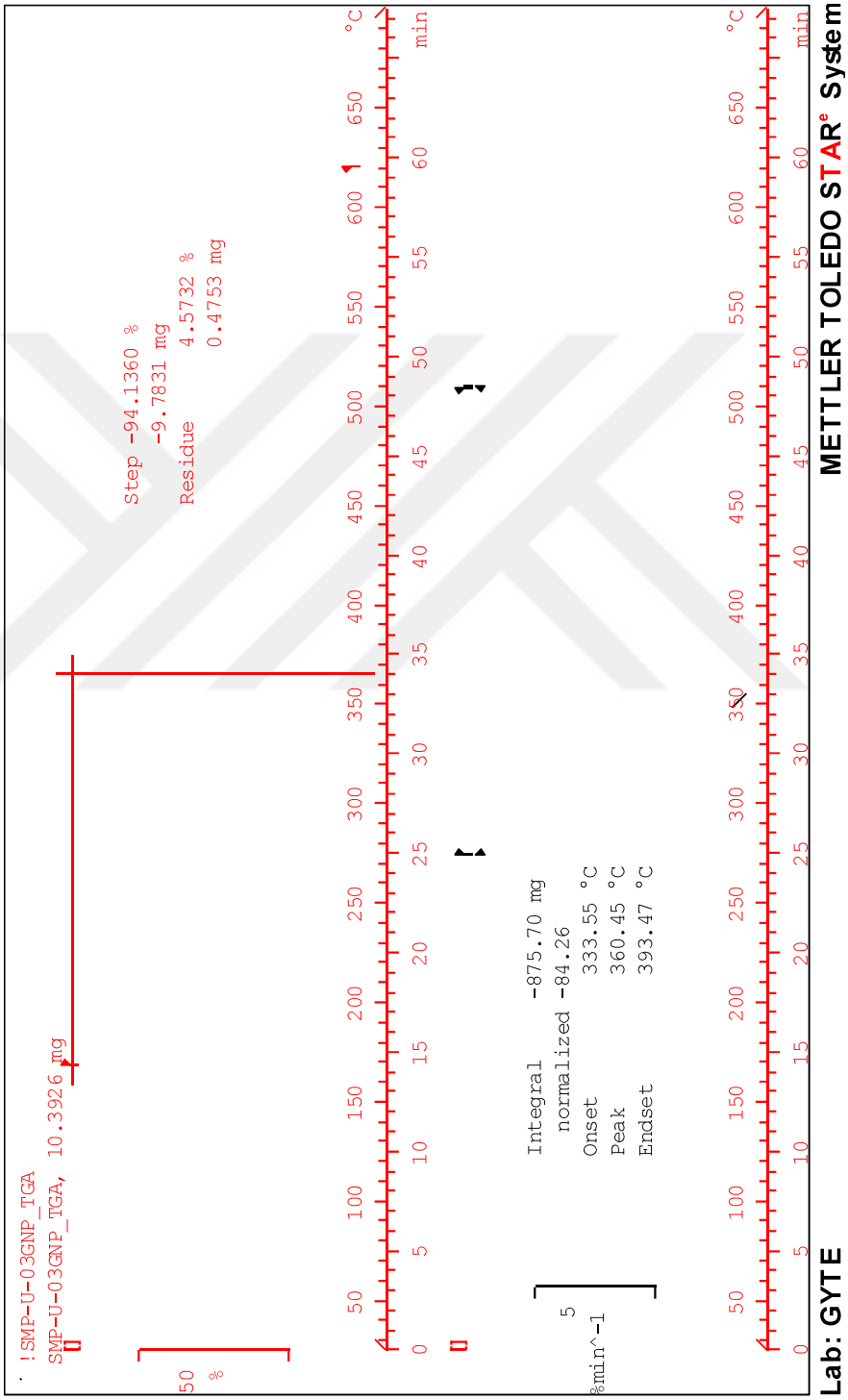


Figure B.6 Thermogravimetric Analysis Results – 0.3% GNP/SMP Nanocomposite produced by hybrid method including ultrasonic mixing-high speed mechanical mixing

Appendix B7 - Thermogravimetric Analysis Results – 0.5% GNP/SMP Nanocomposite produced by hybrid method including ultrasonic mixing-high speed mechanical mixing

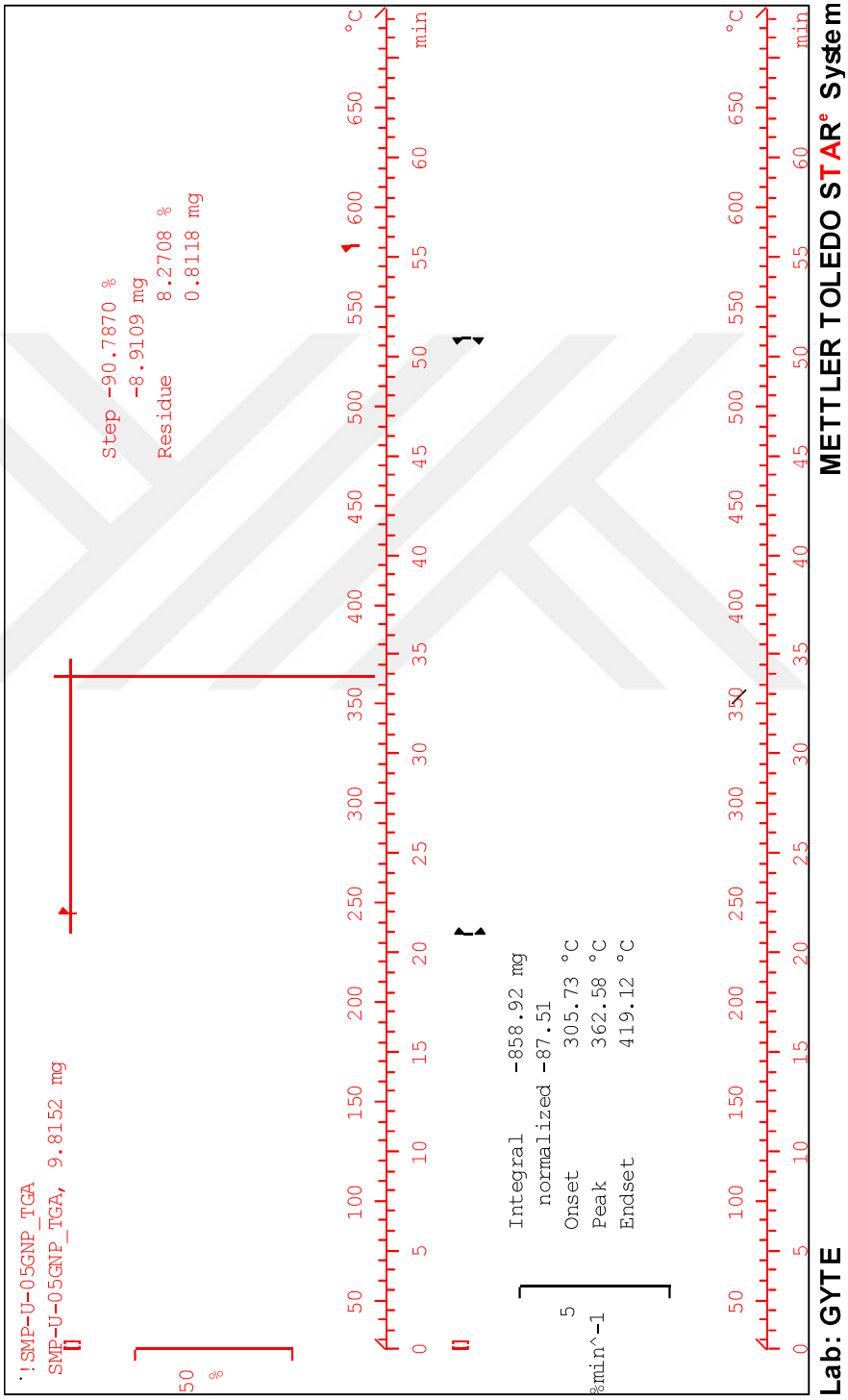


Figure B.7 Thermogravimetric Analysis Results – 0.5% GNP/SMP Nanocomposite produced by hybrid method including ultrasonic mixing-high speed mechanical mixing

Appendix C1 - 3-Point Bending Test Results – Pure SMP

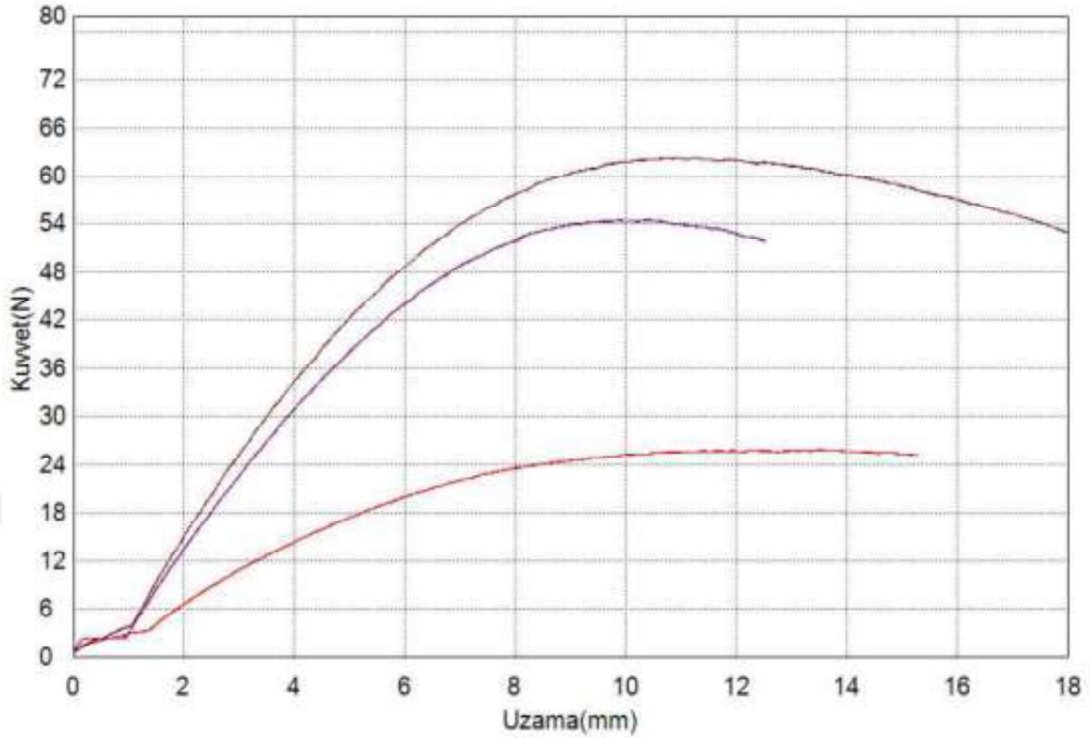


Figure C.1 Force vs. displacement curve of pure SMP

Table C.1 3-Point Bending Test Results – Pure SMP

	Flexural Strength (MPa)	**Flexural Modulus (MPa)**
Sample 1	29.89	928.64
Sample 2	33.38	1016.10
Sample 3	Measurement Error	Measurement Error
Average	31.63	972.37
Standard Deviation	2.47	61.85

Appendix C2 - 3-Point Bending Test Results – 0.1% GNP/SMP Nanocomposite produced by high speed mechanical mixing method

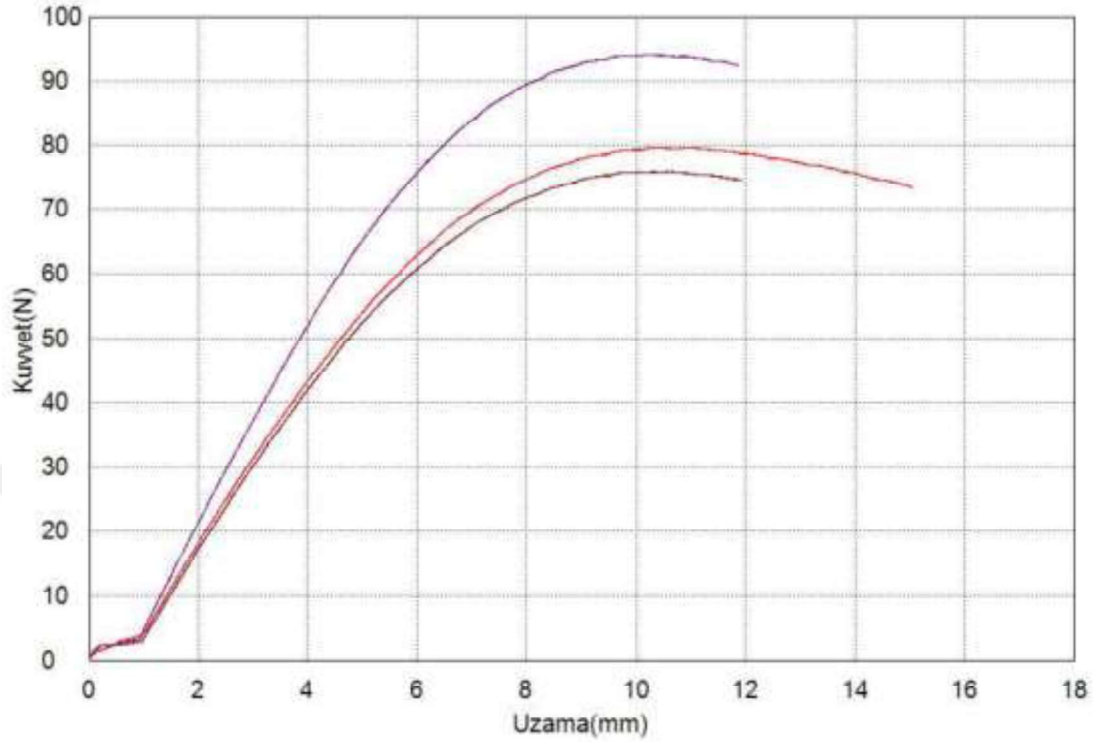


Figure C.2 Force vs. displacement curve of 0.1% GNP/SMP Nanocomposite produced by high speed mechanical mixing method

Table C.2 3-Point Bending Test Results – 0.1% GNP/SMP Nanocomposite produced by high speed mechanical mixing method

	Flexural Strength (MPa)	**Flexural Modulus (MPa)**
Sample 1	52.34	1617.83
Sample 2	48.78	1496.41
Sample 3	52.66	1548.84
Average	51.26	1554.36
Standard Deviation	2.15	60.90

Appendix C3 - 3-Point Bending Test Results – 0.3% GNP/SMP Nanocomposite produced by high speed mechanical mixing method

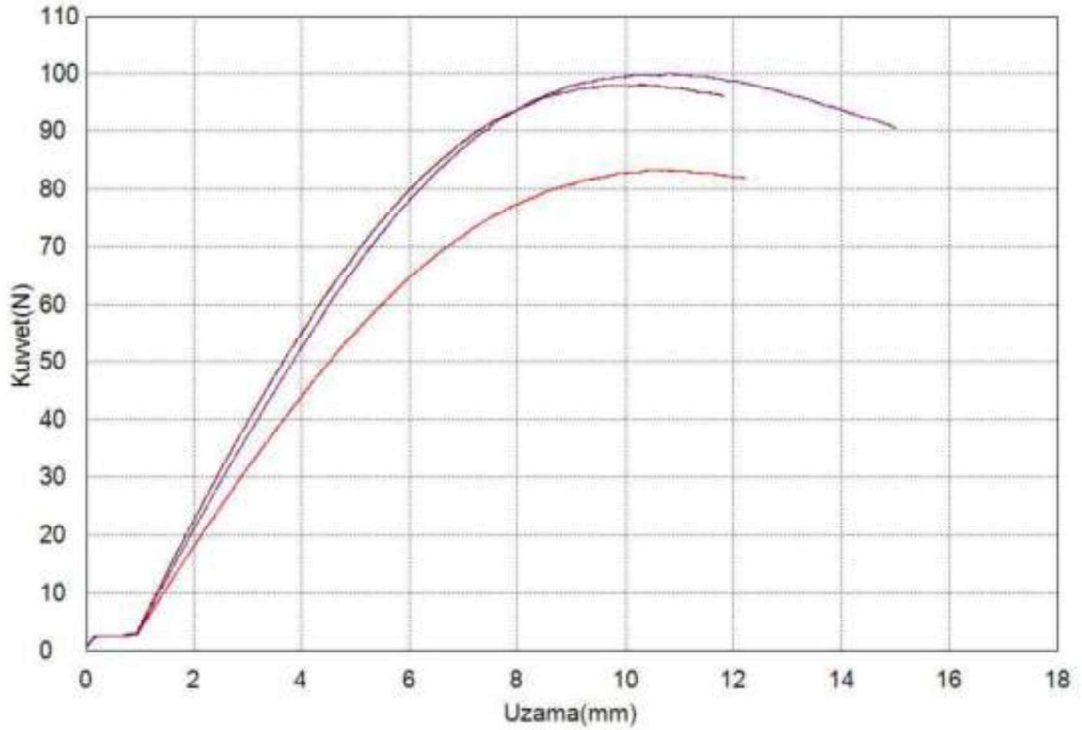


Figure C.3 Force vs. displacement curve of 0.3% GNP/SMP Nanocomposite produced by high speed mechanical mixing method

Table C.3 3-Point Bending Test Results – 0.3% GNP/SMP Nanocomposite produced by high speed mechanical mixing method

	Flexural Strength (MPa)	**Flexural Modulus (MPa)**
Sample 1	53.08	1587.58
Sample 2	55.32	1718.42
Sample 3	54.62	1565.82
Average	54.34	1623.94
Standard Deviation	1.15	82.54

Appendix C4 - 3-Point Bending Test Results – 0.5% GNP/SMP Nanocomposite produced by high speed mechanical mixing method

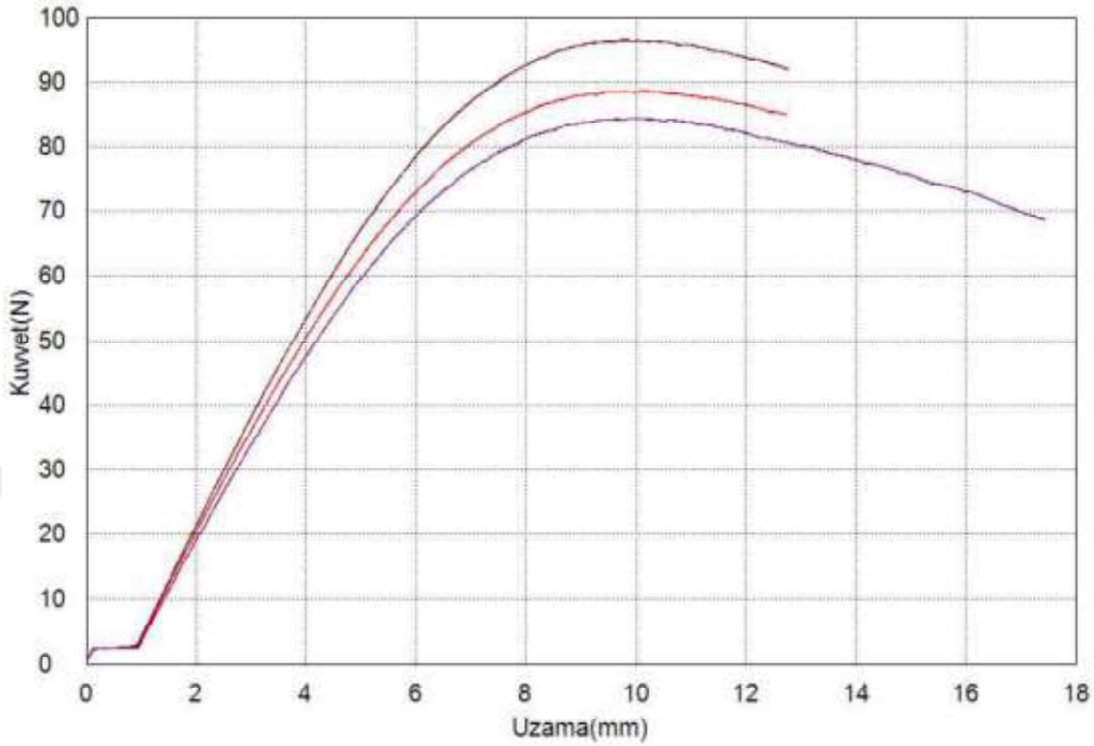


Figure C.4 Force vs. displacement curve of 0.5% GNP/SMP Nanocomposite produced by high speed mechanical mixing method

Table C.4 3-Point Bending Test Results – 0.5% GNP/SMP Nanocomposite produced by high speed mechanical mixing method

	Flexural Strength (MPa)	**Flexural Modulus (MPa)**
Sample 1	52.19	1667.33
Sample 2	53.62	1597.22
Sample 3	48.14	1480.40
Average	51.32	1581.65
Standard Deviation	2.84	94.43

Appendix C5 - 3-Point Bending Test Results – 0.1% GNP/SMP Nanocomposite produced by hybrid method including ultrasonic mixing-high speed mechanical mixing

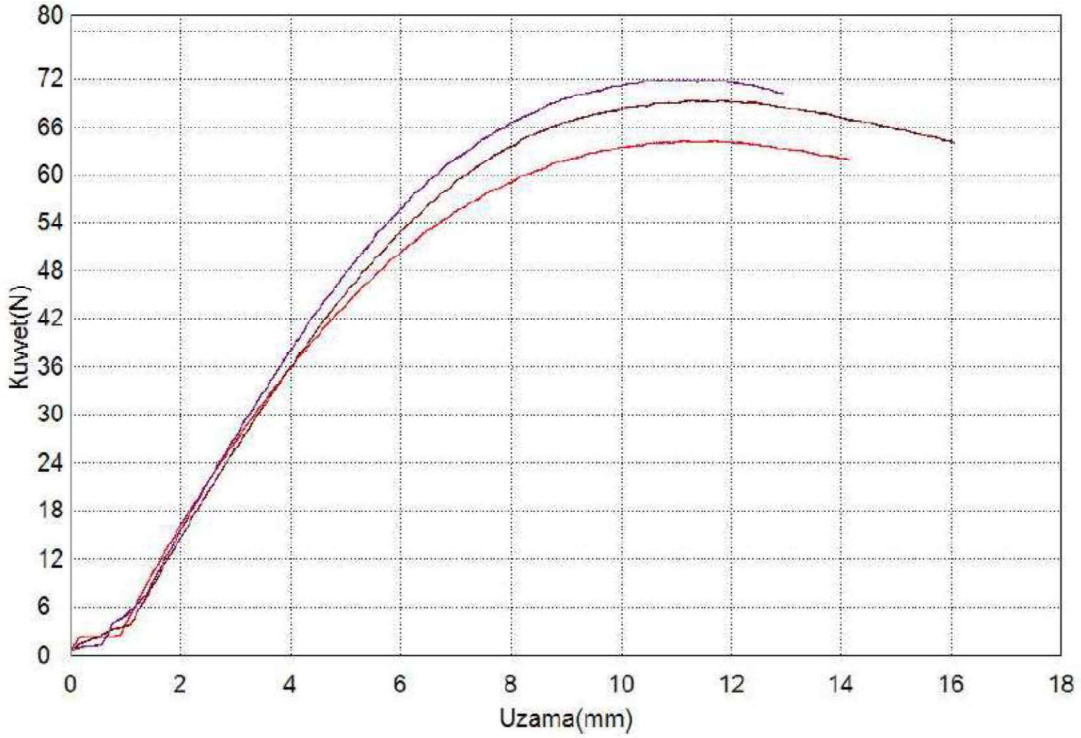


Figure C.5 Force vs. displacement curve of 0.1% GNP/SMP Nanocomposite produced by hybrid method including ultrasonic mixing-high speed mechanical mixing

Table C.5 3-Point Bending Test Results – 0.1% GNP/SMP Nanocomposite produced by hybrid method including ultrasonic mixing-high speed mechanical mixing

	Flexural Strength (MPa)	**Flexural Modulus (MPa)**
Sample 1	35.75	1053.10
Sample 2	38.43	1074.15
Sample 3	41.87	1174.17
Average	38.68	1100.47
Standard Deviation	3.07	64.69

Appendix C6 - 3-Point Bending Test Results – 0.3% GNP/SMP Nanocomposite produced by hybrid method including ultrasonic mixing-high speed mechanical mixing

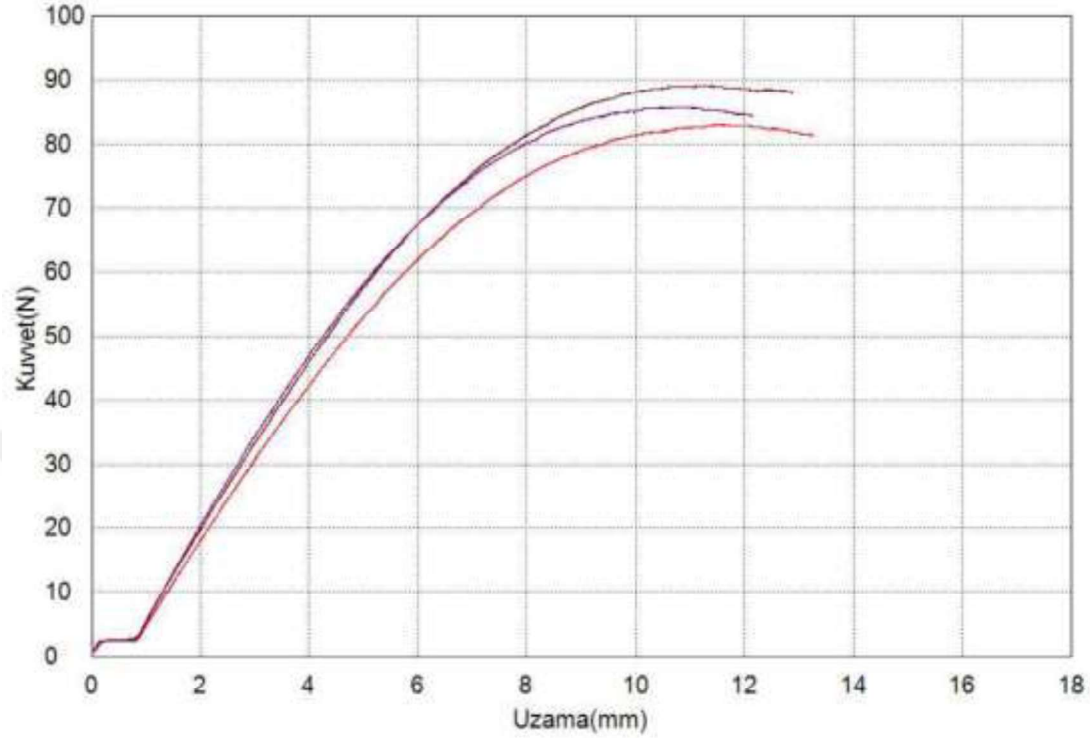


Figure C.6 Force vs. displacement curve of 0.3% GNP/SMP Nanocomposite produced by hybrid method including ultrasonic mixing-high speed mechanical mixing

Table C.6 3-Point Bending Test Results – 0.3% GNP/SMP Nanocomposite produced by hybrid method including ultrasonic mixing-high speed mechanical mixing

	Flexural Strength (MPa)	**Flexural Modulus (MPa)**
Sample 1	48.45	1306.55
Sample 2	48.53	1298.25
Sample 3	48.62	1416.40
Average	48.53	1340.40
Standard Deviation	0.09	65.95

Appendix C7 - 3-Point Bending Test Results – 0.5% GNP/SMP Nanocomposite produced by hybrid method including ultrasonic mixing-high speed mechanical mixing

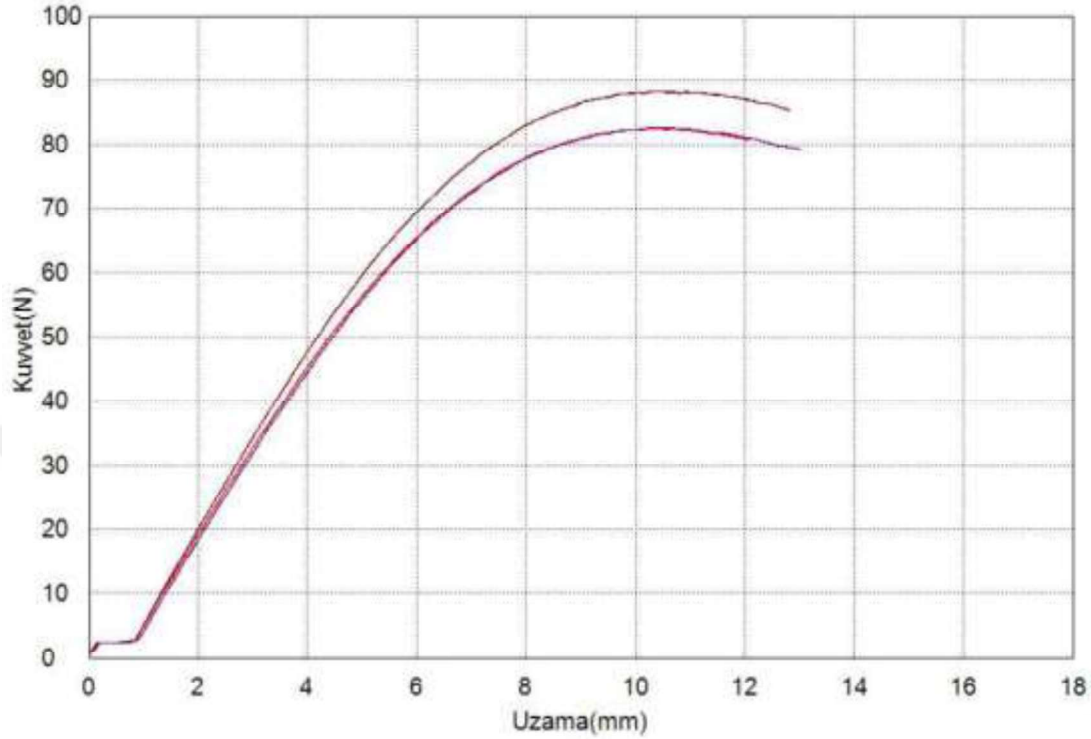


Figure C.7 Force vs. displacement curve of 0.5% GNP/SMP Nanocomposite produced by hybrid method including ultrasonic mixing-high speed mechanical mixing

Table C.7 3-Point Bending Test Results – 0.5% GNP/SMP Nanocomposite produced by hybrid method including ultrasonic mixing-high speed mechanical mixing

	Flexural Strength (MPa)	**Flexural Modulus (MPa)**
Sample 1	54.90	1680.60
Sample 2	52.15	1501.89
Sample 3	55.67	1710.80
Average	54.24	1631.10
Standard Deviation	1.85	112.91

Appendix D - Hardness (Shore D) Test Results Table

Table D.1 Hardness (Shore D) Test Results

	First Measurement	Second Measurement	Third Measurement	Average	Standard Deviation
Pure SMP	57.2	60.7	47.9	**55.2**	6.6
0.1% GNP/SMP nanocomposite produced by high speed mechanical mixing method	62.7	63.5	63.2	**63.1**	0.4
0.3% GNP/SMP nanocomposite produced by high speed mechanical mixing method	65.8	63.3	64.8	**64.6**	1.3
0.5% GNP/SMP nanocomposite produced by high speed mechanical mixing method	61.2	65.2	62.3	**62.9**	2.1
0.1% GNP/SMP nanocomposite produced by hybrid method including ultrasonic mixing-high speed mechanical mixing	62.8	59.3	59.4	**60.5**	1.9
0.3% GNP/SMP nanocomposite produced by hybrid method including ultrasonic mixing-high speed mechanical mixing	60.9	63.9	63.0	**62.6**	1.5
0.5% GNP/SMP nanocomposite produced by hybrid method including ultrasonic mixing-high speed mechanical mixing	65.2	66.2	63.7	**65.0**	1.3